Conceptual Design of a Coupling Process of Hydrodynamic Cavitation and Hydrothermal Separation for Extractives and Biopolymers Extraction

MD. BAYAZID AHMED

SUPERVISOR
Souman Rudra
Abu Shadat Muhammad Sayem

University of Agder, 2023
Faculty of Engineering and Science
Department of Engineering Sciences

Abstract

Lignocellulosic biomass is an abundant and sustainable resource for producing biopolymers, chemicals, biofuels, and high-value-added compounds. The primary refining processes, which includes pretreatment, fractionation, and separation of components, as well as structural disconnection or partial structural change, are necessary to achieve high-value utilization of lignocellulosic materials. However, conventional pretreatment processes for biomass valorization aim to obtain high yields of cellulose without concern for utilizing other components. Focusing on a single component of lignocellulose is not only a waste of resources but also causes serious environmental pollution. This study proposed a novel and efficient biomass processing concept that, for the first time, couples two key technologies (hydrodynamic cavitation and hydrothermal separation) to enable almost all the biomass to be used for a range of high-valued products, including biopolymers and extractives. The conceptual design of coupling of hydrodynamic cavitation and hydrothermal separation was then modeled and simulated to evaluate the ease of coupling in terms of component yield and overall extraction efficiency and observed how the coupling process was affected by the process parameters with an optimal overall extraction efficiency. The simulation results showed that the coupling of the HC and HTS processes had a maximum of 25.5% higher overall extraction efficiency than the single HC process and 18.2% higher efficiency than the single HTS process for woodchips. The process parameters, including HTS temperature, HTS residence time, and S/L ratio affected component yield and overall extraction efficiency. The maximum overall extraction efficiency was predicted by the statistical approach of 80.20 ± 5.04% with a regression coefficient (R-sq) of 99.33% at optimal conditions (S/L ratio 10%, HC pressure 3 bar, HC temperature 60℃, HC residence time 20 min, HTS temperature 210 ℃, HTS residence time 25 min, and HTS pressure of 19.04 bar). The coupling of hydrodynamic cavitation and hydrothermal separation showed better biomass utilization than the conventional pretreatment processes. This coupled process focuses on more utilization of biomass rather than only one yield, which will reduce the waste with minimal environmental effect and increase the potential use of biomass from different perspectives.

Sammendrag

Lignocelluloseholdig biomasse er en rikelig og bærekraftig ressurs for produksjon av biopolymerer, kjemikalier, biodrivstoff og forbindelser med høy verdi. De primære raffineringsprosessene, som inkluderer forbehandling, fraksjonering og separering av komponenter, samt strukturell frakobling eller delvis strukturell endring, er nødvendige for å oppnå høyverdig utnyttelse av lignocellulosematerialer. Imidlertid har konvensjonelle forbehandlingsprosesser for biomassevalorisering som mål å oppnå høye utbytter av cellulose uten bekymring for å bruke andre komponenter. Å fokusere på en enkelt komponent av lignocellulose er ikke bare sløsing med ressurser, men forårsaker også alvorlig miljøforurensning. Denne studien foreslo et nytt og effektivt biomasseprosesseringskonsept som for første gang kobler to nøkkelteknologier (hydrodynamisk kavitasjon og hydrotermisk separasjon) for å gjøre det mulig å bruke nesten all biomassen til en rekke høyt verdsatte produkter, inkludert biopolymerer og ekstraktiver. . Den konseptuelle utformingen av kobling av hydrodynamisk kavitasjon og hydrotermisk separasjon ble deretter modellert og simulert for å evaluere den enkle koblingen når det gjelder komponentutbytte og total ekstraksjonseffektivitet og observerte hvordan koblingsprosessen ble påvirket av prosessparametrene med en optimal total ekstraksjonseffektivitet. Simuleringsresultatene viste at koblingen av HC- og HTS-prosessene hadde maksimalt 25,5 % høyere total utvinningseffektivitet enn enkelt-HC-prosessen og 18,2 % høyere effektivitet enn enkelt HTS-prosessen for flis. Prosessparametrene, inkludert HTS-temperatur, HTS-oppholdstid og S/L-forhold, påvirket komponentutbytte og total ekstraksjonseffektivitet. Den maksimale totale ekstraksjonseffektiviteten ble spådd ved den statistiske tilnærmingen på 80,20 ± 5,04 % med en regresjonskoeffisient (R-sq) på 99,33 % ved optimale forhold (S/L-forhold 10 %, HC-trykk 3 bar, HC-temperatur 60 ℃, HC oppholdstid 20 min, HTS-temperatur 210 ℃, HTS-oppholdstid 25 min, og HTS-trykk på 19,04 bar). Koblingen av hydrodynamisk kavitasjon og hydrotermisk separasjon viste bedre biomasseutnyttelse enn de konvensjonelle forbehandlingsprosessene. Denne koblede prosessen fokuserer på mer utnyttelse av biomasse i stedet for kun ett utbytte, noe som vil redusere avfallet med minimal miljøeffekt og øke potensiell bruk av biomasse fra ulike perspektiver.

Preface

This thesis work was conducted under the project “Collaborative Action for improving educational capacities in Renewable Energy to mitigate climate crisis (CARE)” between Chittagong University of Engineering & Technology (CUET), Bangladesh and University of Agder (UiA), Norway (Collaboration Agreement No. NORPART-2021/10355).

I would like to express my gratitude to my supervisor Prof. Dr. Souman Rudra, UiA, for his excellent guidance and supervision throughout the project. I am grateful to Prof. Abu Shadat Muhammad Sayem, CUET, for his motivation and mentorship during my thesis work.

Lastly, my father, Md. Anisuzzaman, and my mother, Mst. Zahanara Begum and other family members deserve particular thanks for their unconditional love, mental support, and kind words, which served me well.

Md. Bayazid Ahmed
University of Agder
Grimstad, December 2023

Individual/group Mandatory Declaration

The individual student or group of students is responsible for the use of legal tools, guidelines for using these and rules on source usage. The statement will make the students aware of their responsibilities and the consequences of cheating. Missing statement does not release students from their responsibility.

1.	I/We hereby declare that my/our report is my/our own work and that I/We have not used any other sources or have received any other help than mentioned in the thesis.	☒
2.	I/we further declare that this thesis: - has not been used for another exam at another department/university/university college in Norway or abroad; - does not refer to the work of others without it being stated; - does not refer to own previous work without it being stated; - have all the references given in the literature list; - is not a copy, duplicate or copy of another's work or manuscript.	☒
3.	I/we am/are aware that violation of the above is regarded as cheating and may result in cancellation of exams and exclusion from universities and colleges in Norway, see Universitets- og høgskoleloven §§4-7 og 4-8 og Forskrift om eksamen §§ 31.	☒
4.	I/we am/are aware that all submitted theses may be checked for plagiarism.	☒
5.	I/we am/are aware that the University of Agder will deal with all cases where there is suspicion of cheating according to the university's guidelines for dealing with cases of cheating.	☒
6.	I/we have incorporated the rules and guidelines in the use of sources and references on the library's web pages.	☒

Publishing Agreement

Authorization for electronic publishing of the thesis.

Author(s) have copyrights of the thesis. This means, among other things, the exclusive right to make the work available to the general public (Åndsverkloven. §2).

All theses that fulfill the criteria will be registered and published in Brage Aura and on UiA's web pages with author's approval.

Theses that are not public or are confidential will not be published.

I hereby give the University of Agder a free right to

make the task available for electronic publishing: ☒JA ☐NEI

Is the thesis confidential? ☐JA ☒NEI

(confidential agreement must be completed and signed by the Head of the Department)

- If yes:

Can the thesis be published when the confidentiality period is over? ☐JA ☐NEI

Is the task except for public disclosure? ☐JA ☒NEI

(contains confidential information. see Offl. §13/Fvl. §13)

Table of Contents

List of Figures

List of Tables

Abbreviations

HC	Hydrodynamic Cavitation
HTS	Hydrothermal Separation
LCB	Lignocellulosic Biomass
S/L ratio	Solid-to-Liquid Ratio
RSM	Response Surface Methodology
CCD	Central Composite Design
ANOVA	Analysis of Variance

Chapter 1 Introduction

1.1. Background

The global energy dependency on traditional energy sources, such as fossil fuels, has heightened the need for alternative, renewable and sustainable energy sources because of several factors: an increase in the demand for energy, a finite supply of traditional sources, greenhouse gas emissions, and global warming. The objective of attaining the long-term goal of a sustainable circular economy, which prioritizes the "recovery and reuse" of bio-based raw materials instead of the traditional industrial approach of "take, make, and dispose of" raw materials, has also spurred the utilization of renewable energy sources [1]. The use of Lignocellulosic biomass (LCB) as a plentiful (200 billion tons/year) and sustainable energy source has attracted considerable interest in this context [2]. LCB presents a promising solution for meeting future energy demands while simultaneously alleviating the environmental concerns associated with traditional energy sources [3]. The utilization of waste and residual biomass in energy production currently contributes to approximately 14% of global energy consumption, with the potential to meet up to 50% of future energy demands by the next century while significantly reducing carbon emissions [4].

A wide range of biomasses are in the lignocellulosic group, including woody biomass, agricultural residue, municipal solid waste, cattle manure, forest waste and so on. The main components of lignocellulosic biomass are cellulose, hemicellulose, and lignin, accounting for 60–90% of entire dry weight; other components include extractives, minerals and ash [5]. Depending on material types, a typical lignocellulosic biomass consists of cellulose in 35-50%, hemicellulose in 20-45%, and lignin in 15-20%, the three main components, which are interconnected, constituting a recalcitrant structure [6]. In LCB, Cellulose and hemicellulose are densely compacted within the outer surface of plant cells, forming a layer enriched with lignin. The layer of lignin protects the biomass from microbial attack or chemical degradation [7], [8]. Lignocellulosic biomass is an abundant feedstock for production of biofuels, platform chemicals, pharmaceuticals, nutritional components, and other value-added components [8].

“Biorefinery” refers to an industrial facility that converts biomass into energy, chemicals, and materials. It is a refinery that uses biomass to produce bio-based materials, chemicals, and bioenergy (biofuel, power, or heat) [9]. Lignocellulosic biomass can be used in biorefineries to produce biofuels such as bioethanol, biobutanol, biogas, and bio-jet fuel; as well as platform chemicals like sorbitol, xylitol, and glucaric acid, as shown in Table 1.1 (summarized from this study [9]) ; and biomaterials such as biochar, carbon fiber, hydrogel, and coatings [10]. These biorefinery products have diverse applications, including in power and heat production, automobile and aviation industries, food and agriculture sectors, pharmaceuticals and medical appliances, cosmetics, and packaging. However, the production of these products involves various routes, such as chemical, biological, or combined processes, by which, the products are produced using different chemicals or microorganisms [9]. The conversion of lignocellulosic biomass into chemicals and polymers remains a challenging endeavor. The recalcitrant structure and intrinsic properties of lignocellulosic biomass make it resistant to degradation [9]. In this regard, the primary refining processes, which includes pretreatment,

fractionation, and separation of components, as well as structural disconnection or partial structural change, are necessary to achieve high-value utilization of lignocellulosic materials [11].

Table 1.1: Platform chemicals from lignocellulosic biomass [9]

Platform Chemicals	Production Route	Produced From	Applications
Sorbitol	Chemical process	Glucose (Cellulose)	Food industry, medical appliance, and oral health
Xylitol	Chemical process	Xylose (Hemicellulose)	Additive in food, cosmetic, and pharmaceutical industries
Glucaric Acid	Chemical process	Glucose (Cellulose)	Detergents to biodegradable polymers
Succinic Acid	Biological process	Glucose (Cellulose)	Food, agricultural, and pharmaceutical products
Glutamic Acid	Biological process	Glucose (Cellulose)	Flavor enhancer
Lactic Acid	Biological process	Glucose (Cellulose)	Food industry, cosmetics, and pharmaceuticals products
Furfural	Chemical process	Xylose (Hemicellulose)	Chemicals, pharmaceuticals, cosmetics, fragrances, flavors, biofuels, and biomaterials
5-HMF	Chemical process	Glucose (Cellulose)	Chemical, pharmaceuticals, and food packaging industry
Levulinic Acid	Chemical process	Glucose (Cellulose) and Xylose (Hemicellulose)	Herbicides, pharmaceuticals, flavoring agents, solvents, plasticizers, antifreeze agents, and biofuels, resins, and polymers

Pretreatment methods are categorized into mechanical, chemical, physicochemical and biological, or combinations of these. Various pretreatment options are available to solubilize, hydrolyze and fractionate cellulose, hemicelluloses, and lignin. [12]. Physical and physiochemical pretreatments include steam explosion, ammonia fiber explosion, carbon dioxide explosion, liquid hot water pretreatment, mechanical pretreatment, ultrasound, microwave pretreatment, oxidation pretreatment. Chemical pretreatment includes acid pretreatment, alkaline, organosolv, and ozone treatment. The chemical pretreatment is use different chemicals as catalyst to degrade mainly lignin from lignocellulosic matrix to make better enzymatic hydrolysis of cellulose [13]. Biological

pretreatments use the microorganisms to degrade the hemicellulose and lignin, and does not involve the addition of chemicals [13].

However, all the pretreating technologies were aimed at obtaining high yields of cellulose without concern for the utilization of other components. Pretreatment method focusing on a single component of lignocellulose not only was a waste of resources but also would cause serious environmental pollution. The composition of lignocellulose is complex; thus, it is difficult to separate it into useful molecular components. Therefore, plants for the industrialization of biomass raw materials, such as furfural plants, paper mills, xylitol plants, and so on, just emphasize the use of a single component of lignocellulose; other components are discarded as waste, causing a serious waste of resources and environmental pollution. Therefore, insufficient utilization of lignocellulose did not play an important role in improving economic efficiency but became the burden of efficiency [11].

H. Chen mentioned in his book [11] that, there are three common problems in the conversion and utilization of lignocellulosic materials, the singular utilization of each component, the singular utilization of technology, and lack of systematic integration of technologies and research of ecological processes and engineering.

This study proposed a novel and efficient biomass processing concept that, for the first time, couples two key technologies (hydrodynamic cavitation and hydrothermal separation) to enable almost all the biomass to be used for a range of high-valued products, including biopolymers and extractives. The approach will be used to transition to a biobased economy and new technology challenge, which is expected to be the sustainable source of chemical raw materials for the circular bioeconomy.

The coupling of hydrodynamic cavitation (HC) and hydrothermal separation (HTS) is shown in Fig. 1.1. The biomass arrives from the field milled into particles and mixed with water. Then the slurry is fed directly to the HDC reactor through pump. Soluble extractive and lignin would then be separated from the process water. Hydrodynamic cavitation will play a useful role in such processing as a pretreatment of biomass for further processing. The solids are mixed with additional water before it is transported to the hydrothermal separation (HTS) reactor. They are smaller, and thus mass transfer is better as well as the structure is more accessible due to the biomass structures' cavitation breakdown. The HTS reactor converts the biomass slurry to biopolymers for advanced biomaterial production. Both hydrodynamic cavitation and hydrothermal separation use water as a reactant that is environmentally friendly and cost-effective to provide clean feedstocks to produce advanced materials. However, this work will conduct a process simulation of the coupled process based on the mechanism of HC and HTS process to evaluate the feasibility of process coupling in order to components yield and overall extraction efficiency.

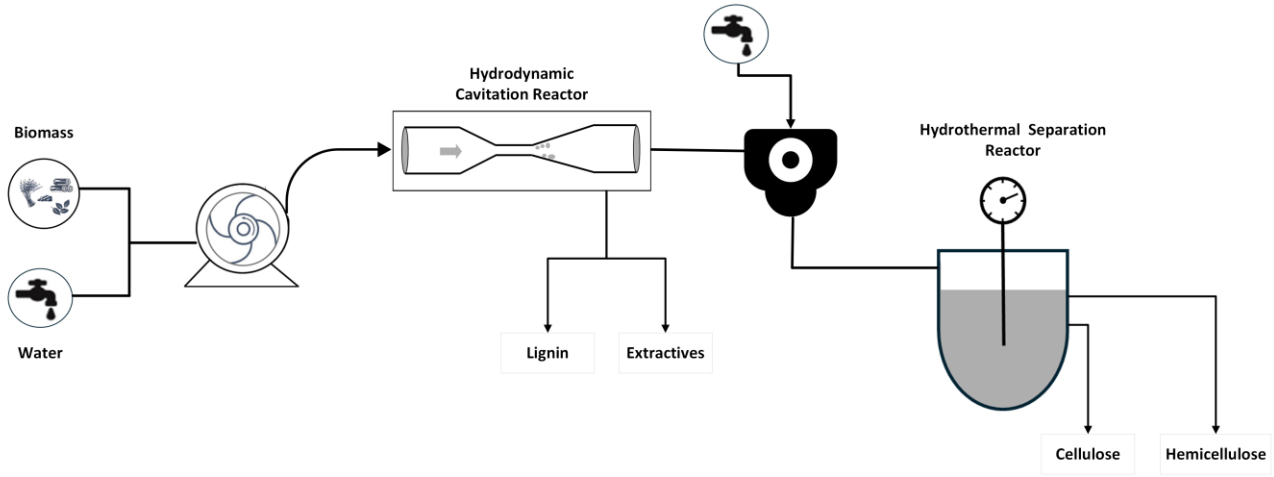

Figure 1.1: Coupling process of hydrodynamic cavitation and hydrothermal separation.

1.2. Objectives

This research aims to study the feasibility of coupling process of hydrodynamic cavitation and hydrothermal separation for extractives and biopolymers extraction. This aim is achieved through the following objectives**:**

- To design a model of coupling of hydrodynamic cavitation and hydrothermal separation process
- To simulate and evaluate the process models in order to components yield and overall extraction efficiency.
- To analyze the effect of process parameters on component yield and overall extraction efficiency of coupled process.
- To optimize the overall extraction efficiency based on process parameters like temperature, residence time, feed ratio.

1.3. Research Question

The following research questions to be answered in this thesis are listed below as follows.

RQ1: How does the coupling process of hydrodynamic cavitation and hydrothermal processes affect the yield of extractives and biopolymers, and overall extraction efficiency?

RQ2: How process parameters affect the performance of the coupled process?

RQ 3: What are the optimal process parameters such as, temperature, pressure, and residence time, for maximizing overall extraction efficiency?

1.5. Limitations

This study was intended to analyze the composition of raw biomass samples; unluckily, we could not conduct the experiment due to malfunctioning of the machines in the laboratory. We waited a few weeks to resolve the issue, but our time was limited. That's why we adopt the compositional data from the literature, and based on the collected data we conduct our simulation to analyze the process.

In this simulation study, the hydrodynamic cavitation reactor was considered as a balanced-based reactor block (RYield) owing to its mechanical effect, and there was no developed reaction kinetics found in the literature for lignocellulosic biomass. The yield distribution for the reactor block in Aspen Plus simulation was specified based on an experimental study by Teran et al. [14], where they studied the HC in a batch process, whereas we intended to simulate it as a continuous operation, which can yield significant cost and energy savings. For extractives, yield distribution was adopted from this study [15], where extractives were separated from wheat straw by simple hot water (80–90 °C). As the hydrodynamic cavitation reactor uses simple hot water as a solvent and there is a lack of literature on extractive separation by HC reactor from lignocellulosic biomass, we, therefore, consider the extraction ratio from this study.

For extractives, yield distribution was adopted from this study [15], where extractives were separated from wheat straw by simple hot water (80–90 °C). As the hydrodynamic cavitation reactor uses simple hot water as a solvent and there is a lack of literature on extractive separation by HC reactor from lignocellulosic biomass, we, therefore, consider the extraction ratio from this study.

The simulation undertaken in this study focused solely on the chemical aspects of biomass processing and did not incorporate the physical effects of hydrodynamic cavitation and hydrothermal separation.

As the coupling of hydrodynamic cavitation and hydrothermal separation is a new concept and we did not perform any experiments in the laboratory, it was not possible to validate the simulation results of the coupled process.

Despite these limitations, there are opportunities for future research to address these gaps and further explore the potential of this coupled process.

1.6. Thesis Outline

This thesis focuses on the design, simulation, and optimization of coupling process of hydrodynamic cavitation and hydrothermal separation process. The report is organized into chapters and subchapters. The sections are arranged in the following way.

Chapter 1 presents an introduction and background information on the selected problem and the objectives of this study followed by Research questions and limitations.

Chapter 2 describes relevant theoretical background and concepts of hydrodynamic cavitation process and hydrothermal separation process and their relevant studies.

Chapter 3 presents the method and simulation procedure for individual pretreatment process and coupled process.

Chapter 4 presents the results and discussion of individual and coupled process for different feedstocks. The subsections present the results and discussion of case studies, sensitivity analysis and optimization.

Chapter 5 concludes the thesis with different findings and implications. Finally, some further work is suggested.

.

Chapter 2 Theory

2.1 Introduction

This chapter discusses the structure of lignocellulosic biomasses, theory of hydrodynamic cavitation process and effects of HC reactor on lignocellulosic biomass and their relevant studies. And mentioned the mechanism of hydrothermal separation process with relevant studies.

2.2. Structure of Lignocellulosic Biomass

Lignocellulosic biomass (LCB) consists of cellulose, hemicellulose, lignin, extractives, and ash, which are organized in intricate, non-uniform, and three-dimensional structures [12]. Cellulose and hemicellulose are densely compacted within the outer surface of plant cells, forming a layer enriched with lignin [7], [8] as shown in Fig. 2.1. The specific arrangement and three-dimensional configuration of these components can vary depending on the particular type of LCB being considered. LCB has developed structures to resist degradation, which include the crystalline nature of cellulose, the hydrophobic properties of lignin, and the encapsulation of cellulose within a lignin-hemicellulose matrix [16].

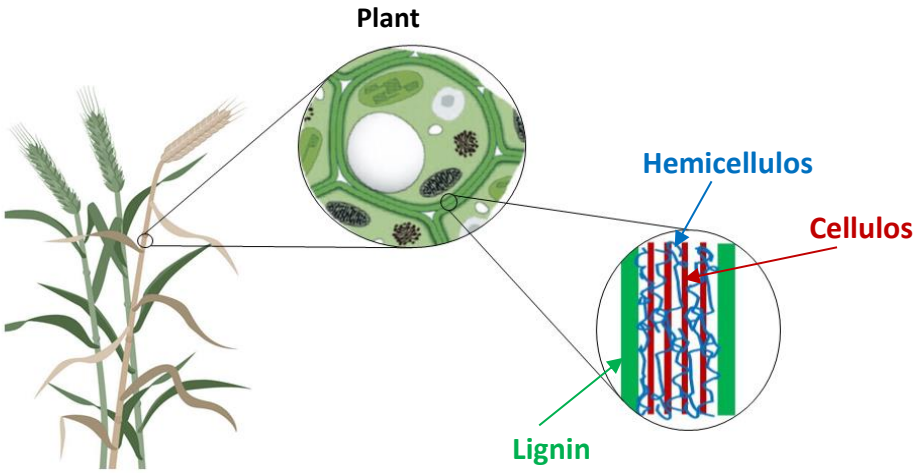

Figure 2.1: Plant cell wall structure of a lignocellulosic biomass

Cellulose is the primary constituent of lignocellulosic biomass and is characterized by its linear and unbranched polymer structure, which consists of numerous parallel chains of glucose units linked together through β-1,4-glycosidic bonds [12]. These chains possess a molecular formula of $(C_6H_{12}O_6)_n$, and their varying degrees of polymerization result in the formation of microfibrils that can interact with hydroxyl groups to create intra- and intermolecular hydrogen bonds [8]. The unique structure of cellulose, with its tightly packed, highly crystalline arrangement, renders it resistant to depolymerization [17]. The cellulose molecule contains both crystalline and amorphous regions that are interwoven to form the overall cellulose structure. The integration of these cellulose chains leads to the formation of cellulose fibrils or bundles [18]. These fibrils are connected by hemicelluloses, amorphous polymers of various sugars, and other polymers, such as pectin, and coated by lignin [19]. However, cellulose begins to decompose at a temperature of 200 °C, and the reaction rate is faster as the temperature increases [20]. Complete hydrolysis of cellulose gives monosaccharides, for example, glucose, but partial hydrolysis of cellulose results in disaccharide, for example, cellobiose. [13]

Hemicellulose is the second most abundant biopolymer with an amorphous and random structure. The composition consists of short, extensively branched heteropolymers, composed of pentose sugar monomer (xylose, arabinose), hexose sugar monomer (mannose, glucose, galactose), and sometimes sugar acid (uronic acids) [12]. Hemicellulose is more readily degraded in acidic or hot aqueous medium compared to cellulose due to its lower degree of polymerization (50–200) and amorphous structure [11]. In hemicellulose, xylose ($C_5H_{10}O_5$) is one of the predominant sugars, has a molecular weight of 150.1 g/mol [21]. Hemicelluloses are categorized into xyloglucans, xylans, mannans, or galactans, depending on the types of substituents present [12]. Xylans are the primary polysaccharides found in hemicelluloses, with their polymeric chains consisting of 1,4-linked β-d-xylose units [21]. The composition of xylan can vary depending on its origin. For instance, xylan derived from birch wood is composed of 89.3% xylose, 1.4% glucose, 1% arabinose, and 8.3% anhydrouronic acid [22]. On the other hand, xylan obtained from corn fiber contains 48–54% xylose, 33–35% arabinose, 5–11% galactose, and 3-6% glucuronic acid [23]. However, the decomposition temperature of hemicellulose is between 160 to 210℃ [24]. Hydrolysis of hemicellulose yielded into monomeric sugar with an intermediate of oligomers.

Lignin is a complex amorphous heteropolymer composed of three distinct phenylpropane units: p-coumaryl, coniferyl, and sinapyl alcohol. P-hydroxyphenyl (H), guaiacyl (G), and syringyl (S) units are the corresponding phenylpropanoid monomeric units in lignin, respectively. Lignin serves the purpose of providing plant structural support, impermeability, and resistance to microbial attack and oxidative stress [9]. Due to its hydrophobic nature, lignin is insoluble in water under ambient conditions [21] and insoluble even at 160 to 210℃. Different lignocellulosic biomasses exhibit variations in both the composition and quantity of lignin. For instance, the lignin content in hardwood, softwood and grasses follows the sequence of grasses having the lowest concentration, followed by hardwood, and then softwood [21]. The distribution of cellulose, hemicellulose, and lignin within the cell walls is non-uniform, and the composition and quantity of cell wall components vary considerably depending on factors such as the species, tissue type, and maturity of the plant cell wall [25]. Extracting cellulose and hemicellulose from biomass to yield sugars is strongly hindered by the presence of lignin [21].

Extractives refer to the soluble components of lignocellulosic biomass that are not part of its structure. These components can dissolve in water or neutral organic solvents such as ethanol, toluene, hexane, benzene, acetone, and dichloromethane [26]. Lipophilic extractives, which are insoluble or partly soluble in water but soluble in organic solvents, include fatty acids, sterols, wax, terpenes, tannins, lignan, flavonoids, glycerol, and sterols [27]. Meanwhile, water-soluble constituents contain inorganic compounds, proteins, and unstructured sugar [28]. A simple hot water extraction step removed more than half of the water-soluble extractives [15]. A study by R. C. Sun et al. [15] showed that, treatment of wheat straw with liquid hot water at 80-90℃ realized 41 to 53% of original lipophilic extractives. However, the quantity of extractives differs among similar species or even distinct parts of the same plant, such as bark, stem, leaves, roots, and so on [28].

Ash refers to the inorganic, non-combustible solid substance that remains after the complete combustion of biomass waste. It contains various minerals and elements, including silicates, sodium, potassium, calcium, magnesium, phosphates, carbonates, and so on [29], [30]. Silica, a principal biomass ash constituent, exists as silicates within plants, such as kaolinite, feldspars, plagioclase, chlorite, quartz, opal, etc. [30]. Silicates give structural integrity to the supporting tissues, such as bark,

in bigger plants like trees [31]. The amount of ash content varied for different biomasses. It has been shown that woody biomass contains a lower ash content than agricultural residual biomass [21], [29].

2.3 Hydrodynamic Cavitation Process

Cavitation is initiated by creating vapor bubbles inside a liquid flow due to a localized reduction in pressure below the boiling point of the liquid at a specific temperature. More precisely, when exposed to increased pressure, the created cavities burst, leading to a localized rise in temperature, pressure, and micro- and turbulent mixing events, a cavitation phenomenon is shown in Fig.2.2. When cavitation occurs in a reactive flow, it results in turbulent mixing and rapid mass transfer, which improves the environment for favorable reactions, increases selectivity, and reduces energy consumption. Cavitation arises with reduced power consumption due to the decreased reaction pressure and temperature in these processes [32], [33]. Cavitation is categorized into four types based on its generation modes: acoustic, hydrodynamic, optic, and particle. However, only acoustic, and hydrodynamic cavitation were effectively taken into account in the creation of physical-chemical changes, which is desirable in pretreatment procedures [34]. Acoustic cavitation is achieved by transmitting a high-amplitude ultrasonic signal (20–100 kHz) into a liquid, the most common method for generating cavitation on a laboratory scale [35].

Hydrodynamic cavitation surpasses acoustic cavitation in numerous applications due to its ability to oxidize organic molecules, along with its cost-effectiveness, high power efficiency, scalability, and minimal pollution without the formation of any byproducts [36],[37]. It is generated via mechanical restrictions, such as Venturi pipes, orifice plates, and throttling valves. Cavitation can be understood by considering the link between fluid velocity and pressure, as described by Bernoulli's equation [34]. As the fluid passes through the narrow section, the pressure drops below the liquid-vapor pressure at the current temperature. This causes vapor cavities to form, which subsequently collapse in the area farther downstream. The collapsing cavities produce powerful shockwaves with very high pressures and intense turbulence, resulting in significant strain [38]. The collapse is of significant magnitude, resulting in the rapid release of substantial energy. The implosion of the vapor cavity can create intense localized temperatures ranging from 5000 to 10,000 K and pressures of 1000 to 2000 atm [34]. This process leads to physical and chemical changes, resulting in the formation of highly reactive radicals like the hydroxyl radical (OH-). These radicals are produced through the decomposition of water molecules and the decomposition or pyrolysis of organic molecules that are trapped inside or in close proximity to the vapor cavities. This ultimately leads to the disintegration of the structure and an increase in the porosity of the biomass [39], [40].

Hydrodynamic cavitation reactors can be classified into two categories. One is non-rotating reactors, such as Venturi pipes or orifice plates, and another is rotating reactors, in which cavitation is induced within a region swept by high-velocity propellers [41].

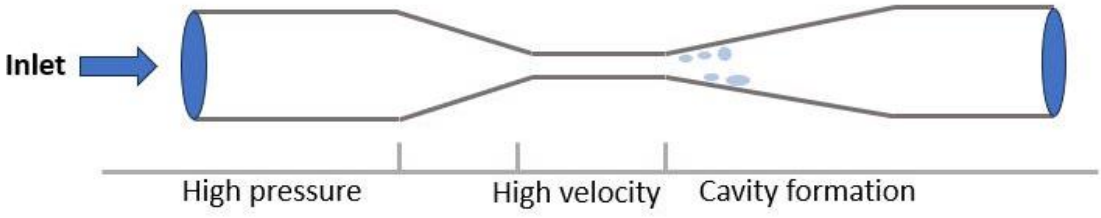

Figure 2.2: Schematic presentation of cavitation phenomena in a venturi tube reactor

The energy efficiency of HC is recognized to be superior to that of other alternative energy sources in process intensification [42]. The fundamental properties of HC reactors dictate that HC technology is suitable for large-scale industrial applications [43]. HC reactors can be readily produced through mechanical machining without costly electrical components, thus explaining their feasibility. Furthermore, the cavitation intensity of HC reactor can either remain constant or increase by scaling up with a suitable alteration, as the same percentage also expands the size of the created cavitation region [44].

2.4 Effects of Hydrodynamic Cavitation on Lignocellulosic Biomass

Research has indicated that hydrodynamic cavitation (HC) is primarily employed for the purpose of delignification in lignocellulosic biomass. Baxi and Pandit conducted the first study to investigate the effectiveness of HC on delignification in 2012 [45]. This experiment treated sawdust using HC (reactor: Venturi, capacity: 5 L) and alkali (5% w/w NaOH). The findings showed that HC had a higher acid-insoluble lignin removal rate (53.3%) and reaction rate (6.8 × 10-1 min−1) compared to an ultrasound bath with a capacity of 500 mL, which achieved 17.3% and 9.78 × 10-1 min−1, respectively. Subsequently, the HC process has been widely utilized for the pretreatment of numerous lignocellulosic biomass (LCB) sources, including wheat straw (WS) [46], corncob [47], sugar cane bagasse (SCB) [35], reed[39], and miscanthus grass. Various hydrodynamic cavitation devices, such as venturi tubes, orifice plates, vortex-based cavitation, and rotational cavitation reactor.

Kim et al.[39] investigated the use of hydrodynamic cavitation to assist in alkali pretreatment of reed. The cavitation device used was an orifice plate containing 27 holes, each with a diameter of 1 mm. The volume of the reaction vessel was 150 mL, and the pressure at the intake was 500 kPa, reaction temperature was 77 °C. The most effective pre-treatment condition was found to be 3% NaOH, 11.8% solid load, and a reaction duration of 41.1 minutes. This resulted in a removal of 35-42% of lignin and a maximum glucose production of 326.5 grams per kilogram of biomass after 72 hours of enzymatic hydrolysis. The utilization of hydrodynamic cavitation as a pretreatment method for biomass has demonstrated its advantageous nature in terms of energy efficiency. The energy consumption for this process is measured at 3.65 MJ/kg of biomass, which is significantly lower than the energy consumption of 14.4 MJ/kg of biomass observed in ultrasonic cavitation conducted under similar conditions.

Even though LCB pretreatment based on HC has been studied for over a decade, the number of related research studies is relatively small (less than 30) compared to other emerging technologies such as microwave, ultrasound, gamma ray, and pulsed electric field [44]. This suggests that this promising method has yet to receive significant research attention. Additionally, the recent progress in this field is poorly understood, and the underlying mechanisms remain unclear [44].

Fig. 2.3 provides a schematic representation of the depiction of cavitation during the processing of lignocellulosic biomass. The mechanical consequences of cavitation result in the generation of shock waves and the rapid movement of micro-jets, which are caused by the forceful implosion of bubbles. These events contribute to the breakdown of organic matter, especially the lignin-carbohydrate bond, as lignin is located in the vicinity of the cavity, and the formation of small cavities on the surface of biomass, which increase the porosity and surface area of cellulose. [37], [48].

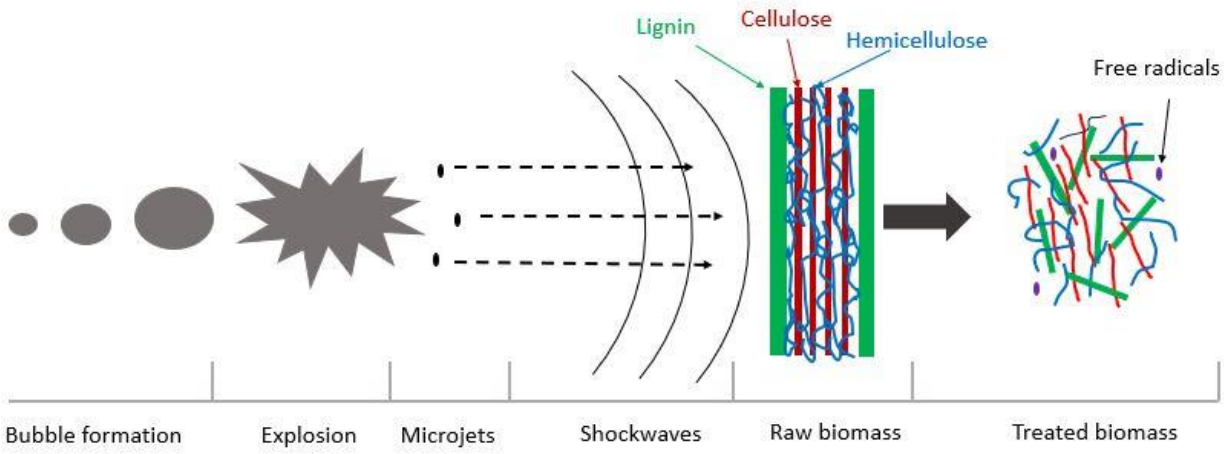

Figure 2.3: Schematic presentation of treatment of lignocellulosic biomass through hydrodynamic cavitation

Due to the increased temperature and pressure from cavitation, water molecules dissociate into OH• and H• as shown in eq. (1). During alkaline conditions, the conjunction of OH• radicals occur, forming H_2O_2 as shown in eq. (2). H_2O_2 then breaks down, yielding HOO• and H• shown in eq. (3). The produced HOO• reacts with any remaining water to produce O_2 and extremely reactive OH• which is shown in eq. (4) [49].

$$H_2O \xrightarrow{HC} H\bullet + OH\bullet \quad (1)$$

$$OH\bullet + OH\bullet \longleftrightarrow H_2O_2 \quad (2)$$

$$H_2O_2 \longleftrightarrow HOO\bullet + H\bullet \quad (3)$$

$$H_2O_2 + HOO\bullet \longleftrightarrow OH\bullet + O_2\bullet + H_2O \quad (4)$$

In an alkaline environment, the phenolic hydroxyl group in the lignin structure dissociates, resulting in the formation of a phenoxy radical that is stabilized through resonance. This intermediate chemical undergoes reactions with the resulting radicals such as HOO• and OH•, leading to the breakdown of lignin by processes including ring opening, side chain elimination, and demethoxylation. As a result of these reactions, carbon dioxide, organic acid, and various low molecular weight organic compounds are generated. In addition, they have the potential to undergo self-reactions, leading to the formation of condensed lignin [49],[50].

Hydrodynamic cavitation process produces two streams after the treatment of lignocellulosic biomass. Mainstream contains solid residue (cellulose rich solids), and the side stream contains the process water; the side stream carries the removed lignin, extractives, and a small fraction of hemicellulose and cellulose with water. Most of the studies for LCB focus on mainstream to produce cellulose rich solids by removing lignin for better enzymatic hydrolysis and maximum sugar production. On the contrary, side stream has the potential for producing valuable lignin derivatives with strong antioxidant properties through the treatment of lignocellulosic biomass (LCB) with HC process. For the first time, Lauberte et al. [46] demonstrated that the lignin-rich fraction obtained through the side stream of HC process followed by ultrasound/NaOH procedures for wheat straw can act as a repository of physiologically active flavonoid-lignin oligomers. The presence of biologically active compounds, including flavonoids, tricin, apigenin, and their derivatives, was confirmed through ultra-performance

liquid chromatography-tandem mass spectrometry analysis of the liquid fraction. Tricin and apigenin possess anti-inflammatory and anti-cancer properties, respectively. Given that the tricin-lignin complex constitutes approximately 30% to 35% of the liquid fraction, the waste lignin streams generated through the HC/ultrasound process may serve as a promising source for the further utilization of LCB.

Ter´an Hilares et al.[35] showed the pretreatment of sugarcane bagasse with HC removed 33.07% of lignin and 25.01% of hemicellulose at optimal conditions (3 bar, 70℃, 0.3M NaOH), where the enzymatic hydrolysis reached 93.05% and 94.45% for hemicellulose and cellulose, respectively by response surface methodology (RSM). Pretreatment through HC removes a small amount of cellulose and hemicellulose from the feed biomass with lignin. Nagarajan and Ranade's [51] research found that the Fourier transform infrared spectroscope (FT-IR) profiles of SCB samples treated with HC decreased in all three(cellulose, hemicellulose and lignin) fractions. Another study by Ter´an Hilares et al. [14] showed 48.31% lignin removal along with 19.81% hemicellulose and 9.20% cellulose, whereas solid recovery was 76.44% at the same condition (Inlet pressure 3 bar, 60℃, 20 min). Hilares et al. [48] employed hydrodynamic cavitation to enhance the efficiency of the alkaline pre-treatment of sugarcane bagasse. Under the specified conditions (0.48 M NaOH, 4.27% solid loading, and 44.48 min.), it was found that 60.4% of lignin removal, 52.1% of glucan content, and 97.2% enzymatic digestibility were achieved after 48 hours of hydrolysis. Those results suggest that HC is an efficient process for removing lignin from biomass slurry. Some other studies that focus on lignin removal by the HC process are presented in Table 2.1. Overall, the application of HC alone or in combination with conventional techniques such as alkalis and acids can achieve hemicellulose and lignin removal rates of 6.57% to 19.81% and 25% to 77.4%, respectively, in LCB [44]. However, there still needs to be a greater understanding of the mechanisms and kinetics of reaction happening for cellulose, hemicellulose, and cellulose in HC process.

In accordance with prior research, it has been determined that the factors of cavitation intensity, temperature, treatment duration, and feedstock characteristics are the most influential in the realm of HC process. The effect in cavitation intensity can be observed by changing pressure between inflow and outflow of the cavitation device. The concept was notably illustrated in a study by Ter'an Hilares et al. [35]. The researchers found that increasing the inflow pressure of an orifice from 1 to 3 bar led to higher removal rates of hemicellulose and lignin. Specifically, the removal rate of hemicellulose increased from 27.49% to 29.33%, and the removal rate of lignin increased from 9.23% to 19.23%. These changes occurred under the same temperature conditions (40°C) and NaOH concentration (0.2 mol/L). Nevertheless, it is crucial to acknowledge that overly augmenting pressure is unnecessary and undesirable. This occurs because once the point of choke cavitation is achieved, the cavitation's strength and flow velocity stay consistent, regardless of the input energy level.

The cavitation intensity generated by the HC reactor exhibits a steady rise as the temperature increases but begins to decline once it reaches the range of 50–70°C [44]. In their study, Baxi and Pandit [45] found a link between temperature and cavitation intensity of HC process for lignocellulosic biomass (LCB). They discovered that the HC (Venturi) treatment, when not cooled, can eliminate an additional 9.5% of acid-insoluble lignin content (17.05% w/w) from sawdust, in comparison to the cooled HC method (15.57% w/w). Ter´an Hilares et al. [35] provided more detailed information: under identical conditions (inlet pressure of the orifice: 1 bar, duration: 30 min, NaOH concentration: 0.2 mol/L),

raising the temperature from 40◦ to 70◦C increased the elimination rates of hemicellulose and lignin components in SCB from 27.49% to 34.09% and 9.23% to 27.64%, respectively.

When it comes to feedstock, a smaller loading is usually more advantageous in terms of efficacy because of the comparatively high rate of mass transfer and mixing effect. Kim et al. [39] demonstrated this using HC (orifice) technology. They found that decreasing the S/L ratio of reed from 10% to 5% resulted in a rise in lignin removal from 36.2% to 38.3% under the same conditions (NaOH concentration: 5%, duration: 40 min, pressure difference: 0.54 MPa). However, it is important to acknowledge that high-solids loadings have a significant advantage over low- and moderate-solids loadings. This advantage lies in their greater efficiency, cost-effectiveness, and environmental friendliness due to reduced water and energy consumption, including heating and cooling [52]. Due to the varying compositions of various types of LCB, it is necessary to carefully determine the optimal treatment procedure or condition for each individual case and subsequent process, in order to achieve the most effective results when utilizing HC-based treatments under the same conditions [44].

The potential of hydrodynamic cavitation has led to the exploration of various operating modes, including semi-continuous and continuous processes. These modes are appealing from an operational standpoint for biorefining series and other industrial applications, as they save time, energy, and operating costs compared to batch processes. In the semi-continuous and continuous processes, the biomass is treated only once, without recirculation in the reactor, ensuring greater productivity [53], [54].

Table 2.1: Several studies on hydrodynamic cavitation process

HC Process	Feedstock	Catalyst	Optimal Conditions	Findings	References
Venturi tube	Sugarcane bagasse	NaOH (4.9%)	Inlet pressure 6.89 bar, S/L ratio 2.03%, residence time 58.33 min, operating temperature 65℃	56.1% lignin removal at optimal conditions by RSM in terms of S/L ratio, NaOH concentration, and duration as the design variables	[55]
Orifice plate	Sugarcane bagasse	NaOH (0.48 M)	Inlet pressure 3 bar, S/L ratio 4.27%, residence time 44.48 min, operating temperature 64℃	60.4% of lignin removal with 52.1% of glucan content and 97.2% of cellulose by hydrolysis in 48 h.	[48]
Orifice Plate	Sugarcane bagasse	NaOH (0.3 M)	Inlet pressure 3 bar, residence time 30 min, operating temperature 70℃	41.83% lignin removal with 94.43% hydrolysis yield of hemicellulose and 93.05% of cellulose in 30 min of pretreatment.	[35]
Orifice Plate	Corncob	Laccase enzyme	Inlet pressure 0.5 bar, solid loading 5% w/v, residence time 60 min, operating temperature 30℃	47.4% lignin removal, energy consumption 1.35 MJ/kg of biomass	[47]
Vortex based cavitation	Sugarcane bagasse	NaOH (0.75 M)	Solid loading 1% w/v, residence time 60 min, operating temperature 30℃	77.4% lignin removal, 70.3% cellulose and 69.4% of hemicellulose conversion by hydrolysis	[56]
Rotational HCR	Wheat straw	NaOH (0.4 M)	S/L ratio 1:50, residence time 30 min, operating temperature 50℃, 3000 rpm	24.05% of lignin removal	[46]

2.5 Hydrothermal Separation Process and Its Effect on LCB

Hydrothermal separation, also known as liquid hot water extraction, is a process that involves the use of elevated temperatures (160–240 °C) and above saturated vapor pressure with liquid water as the sole solvent and catalyst [57]. In the initial step of the HTS process, water undergoes autoionization to create hydronium ions that cleave O-acetyl and uronic acid substitutions from hemicellulose [58]. Additionally, acetic and other organic acids are generated, which subsequently result in further hydronium ion production through autoionization. The hydronium ions originating from these organic acids are more significant in altering the physicochemical characteristics of biomass, particularly in depolymerizing hemicellulose [59]. Hemicellulose degradation occurs first at temperatures ranging from 160 to 200℃, while cellulose degradation occurs at temperatures between 200 and 230 ℃, and lignin degradation takes place between 220 and 260 ℃. Lignin is thought to remain relatively intact at lower temperatures but begins to degrade above 250 °C [60]. Treating biomass with HTS results in the production of both liquid and solid fractions. In the liquid stream, hemicellulose is primarily degraded, while cellulose and lignin are mainly preserved in the solid fraction [7].

The elevation of temperature during the pretreatment process with lignocellulosic biomass leads to an increase in the content of lignin degradation products in the liquid phase. A portion of these degradation products will recondense on the surface of the solid residue that has been treated with lignocellulosic biomass, forming droplets, spheres, or layers. This occurs when the pretreatment liquid cools down. The majority of lignin remains in the solid residues after the lignocellulosic biomass [24]. Several studies focus the hemicellulose and cellulose separation by HTS process, as shown in Table 2.2.

Lignocellulose undergoes significant changes in its microstructure following LHW pretreatment. Specifically, its surface morphology becomes more porous, its cell walls are altered, and its micropores are enlarged. Additionally, the crystallinity of lignocellulose is affected by pretreatment. Consequently, the surface morphology of the lignocellulose becomes less compact, and longitudinal cracks appear in the fascicular structure [7].

Table 2.2: Several studies showed the separation of hemicellulose and cellulose by using hydrothermal separation.

Feedstock	Conditions	Findings	References
Corn stover	Temperature 185℃, and residence time 40 min	82.4% of hemicellulose removal, and 11% of cellulose removal with 87% of enzymatic hydrolysis yield	[61]
Sugarcane straw	Temperature 195℃, and residence time 10 min	85.45% hemicellulose removal and 9.80% of cellulose removal	[62]
Sugarcane straw	Temperature 195℃, and residence time 15 min	85% of hemicellulose removal with 21% of cellulose removal	[63]

Chapter 3 Methods

3.1. Introduction

This chapter represents the overall working procedure of this study. The overall methodology is shown in Fig. 3.1.

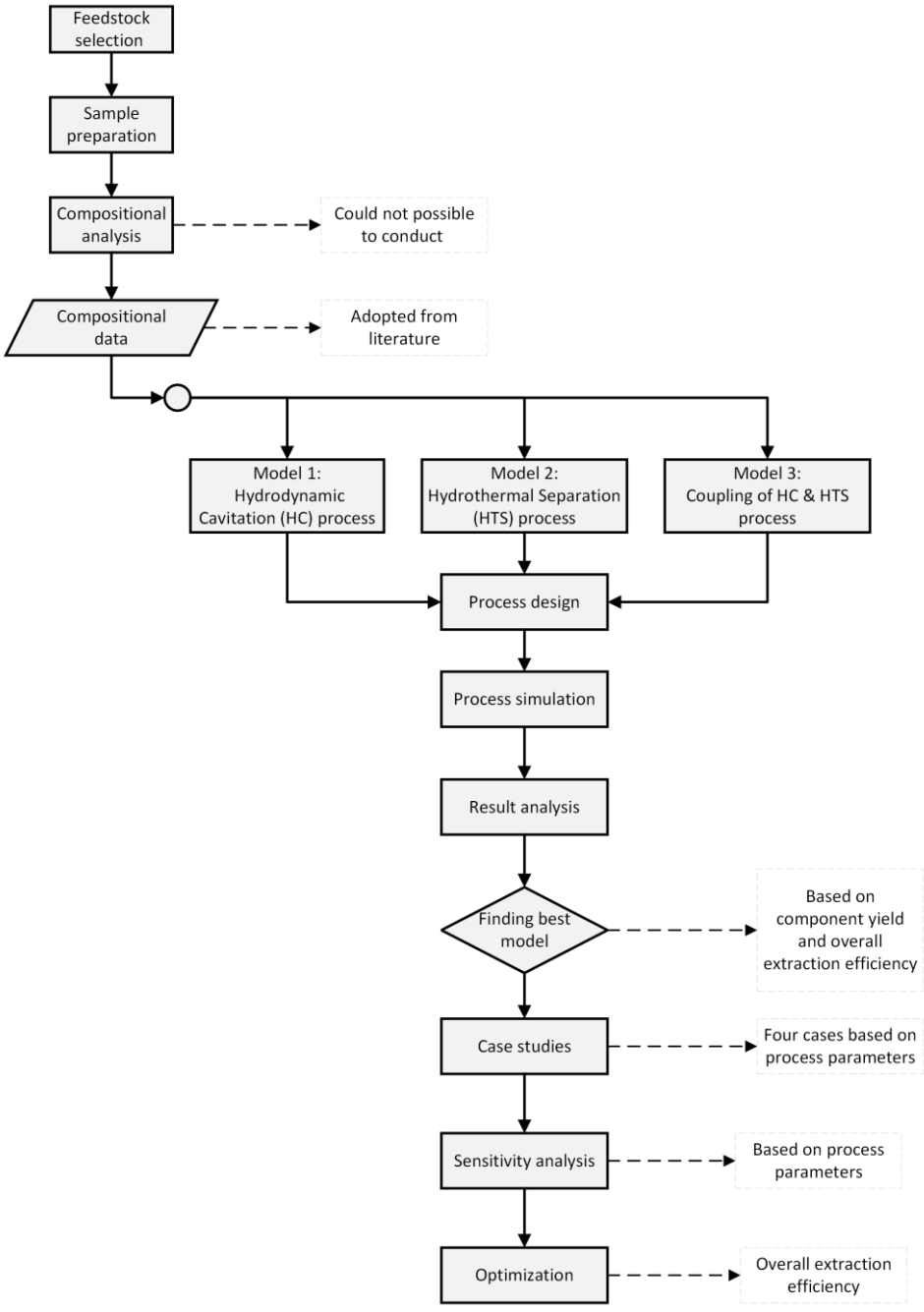

Figure 3.1: Flow diagram of methodology

3.2. Feedstocks Selection and Sample Preparation

Three lignocellulosic biomass feedstocks were selected in this work, of which two were agricultural residue biomass (wheat straw and corn stalk) and the third was woody biomass (woodchips). The Combustion Laboratory at the University of Agder provided all the raw biomass samples. After collection, samples were prepared for grinding by manually making them into smaller pieces, as shown in Fig. 3.2.

Figure 3.2: Prepared raw biomass samples for grinding: woodchips, corn stalks, and wheat straw, left to right, respectively.

Prepared raw samples were then ground in a hammer mill (Polymix® System PX-MFC 90 D**,** Kinematica AG, Malters, Switzerland) to obtain the fine particles. Polymix® System PX-MFC 90 D is a hammer grinding/laboratory mill that has a hammer grinding attachment, a funnel volume of 300 ml, sieves of 0.2 to 6 mm mesh size, and a speed range of 50–6000 rpm for a supply voltage of 100–230 V [73] have shown in Fig. 3.3. Operating conditions for this study was 3500 rpm and sieve size were 0.8 mm. Final products after grinding have shown in Fig. 3.4.

Figure 3.3: Polymix® System PX-MFC 90 D hammer mill.

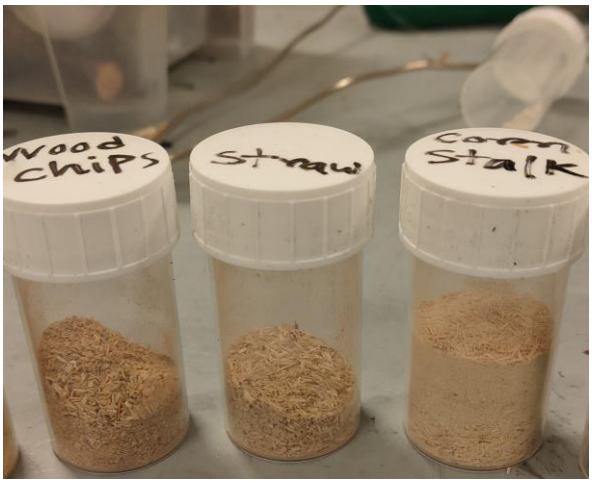

Figure 3.4: Raw samples after grinding in Polymix® System PX-MFC 90 D hammer mill. (Left to right, woodchips, wheat straw and corn stalk, respectively)

After grinding, the samples were dried in Termaks® TS4057. The Termaks® TS4057 oven is a laboratory oven designed for heat treatment processes and material drying. Key features are power of 730 W, voltage of 230V/50Hz, and a temperature range above 5°C of ambient temperature to 180 °C [74], shown in Fig.3.5. In this study, ground samples are dried for 24 hours at 105°C to remove moisture to make fully dry and prepared for compositional analysis.

Figure 3.5: Termaks TS4057 laboratory oven

3.3. Feedstocks Compositional Analysis

As described in the limitation section of this study, we intended to analyze the composition of raw biomass samples; unluckily, we could not conduct the compositional analysis experiment due to malfunctioning of the machines in the laboratory. We waited a few weeks to resolve the issue, but our time was limited.

As representative of the samples, we adopted the compositional analysis data (shown in Table 3.1) for wheat straw [64], corn stalk [4], and woodchips [65]. The compositional analysis of those studies showed that the amount of cellulose, hemicellulose, lignin, extractives, and ash varied based on the types of biomasses. Finally, the compositional data was imported into the simulation model to run the process.

Table 3.1: Biochemical composition of different feedstocks

Components	Sample 1 [64]	Sample 2 [4]	Sample 3 [65]
% (Dry mass)	Wheat Straw	Corn Stalk	Woodchips
Cellulose	36.42	42.7	41.2
Hemicellulose	26.11	23.2	26
Lignin	18.5	17.5	27.8
Extractives	7.62	9.8	1.9
Ash	11.35[a]	6.8	3.1[a]

a-By differences

3.4. Process Simulation

Aspen Plus is a commercial process simulation software developed by AspenTech that is used for the pharmaceutical, chemical, petrochemical, and process industries. The software frequently analyzes steady-state chemical processes involving solid, liquid, and gaseous streams under specified conditions by utilizing mass and energy balance equations and phase equilibrium databases. It employs an extensive built-in physical properties database and user-defined data in most of its computational thermochemical process simulations.

The software package Aspen Plus V.11 was utilized in this research endeavor. Initially, three distinct process flowsheets were conceptualized and modeled, named Model 1 (hydrodynamic cavitation), Model 2 (hydrothermal separation), and Model 3 (combination of hydrodynamic cavitation and hydrothermal separation). Model 1 and Model 2 were developed based on the mechanisms described in the literature, and Model 3 was an integration of Model 1 and Model 2. The compositional data for each sample (as shown in Table 3.1) was input into every model in order to evaluate the efficiency of component extraction for each model.

3.4.1. Component Specification and Property Method

In this study, we consider the lignocellulosic biomass was made up of cellulose, hemicellulose, lignin, extractives, and ash. And also consider the hydrolysis of cellulose yielded only gluco-oligomers and glucose, hydrolysis of hemicellulose consists of xylo-oligomers and xylose. The total sugar in this study means a sum of xylose and glucose. Due to the limitation of Aspen Plus, all the components excluding

cellulose were not found in the aspenONE databank. Therefore, we consider a representative for all components excluding cellulose. The representative components are shown in Appendices A.

The Aspen Plus property method is used to estimate the thermodynamic properties of any components, like enthalpy, entropy, viscosity, Gibbs free energy, thermal conductivity, and so on. This computer program has various property methods, including IDEAL, equation of state, activity coefficient methods, and unique system methods. A suitable thermodynamic property methodology is necessary to simulate a process accurately and provide reliable outcomes. Under specific process conditions, the physical property method helps to understand the behavior of the interpretation of components. The components and the simulation conditions are considered while selecting an appropriate property method.

This study uses the Soave-Redlich-Kwong (SRK) equation of state as a thermodynamic property method for all flowsheet models. Because of its simplicity and engineering flexibility, the SRK method became widely used and occupied numerous thermodynamic packages, including Aspen Plus. Furthermore, this method is highly recommended for high-pressure conditions [66]. The SRK equation of state is also applicable to non-polar or mildly polar mixtures, delivering reasonable outcomes at all temperatures and pressures within the critical region.

3.4.2 Assumptions

Following assumption are considered during this process simulation-

- Steady state process condition
- Separators were ideal.
- No pressure drop occurred throughout the process.
- The efficiency of the pump considered as 90%
- In the coupled process, extractives are considered to be extracted only after HC reactor with as extraction ratio of 45% based on literature [15].

3.4.2. Model 1: Hydrodynamic Cavitation (HC) process

As described in the theory section, a hydrodynamic cavitation reactor has a mechanical and chemical effect on lignocellulosic biomass due to the formation of cavities, bubble collapse, and shock waves during the cavitation process. The overall process is described in Fig. 3.6. The composition of each biomass sample was given as input in the BIOMASS stream. The BIOMASS and WATER streams mixed in the MIXER block and made the SLURRY-1 stream. The slurry was then pumped and heated through the PUMP and HEATER blocks, respectively, according to the process conditions shown in Table 3.2. As mentioned in the literature, the HC process's mechanism is poorly understood. Therefore, we consider the HC as a RYIELD reactor block (HCR block in Fig. 3.6). The yield distribution of the RYIELD block was considered from the study by Teran et al. [14] for the same process conditions (reactor temperature 60℃, pressure 3 bar and residence time 20 min) for cellulose, hemicellulose, and lignin. The yield distribution for extractives was considered as of 45% based on literature [15].

Furthermore, the separator block SEP-1 divided the SLURRY-4 stream into two process streams; the S-RESIDU stream contains the solid residue of treated biomass, whereas the P-WATER stream contains the removed lignin, extractives, and a small fraction of hemicellulose and cellulose. The amount of lignin and extractives from the process water was separated after the S-SEP block and DIST-COL block,

respectively. On the other hand, fractional cellulose and hemicellulose content was observed in WAST-H2O stream.

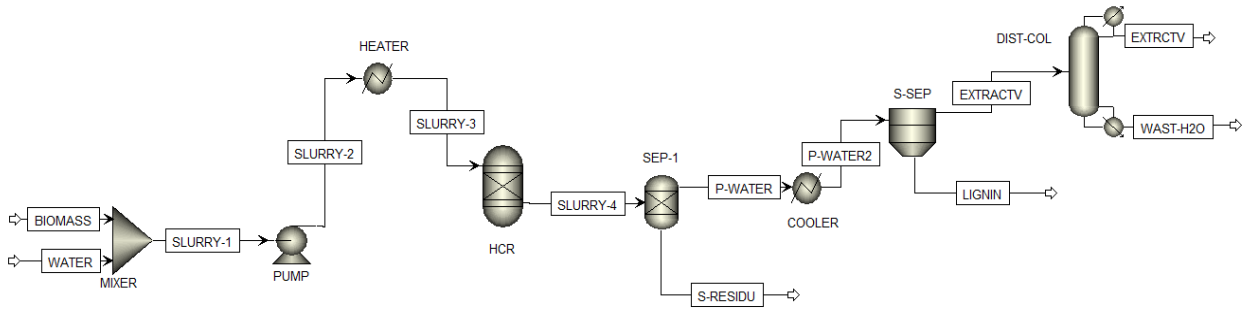

Figure 3.6: Process flowsheet of hydrodynamic cavitation (HC) process

Table 3.2: Process conditions used for hydrodynamic cavitation.

Aspen Plus block name	Model block name	Process conditions
Pump	PUMP	3 bar
Heater	HEATER	60℃ and 3 bar
RYIELD raector	HCR	60℃ and 3 bar

3.4.3. Model 2: Hydrothermal Separation (HTS) Process

Hydrothermal separation or hydrothermal extraction process use liquid hot water with high temperature and pressure. Overall process flowsheet is presented in the Fig. 3.7. In HTS, water at elevated temperature and pressure condition make auto-ionization effect which results in the hydrolysis of hemicellulose and cellulose and produced corresponding monomer and oligomer. On the other hand, lignin also made a partial depolymerization, but the range of temperature used in HTS process are not favourable for lignin solubilization in water, which results condensation of lignin at the same time.

By increasing the temperature, hydrolysis of cellulose and hemicellulose increased, which results more hydrolysate yield. For hydrothermal separation, we consider the hydrothermal separation reactor as a Continuous Stirred Tank (CSTR) reaction with known kinetics parameters shown in Table 3.3. We consider that, hydrolysis of cellulose produce gluco-oligomer and glucose and hemicellulose produced xylo-oligomer and xylose, respectively. The reaction was considered as first order Arrhenius type (eq. (3.1)) kinetic reaction.

$$\ln k = -\frac{Ea}{RT} + lnA \qquad (3.1)$$

Table 3.3: Reaction considered in hydrothermal separation process with Arrhenius parameters [63]

Reactions	**ln(A)**	**E_a, kJ/mol**
Cellulose + H_2O —> Gluco-oligomers	49.67	216.44
Gluco-oligomers —> Glucose	25.32	105.60
Hemicellulose + H_2O —> Xylo-oligomers	25.75	109.49
Xylo-oligomers —> Xylose	53.66	220.23

The overall HTS process is described in Fig. 3.7. The composition of each biomass sample was given as input in the BIOMASS stream. The BIOMASS and WATER streams mixed in the MIXER block and made the SLURRY-1 stream. The slurry was then pumped and heated through the PUMP and HEATER blocks, respectively. The CSTR (HSTR) reactor block was used as HTS reactor, which perform the reaction according to the kinetic parameters and reaction shown in Table 3.3. The hydrolysate and untreated solid made the SLURRY-4 stream, from which solid residues was separated after S-SEP block. The process water after S-SEP block contains the hydrolysate products of cellulose and hemicellulose which was then separated by SEPARTOR and SEP block respectively.

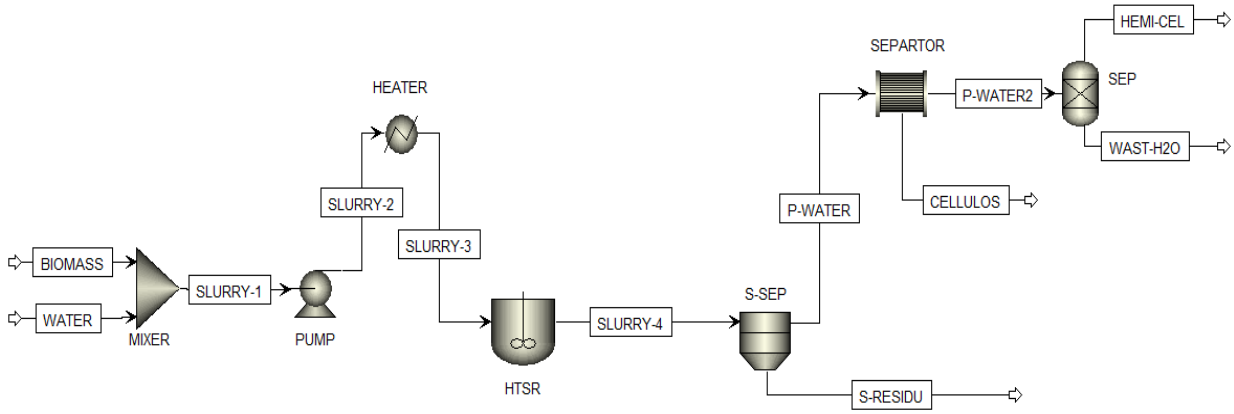

Figure 3.7: Process flowsheet of hydrothermal separation (HTS) process (Model 2)

3.4.4. Model 3: Coupling of HC & HTS Process

Fig. 3.8 represents the coupling of hydrodynamic cavitation and hydrothermal separation process. The composition of each biomass sample was given as input in the BIOMASS stream of HC section. The BIOMASS and WATER streams mixed in the MIXER block and made the SLURRY-1 stream. The slurry was then pumped and heated through the PUMP and HEATER blocks, respectively. The HC reactor (HCR block) was considered as RYIELD, and the yield distribution of the RYIELD block was considered from the study by Teran et al. [14] for the same process conditions (reactor temperature 60℃, pressure 3 bar and residence time 20 min). Furthermore, the separator block SEP-1 divided the SLURRY-4 stream into two process streams; the S-RESIDU stream contains the solid residue of treated biomass and went as input of HTS process, whereas the P-WATER stream contains the removed lignin, extractives, and a small fraction of hemicellulose and cellulose. Since, our goal was to separate lignin and extractives from the process water of HC process, the S-SEP block and DIST-COL block separated the lignin and extractives respectively. And the fractional content of cellulose and hemicellulose was considered as waste which went with WAST-H2O stream.

The untreated solid residues from S-RESIDU stream of HC process then mixed with water and made SLURRY-5 stream, which was pumped and heated up in PUMP-2 and HEATER-2 block, respectively. The Aspen Plus CSTR reactor block was considered as HTS reactor (HTSR block in flowsheet). The reactions with Arrhenius kinetic parameters were as shown in Table 3.3. The hydrolysate from HTSR block made the SLURRY-8 stream and remaining solid residue was separated in S-SEP-2 block. Finally, cellulose,

hemicellulose, and wastewater were separated from the P-WATER4 stream by SEPARTOR and SEP-2 block, respectively.

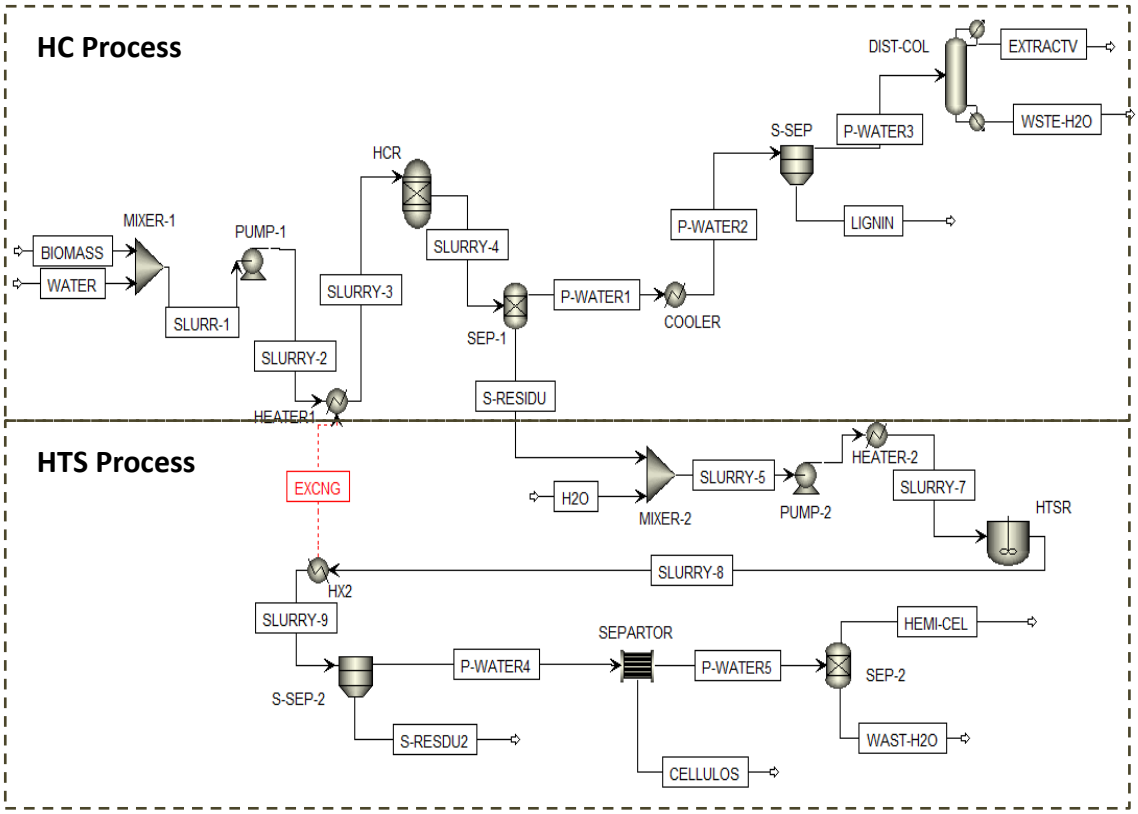

Figure 3.8: Process flowsheet of coupling of HC & HTS Process (Model 3)

3.5. Process Analysis

3.5.1. Case Studies

A total of four cases was studied for Model 3 (coupling of HC and HTS process) to understand how the model behave under different process conditions. In the coupled process, various parameters may affect components yield and overall extraction efficiency, such as the feedstock solid-liquid ratio (S/L ratio), HC inlet pressure, HC reactor temperature, HC residence time, HTS reactor temperature, HTS reactor pressure, and HTS residence time. However, it was not feasible to investigate the impact of all the process parameters in a single study. Additionally, as mentioned in the theory chapter, the mechanism of the HC process was poorly understood. Therefore, we studied the influence of S/L ratio, HTS reactor temperature, HTS pressure, and HTS residence time on components yield and overall extraction efficiency, and remaining process parameters (HC reactor temperature of 60℃, inlet pressure 3 bar and residence time 20 min) were identical throughout the study.

Four cases were studied with different process parameters, whereas Case 1 was for S/L ratio 10%, HTS temperature 190℃, HTS pressure 15 bar, and HTS residence time 10 min. Case 2 was for an S/L ratio of 10%, HTS temperature 205℃, HTS pressure 20 bar, and HTS residence time of 10 min; Case 3 was for an S/L ratio of 15%, HTS temperature 190℃, HTS pressure 15 bar and HTS residence time 20 min and Case 4 stand for S/L ratio 15%, HTS temperature 205℃, HTS pressure 20 bar and HTS residence time 20 min.

3.5.2. Sensitivity Analysis

A sensitivity analysis was performed to understand how individual process parameters affect the extraction ratio and overall extraction efficiency of the coupled process (Model 3). Sometimes, it may be useful to see how the results vary with input changes, either because they are uncertain or represent a range of applications. In the Aspen Plus sensitivity analysis tool, performing "what if" studies by varying one or more flowsheet variables are possible. As mentioned in the previous section, various parameters can affect the performance of Model 3. Here, we performed the analysis by considering the parameters, including S/L ratio, HTS temperature, HTS pressure, and HTS residence time, while the parameters for the HC process (HC reactor temperature of 60 °C, inlet pressure of 3 bar, and residence time of 20 min) remained unchanged. However, the analysis encompassed six HTS reactor temperatures (180, 185, 190, 195, 205, and 210 °C), two S/L values (10% and 15%), six HTS residence times (1, 5, 10, 15, 20, and 25 min), and two HTS pressures (15 bar and 20 bar).

3.5.3. Optimization

Response surface methodology (RSM) was used to optimize the overall extraction efficiency aiming to maximize the efficiency. Four independent variables including, HTS temperature, HTS residence time, HTS pressure and S/L ratio was considered to run the simulation of coupled process (Model 3) by the Aspen Plus simulation and further statistical approach. The range of process conditions was considered as follows: HTS temperature of 180 to 210℃, HTS residence time of 5 to 25 min, HTS pressure of 15 to 20 bar and S/L ratio of 10 to 15%. A total of 31 simulation runs of four variables were designed by Central Composite Design (CCD) using the Minitab 21.4.2 statistical software.

3.6 Formulas for Calculations

The following mathematical formulas was used for calculation of component extraction ratio and overall extraction efficiency.

The component extraction ratio is the ratio of component yield, kg (per hour) to the amount of same components in feed biomass, kg (per hour) in 100%, shown as eq. (3.2).

The overall extraction efficiency is the ratio of difference between amount of feed biomass and untreated biomass to the amount of feed biomass in 100%, shown as eq. (3.3).

$$\text{Component extraction ratio } (\%) = \frac{\text{Component yield, kg (per hour)}}{\text{Amount of same component in feed biomass,kg (per hour)}} \times 100\% \quad (3.2)$$

$$\text{Overall extraction efficiency}(\%) = \frac{\text{Amount of feed biomass} - \text{amount of untreated biomass}}{\text{Amount of feed biomass}} \times 100\% \quad (3.3)$$

Chapter 4 Results and Discussions

4.1. Introduction

This chapter contains the results and discussion of this study. Firstly, the simulated results for three individual models are presented. Then, for the best model (based on component yield and overall extraction efficiency), process analysis is carried out through case studies, followed by sensitivity analysis and process optimization.

4.2. Model Analysis

This section evaluates the outcomes of three simulation models based on component yield and the overall extraction efficiency according to the prescribed process conditions. In the whole study, cellulose consists of gluco-oligomers and glucose, hemicellulose consists of xylo-oligomer and xylose, and total sugar means the sum of glucose and xylose. The results of Model 1, which uses a hydrodynamic cavitation process, are depicted in Fig. 4.1. The same process conditions, including a S/L ratio of 10%, mass flow rate of 1000 kg/h (biomass 100 kg/h and water 900 kg/h), HC reactor temperature 60℃, inlet pressure 3 bar and residence time 20 min were applied to the simulation of all three feed samples, namely wheat straw (sample 1), corn stalk (sample 2), and woodchips (sample 3), as shown in Fig. 4.1.

The results showed that the lignin yield for woodchips and corn stalks was 13.43 kg/h and 8.45 kg/h, respectively. The highest hemicellulose yield was observed for wheat straw at 5.17 kg/h, followed by woodchips and corn stalks. Additionally, the cellulose yield was approximately similar for all three feed samples. However, corn stalks had a higher yield of extractives at 4.41 kg/h, while woodchips had a lower yield. Furthermore, wheat straw yielded the highest of untreated solid, followed by corn stalk and woodchips, which indicates that wheat straw underwent less degradation in the HC process compared to woodchips, and corn stalk.

All samples showed an overall extraction efficiency between 20.89% and 23.23% by the hydrodynamic cavitation process, as depicted in Fig. 4.4. A non-rotating hydrodynamic cavitation process (such as a Venturi tube or orifice) has an overall extraction efficiency of 7.7 to 40% [44]. This result is also supported by Raut-Jadhav et al., who found that HC alone had an overall extraction efficiency of 26% [67]. Another study obtained a efficiency of 21.89% using HC alone [68]. However, the minimum yield of lignin (8.45 kg/h) was also higher than the yield of any other component. This suggests that lignin separation is more favorable in the hydrodynamic cavitation process, which has been the focus of several studies [48], [14]. In contrast, the lower yield of hemicellulose and cellulose indicated that these two-component separations were unfavorable in the HC process. This may be due to the mechanical effect of the HC process and the complex structure of the LCB. The high-energy shock wave generated by the HC process directly strikes the plant's outer cell wall, where the outer shell is densely packed with lignin, resulting in higher lignin yield.

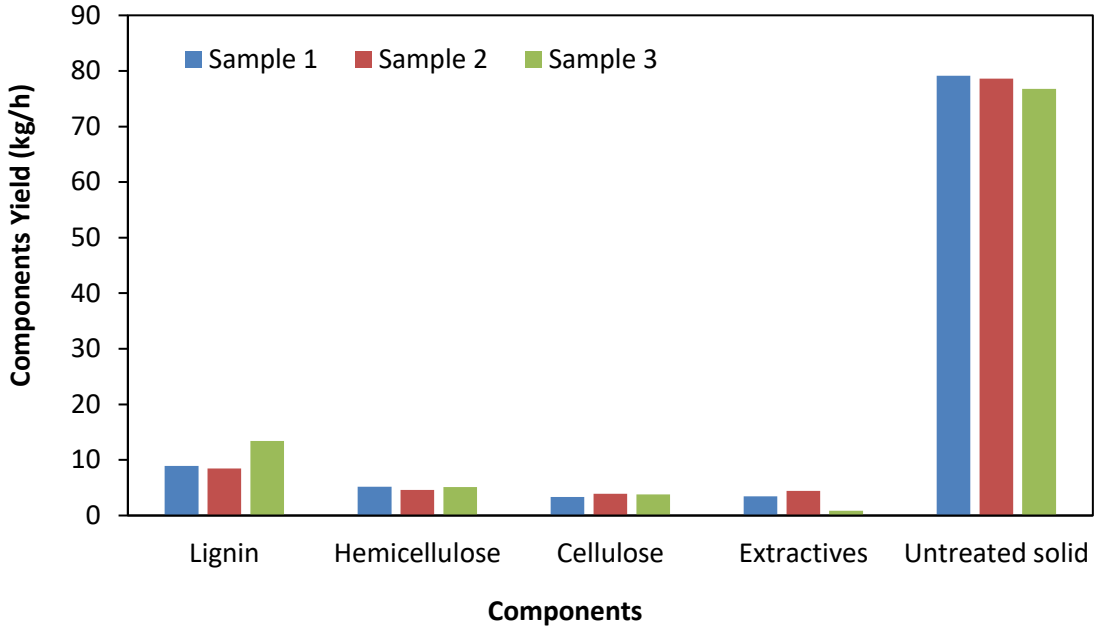

Figure 4.1: Components yield for different feedstock for Model 1.

Fig. 4.2 presents the component yield by Model 2 (hydrothermal separation process) for the three feed samples. Samples 1, 2, and 3 represented wheat straw, corn stalk, and woodchips, respectively. All the samples were subjected to the same process conditions, including a S/L ratio of 10%, mass flow rate of 1000 kg/h (biomass 100 kg/h and water 900 kg/h), HTS reactor pressure of 20 bar, temperature of 190 °C, and residence time of 15 min. As stated previously, the hydrothermal separation process mainly focused on the removal of hemicellulose with a partial fraction of cellulose, and the removal of lignin is not favorable [62]; we considered only hemicellulose and cellulose yield during the hydrothermal separation process.

The results demonstrated (Fig. 4.2) that wheat straw yielded the maximum of hemicellulose (21.17 kg/h), and woodchips had an approximately similar amount, whereas corn stalk yielded only 17.18 kg/h. For these yield the extraction ratio of hemicellulose for wheat straw, corn stalk, and woodchips were 81.1, 72.2, and 81.1%, respectively, based on their feed composition. W. Zhou et al. reported that at 190 °C, the hemicellulose extraction ratio by hydrothermal separation was 83.6% [61]. In the case of cellulose yield, woodchips showed the highest yield (9.46 kg/h), followed by wheat straw and corn stalk. Simultaneously, cellulose extraction ratio was 23%, 16.6%, and 22.9% for wheat straw, corn stalk, and woodchips, respectively. A study by M. S. R. dos Santos Rocha et al. [63] reported that 21% hemicellulose was removed from sugarcane straw by hydrothermal separation at 195℃ for 15 min. Another study reported only 12.2% cellulose extraction at 190 °C for corn stover [61]. The results indicated that the extraction ratio of cellulose and hemicellulose may vary based on the type of feedstock used and the process conditions, such as temperature and residence time. On the other hand, the yield of untreated solid was highest for corn stalk, followed by wheat straw and woodchips. This means that woodchips underwent higher degradation during the hydrothermal separation process than wheat straw and corn stalk.

The yield of hemicellulose was higher than that of the other components in the hydrothermal process, indicating that hemicellulose was more favorable to separate by the HTS process, which has also been the focus of some studies [61], [62]. This may be because of the autohydrolysis of water in the HTS

process. At elevated pressure and temperature condition, water produces hydronium ions, which act as a catalyst to break down O-acetyl and uronic acid substitutions in hemicellulose. Which results in the generation of more hydronium ions from the acids. The hydronium ions derived from these organic acids have a greater impact than those derived from water on modifying the physicochemical characteristics of biomass, particularly depolymerized hemicellulose [24].

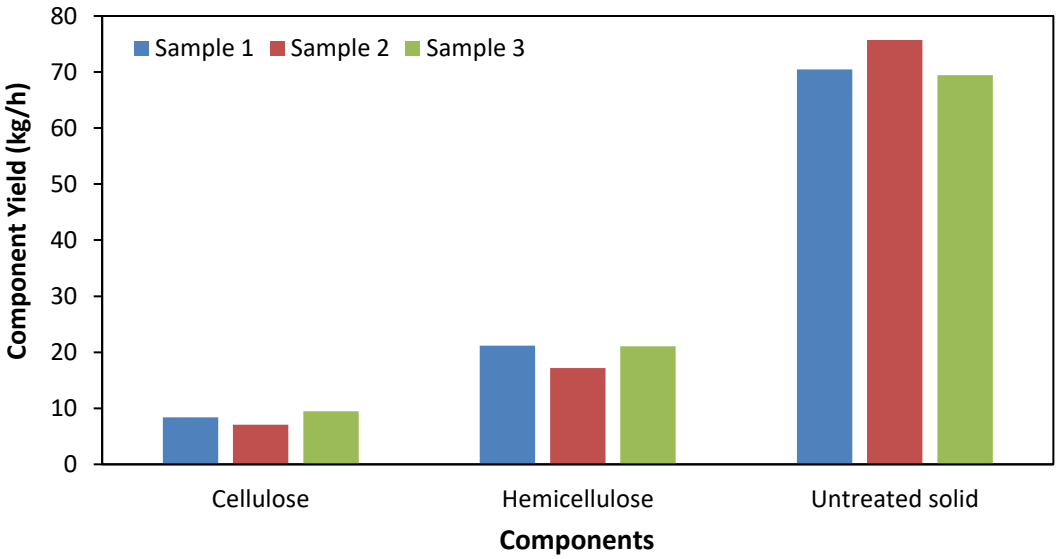

Figure 4.2: Components yield for different feedstock for Model 2.

The components yielded by the coupling process of hydrodynamic cavitation and hydrothermal separation (Model 3) for all three feed samples are shown in Fig. 4.3. As Model 3 involved a combined process, the process conditions for the hydrodynamic cavitation section were identical to those in Model 1, and for the hydrothermal separation section were identical to those of Model 2.

The results showed (in Fig. 4.3) for cellulose yield that, corn stalk (sample 2) had the highest yield (8.90 kg/h), followed by woodchips (sample 3) and wheat straw (sample 1). The extraction ratio of cellulose was 20.85%, 20.86%, and 20.87% for corn stalk, woodchips, and wheat straw, respectively, in order to the composition of each feedstock. Compared with Models 1 and 3, the cellulose yield was almost 127% higher in Model 3 (Fig.4.3) than in Model 1 (Fig. 4.1) for all samples. On the other hand, the cellulose yield between Model 2 and Model 3 showed that Model 3 had 9.2%, 20%, and 10% lower yield of cellulose for wheat straw, corn stalk, and woodchips, respectively. This may happen because the coupled process did not consider the fractional cellulose and hemicellulose yield in process water after the HC reactor (see Fig.3.8), which resulted in a reduced cellulose and hemicellulose content in the stream to the HTS reactor.

For hemicellulose yield in Model 3, wheat straw and woodchips showed an approximately similar yield of 16.9 kg/h, whereas corn stalk yielded 15.1 kg/h. Model 3 showed a higher hemicellulose yield than Model 1 and, at the same time, a lower yield than Model 2. Furthermore, Model 3 showed the same yield for lignin and extractives for all the samples as Model 1 because the HC reactor of both models were performed with the same process conditions.

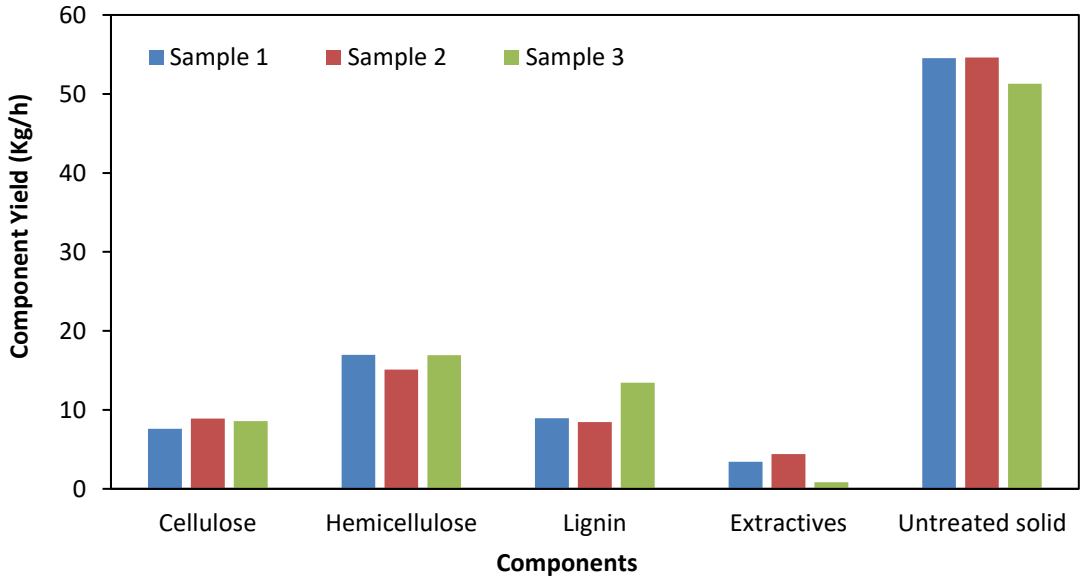

Figure 4.3: Components yield for different feedstock for Model 3

The overall extraction efficiencies of the three models have shown in Fig. 4.4. Model 1 achieved an overall extraction efficiency of 20.89% to 23.23%, Model 2 achieved 24.26% to 30.54%, and Model 3 achieved 45.47% to 48.73%. Wheat straw (sample 1) exhibited an overall extraction efficiency of 20.89%, 29.55%, and 45.47% for Model 1, Model 2, and Model 3, respectively. Additionally, corn stalk displayed an overall extraction efficiency of 21.39%, 24.26%, and 45.37% for Model 1, Model 2, and Model 3, respectively. In each of the models, woodchips showed the highest overall extraction efficiency of 23.23%, 30.54%, and 48.73% for Model 1, Model 2, and Model 3, respectively.

However, Model 3 demonstrated the highest overall extraction efficiency for all the samples when compared to Model 1 and Model 2, indicating that the coupling of the HC and HTS process (Model 3) was more effective in separating components than the individual processes of hydrodynamic cavitation (Model 1) and hydrothermal separation process (Model 2). Woodchips displayed the maximum overall extraction efficiency (48.73%) in Model 3, while wheat straw and corn stalk showed similar overall extraction efficiency (45.4%). This suggests that woody biomass (woodchips) degraded more in the coupled process than agricultural residual biomass (corn stalk and wheat straw). This may be attributed to the biomass composition of the feedstock, as woody biomass contains higher contents of cellulose, hemicellulose, and lignin, and lower ash content compared to agricultural residual biomass [69]. In Model 3, the corn stalk exhibited an overall extraction efficiency similar to wheat straw. In Model 2, the corn stalk displayed the lowest overall extraction efficiency among the three samples, and in Model 1, the overall extraction efficiency of the corn stalk was between the values of wheat straw and the woodchips. This indicated that the overall extraction efficiency can vary in different treatment processes for the same feedstock.

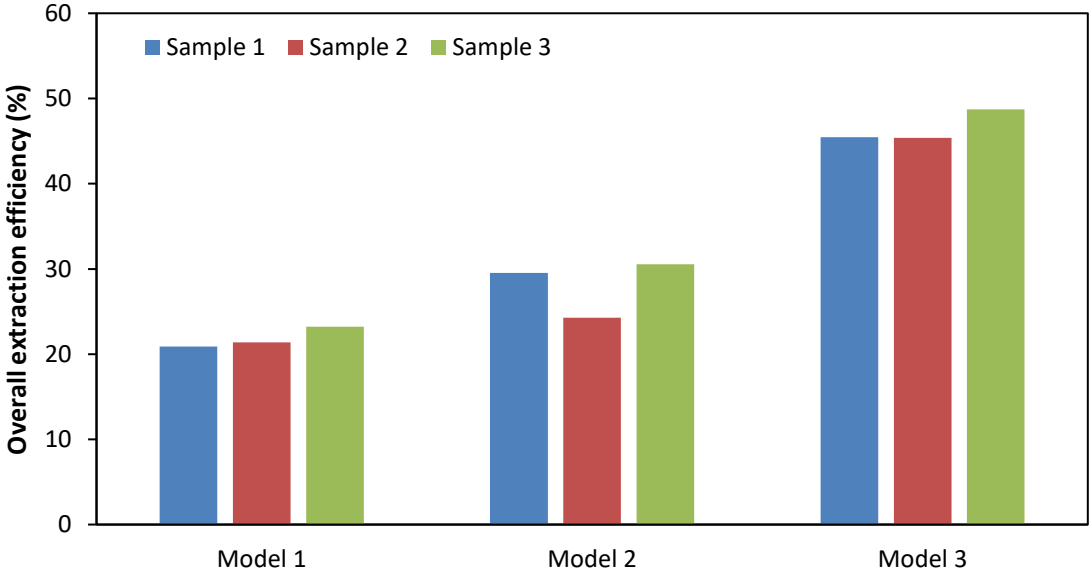

Figure 4.4: Comparison of overall solid degradation in different Model for different feedstock

Finally, it can be concluded that the coupling of the HC and HTS processes (Model 3) can be used for the better utilization of biomass with a higher overall extraction efficiency than that of the individual processes (Models 1 and 2). It can extract valuable components such as extractives and biopolymers from the lignocellulosic matrix to produce raw materials for biochemicals, biofuels, and biomaterials.

4.3. Case Studies

This section presents case studies for Model 3 (coupling of HC and HTS process) to understand how the model behave under different process conditions.

Four cases were studied with different process parameters, whereas Case 1 was for S/L ratio 10%, HTS temperature 190℃, HTS pressure 15 bar, and HTS residence time 10 min. Case 2 was for an S/L ratio of 10%, HTS temperature 205℃, HTS pressure 20 bar, and HTS residence time of 10 min; Case 3 was for an S/L ratio of 15%, HTS temperature 190℃, HTS pressure 15 bar and HTS residence time 20 min and Case 4 stand for S/L ratio 15%, HTS temperature 205℃, HTS pressure 20 bar and HTS residence time 20 min.

Figs. 4.5 to 4.9 showed the yield of different components and overall extraction efficiency for Case 1, 2, 3 and 4. For case 1, Fig. 4.5 showed that cellulose yield was higher for corn stalk (sample 1) of 6.43 kg/h, followed by woodchips (sample 3) and wheat straw (sample 1). In case of hemicellulose, wheat straw and woodchips showed approximately same yield (15.5 kg/h), at the same time corn stalk yielded the lowest amount. For total sugar yield, woodchips showed the highest, 17.75 kg/h, compared to the other two. For lignin, woodchips also showed the highest yield (13.43 kg/h) followed by wheat straw and corn stalk. Furthermore, extractives yield was highest (4.41 kg/h) in corn stalk with the lowest (0.86 kg/h) in woodchips.

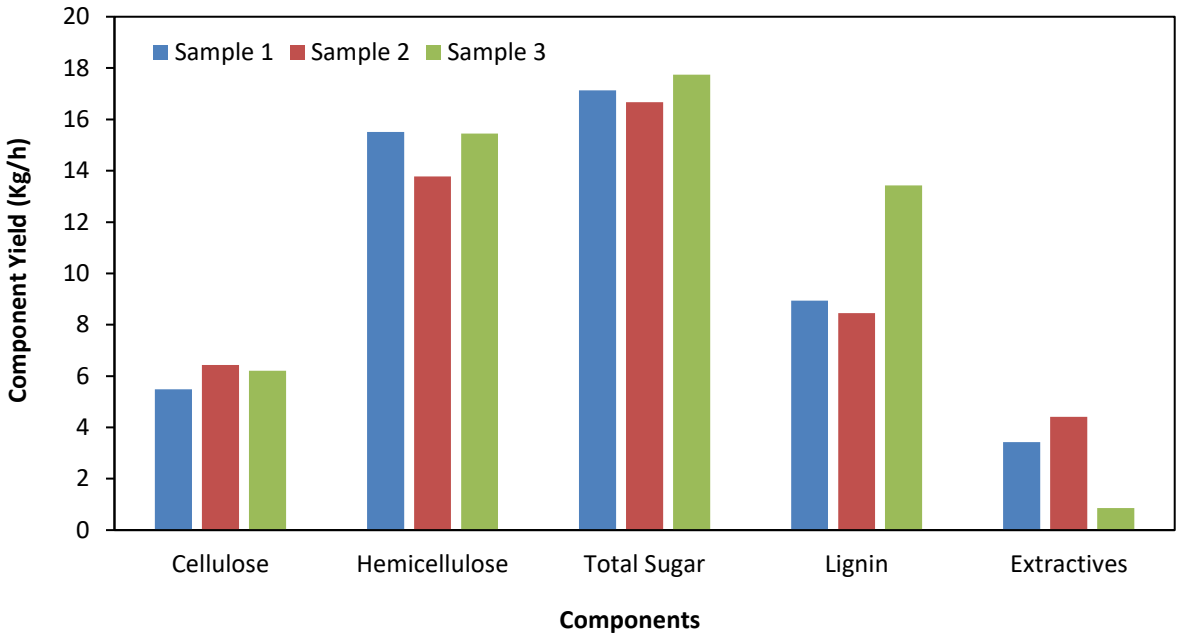

Figure 4.5: Yield of different components by the coupled process for Case 1 (S/L ratio 10%, HTS temperature 190 ℃, HTS pressure 15 bar, and HTS residence time 10 min)

Fig. 4.6 showed the components yield for Case 2. In case 2, it had the same S/L ratio and HTS residence time as Case 1, whereas temperature was higher (205℃) and the pressure of HTS also higher (20 bar) than Case 1. The change in temperature and pressure showed that all the components except lignin and extractives underwent a higher yield for all the samples in Case 2 than Case 1. Comparing Figs. 4.5 and 4.6 showed that, cellulose yielded more than two times (229%) higher than in Case 1, whereas hemicellulose underwent about 20% higher, and total sugar yield was approximately twice in Case 2 than case 1. Furthermore, Fig. 4.9 showed that overall extraction efficiencies for all three samples were higher in Case 2. These results indicated that HTS pressure and temperature, together, influenced the cellulose, hemicellulose, total sugar yield, and overall extraction efficiency when residence time and S/L ratio were fixed. Same trend was observed for cellulose and hemicellulose yield at same residence time by this study [61]. In contrast, since lignin and extractives were separated from the process stream after the HC reactor, HTS pressure and temperature did not show any effect on lignin and extractive yield (by comparing Figs.4.5 and 4.6).

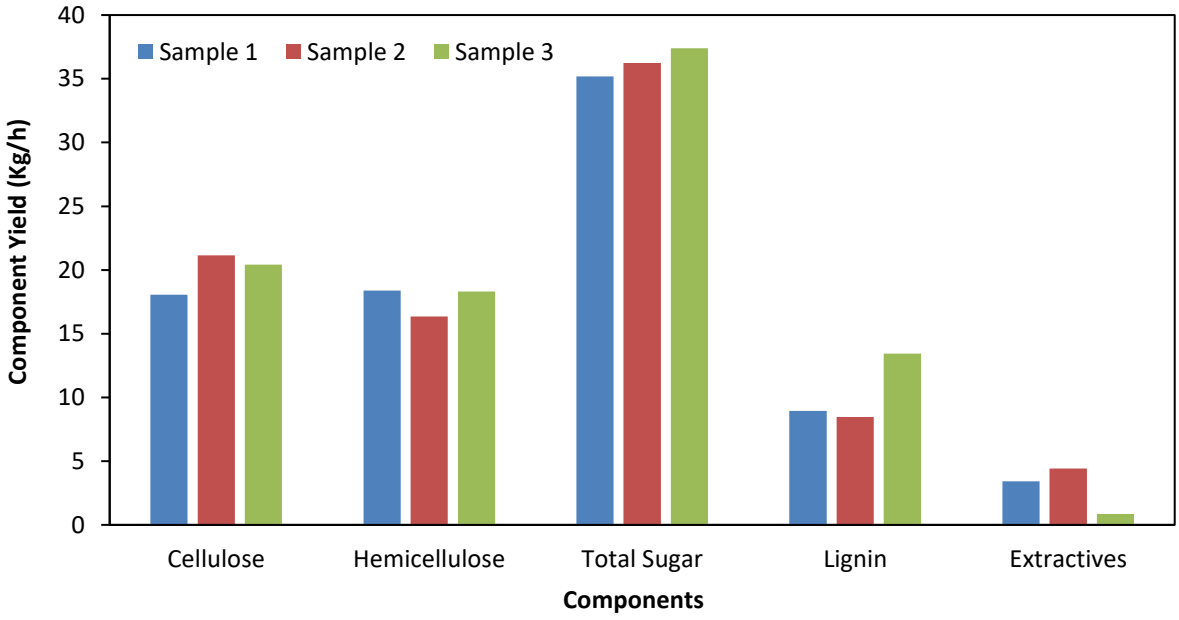

Figure 4.6: Yield of different components by the coupled process for Case 2 (S/L ratio of 10%, HTS temperature 205℃, HTS pressure 20 bar, and HTS residence time 10 min)

Fig. 4.7 shows the component yield for Case 3, whereas HTS temperature and pressure were the same as in Case 1 but there was a change in HTS residence time (20 min) and S/L ratio (15%). Results showed that the components yield (including lignin and extractives) were higher in case 3 for all the samples than Case 1. In Fig. 4.9, the overall extraction efficiency was also higher (approximately 6.5%) for all samples in Case 3 than Case 1. These results indicated that the S/L ratio and HTS residence time had effects on component yield and overall extraction efficiency. However, it was not clear how individual process parameters (S/L ratio or HTS residence time) affect the components' yield and overall extraction efficiency. On the other hand, Fig. 4.9 showed that, overall extraction efficiency was lower (approximately 10.5%) in Case 3 than Case 2 for all the feed samples. Though the S/L ratio and HTS residence time were higher in Case 3 than in Case 2, because of having the lower HTS temperature and residence time, overall extraction efficiency was lower. This indicated that HTS temperature and pressure, together, may have more effect than residence time and S/L ratio on component yield and overall extraction efficiency.

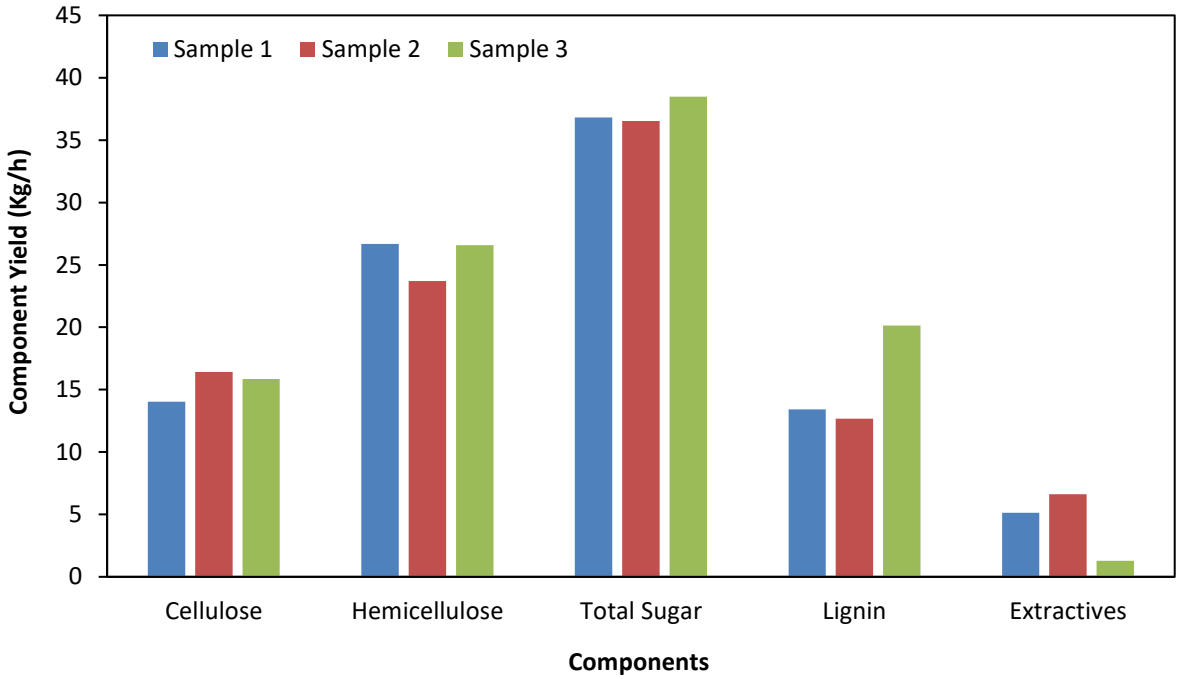

Figure 4.7: Yield of different components by the coupled process for Case 3 (S/L ratio of 15%, HTS temperature 190 ℃, HTS pressure 15 bar and HTS residence time 20 min)

Fig. 4.8 showed the components yield for case 4, whereas S/L ratio, HTS was identical to those in Case 3, but HTS pressure (20 bar) and temperature (205℃) was higher than Case 3. Comparing to Case 1, all the process parameters was higher in Case 4.

However, the results showed that (by comparing Figs. 4.7 and 4.8), the yields of cellulose, hemicellulose, and total sugar were higher in Case 4 than in Case 3, whereas lignin and extractives remained the same as in Case 3. As shown in Fig. 4.9, the overall extraction efficiency was approximately 16% higher in Case 4 than in Case 3. These results indicated that, at a certain S/L ratio and HTS residence time, increasing the HTS temperature and pressure results in higher component yield and overall extraction efficiency.

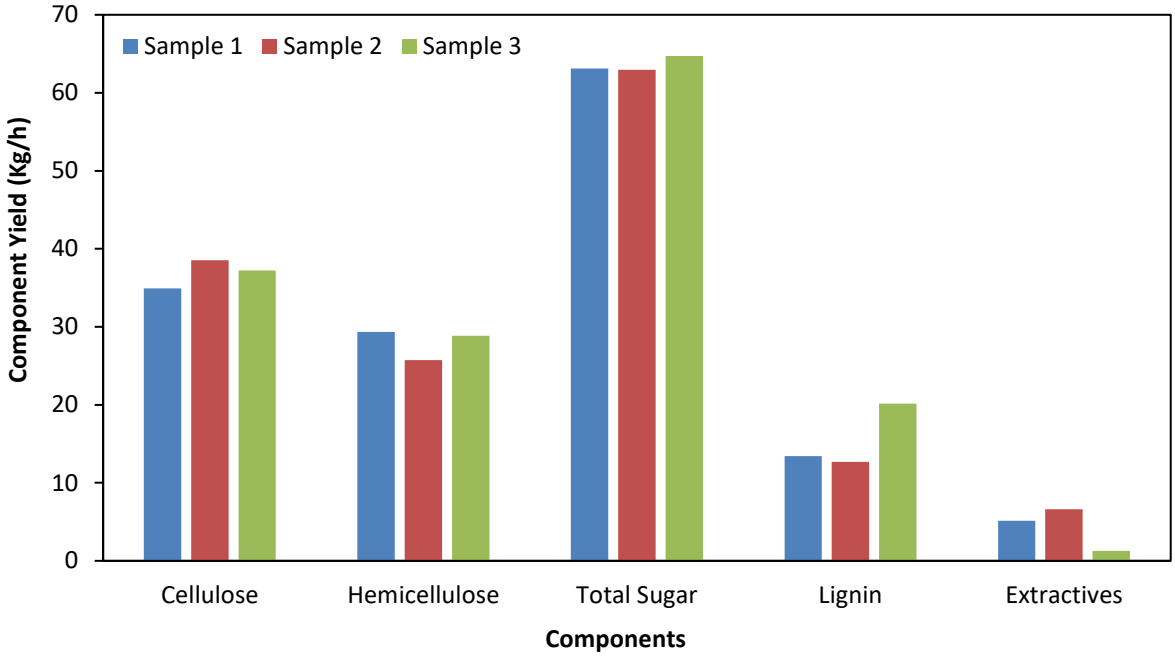

Figure 4.8: Yield of different components by the coupled process for Case 4 (S/L ratio 15%, HTS temperature 205℃, HTS pressure 20 bar and HTS residence time 20 min)

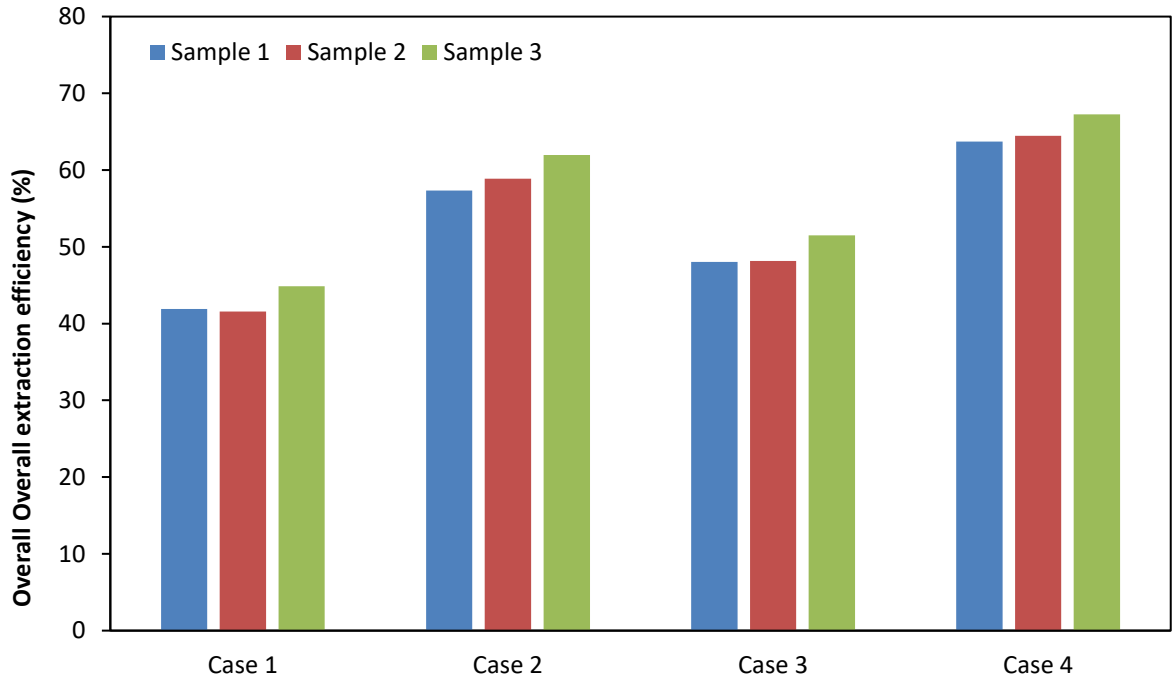

Figure 4.9: Comparison of overall extraction efficiency for different cases

4.4. Sensitivity Analysis

This section performed a sensitivity analysis to understand how individual process parameters affect the extraction ratio and overall extraction efficiency of the coupled process (Model 3). Sometimes, it may be useful to see how the results vary with input changes, either because they are uncertain or represent a range of applications. In the Aspen Plus sensitivity analysis tool, performing "what if" studies by varying one or more flowsheet variables are possible. As mentioned in the previous section, various parameters can affect the performance of Model 3. Here, we performed the analysis by considering the parameters, including S/L ratio, HTS temperature, HTS pressure, and HTS residence time, while the parameters for the HC process (HC reactor temperature of 60 °C, inlet pressure of 3 bar, and residence time of 20 min) remained unchanged. However, the analysis encompassed six HTS reactor temperatures (180, 185, 190, 195, 205, and 210 °C), two S/L values (10% and 15%), six HTS residence times (1, 5, 10, 15, 20, and 25 min), and two HTS pressures (15 bar and 20 bar).

4.4.1. Effects of HTS Temperature

Fig. 4.10 showed the effect of HTS temperature on components extraction ratio and formation of oligomers and sugar monomers for wheat straw (sample 1). Temperature was changed in a certain interval with holding S/L of 15%, HTS pressure of 20bar, and HTS residence time of 15 min.

Fig 4.10 (A) shows that the cellulose and hemicellulose extraction ratio increased with increasing HTS temperature. The extraction ratio of cellulose increased from 55.33% at 180 °C to 75% at 210 °C. Additionally, the cellulose extraction ratio increased from 7.03% at 180 °C to 68.9% at 210 °C. The results showed that the cellulose extraction ratio was lower up to 195 °C. Above 200 °C, the extraction ratio of cellulose increased; this indicates that cellulose depolymerized more at high temperatures, which is likely associated with the structure of cellulose [9]. On the other hand, the ratio of hemicellulose extraction was higher even at lower temperatures (180 °C), which can be attributed to its lower activation energy [63], and a lower degree of polymerization [11]. Furthermore, the extraction ratio of lignin and extractives was constant over the temperature range, indicating that the HTS temperature did not affect lignin and extractive yield throughout the coupled process (Model 3).

As mentioned earlier, cellulose consists of glucose-oligomer and glucose; hemicellulose consists of xylo-oligomer and xylose; total sugar means the sum of glucose and xylose. The yield of the monomers, oligomers, and sugars has been shown in Fig. 4.10 (B). Results showed that the yield of monomeric sugars (glucose and xylose) increased with increasing HTS temperature. For oligomers, xylo-oligomers showed a higher yield at lower temperatures; increasing the temperature reduces the yield of oligomers. Only 9.5% xylo-oligomers were yielded at 205℃ as compared to 180℃. A study by Q. Yu et al. observed that at 200 °C, no oligomers were detected, and oligomers were hydrolyzed into monomeric sugar at a rising temperature [70], which also caused an increase in the yield of total sugar.

The effect of HTS temperature on components extraction ratio and monomer and oligomers formation of corn stalk (sample 2) and woodchips (sample 3) also follow the same trend as wheat straw which has shown in Appendices B.

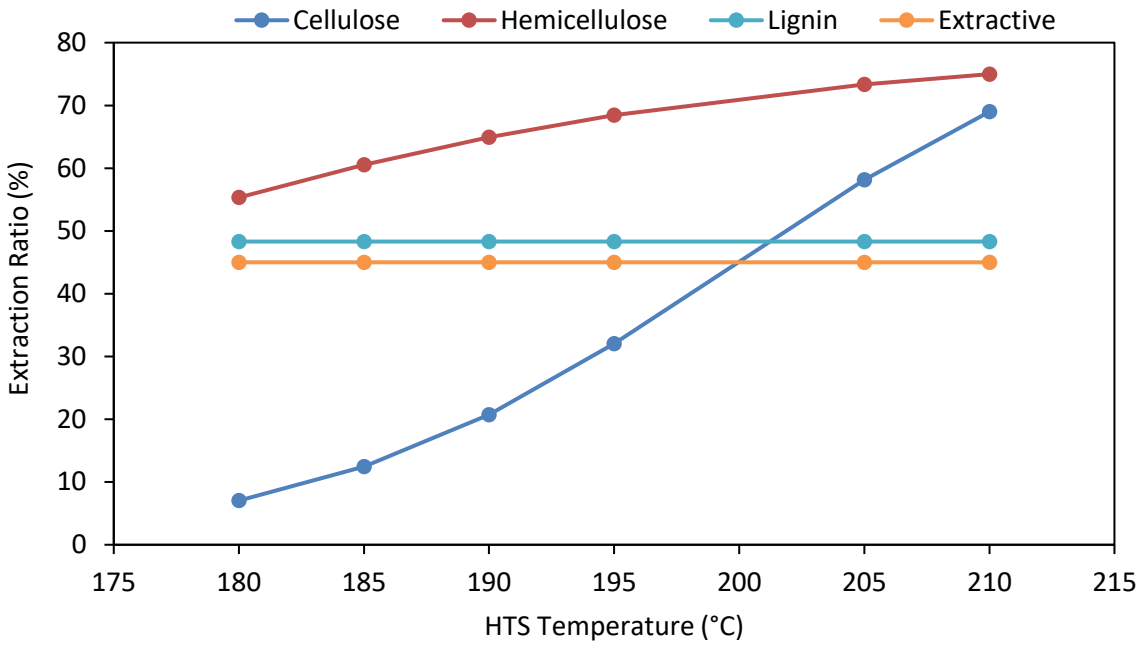

(A)

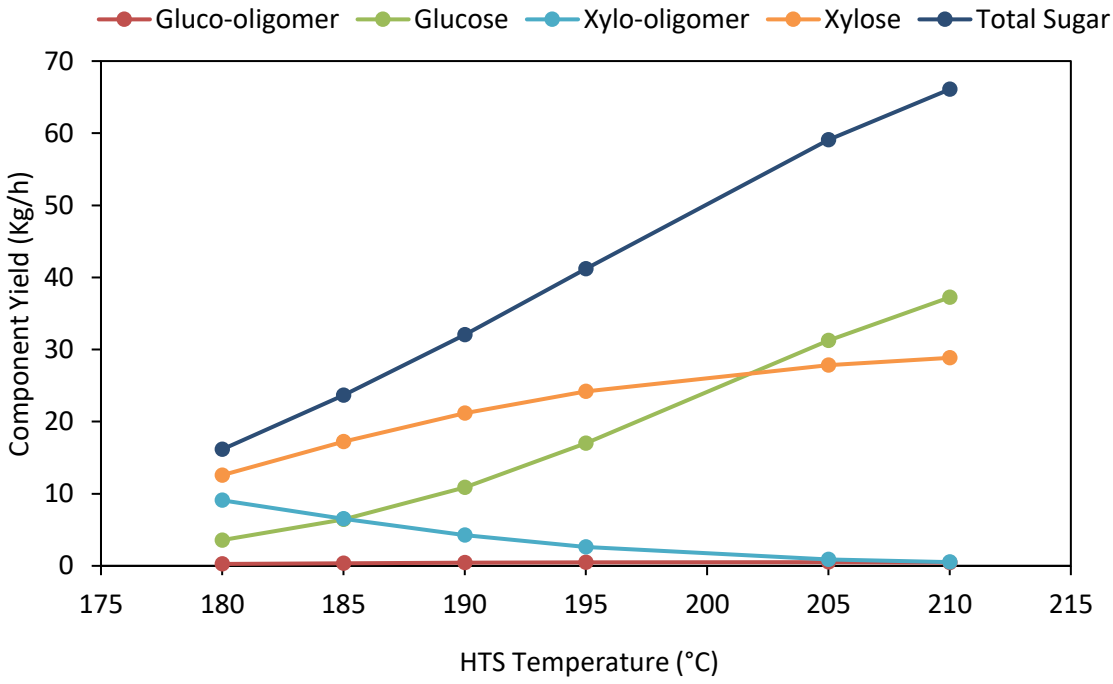

(B)

Figure 4.10: (A) Component extraction ratio and (B) Monomers and oligomers formation with HTS temperature for wheat straw (Sample 1)

Fig. 4.11 showed the change in overall extraction efficiency with HTS temperature for all three feed samples. Results showed that, overall extraction efficiency increased with increasing HTS temperature for all samples. Whereas wheat straw (sample 1) and corn stalk (sample 2) had similar increment of overall efficiency from approximately 38% at 180℃ to 68% at 210℃. On the other hand, woodchips showed a higher overall efficiency than other two, from 40.5% at 180℃ to 71.1% at 210℃. These

results indicated that component yield increased with increasing temperature [61] and that the increment in overall extraction efficiency is associated with the biomass feedstocks' composition and structure.

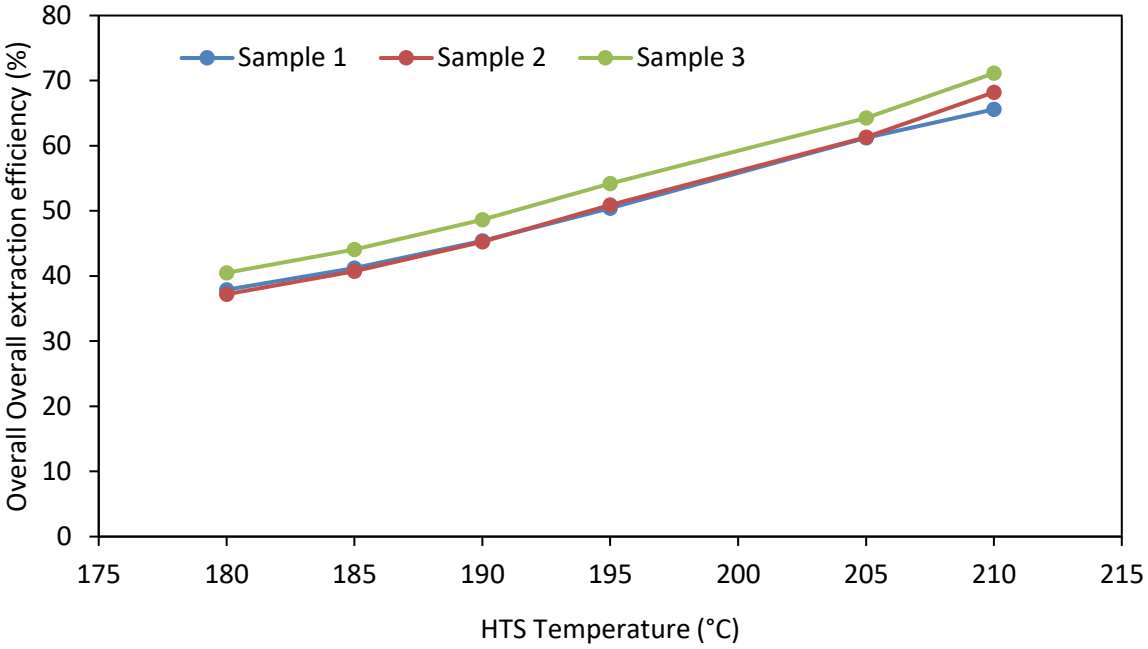

Figure 4.11: Change in overall extraction efficiency with HTS temperature for wheat straw (sample 1), corn stalk (sample 2) and woodchips (sample 3)

4.4.2. Effects of HTS Pressure

Fig. 4.12 showed the effect of HTS pressure on component extraction ratio and the formation of oligomers and sugar monomers for wheat straw (sample 1). The pressure was changed twice (15 and 20 bar) with holding a S/L ratio of 15%, HTS temperature of 190 ℃, and HTS residence time of 15 min.

Fig. 4.12 (A) shows the component's extraction ratio with HTS pressure variation. At 15 bar pressure, the extraction ratio of cellulose, hemicellulose, lignin, and extractives were 20.73%, 64.93%, 48.31%, and 45%, respectively. For 20 bar, results showed that the extraction ratio of all the components was approximately the same as for 15 bar. In Fig. 4.12 (B), the monomer and oligomer formations were also approximately the same for 15 and 20 bar. The overall extraction efficiency for wheat straw (sample 1), corn stalk (sample 2), and woodchips (sample 3) also showed approximately the same, as shown in Fig. 4.13. These results indicated that the pressure change did not affect much the hydrolysis of products and components yield. However, this study only considers two pressure values with smaller differences; to understand the effect of pressure, one needs to consider a wide range of pressure values.

The effect of HTS pressure on components extraction ratio and monomer and oligomer formation of corn stalk (sample 2) and woodchips (sample 3) also follow the same trend as wheat straw, which is shown in Appendices B.

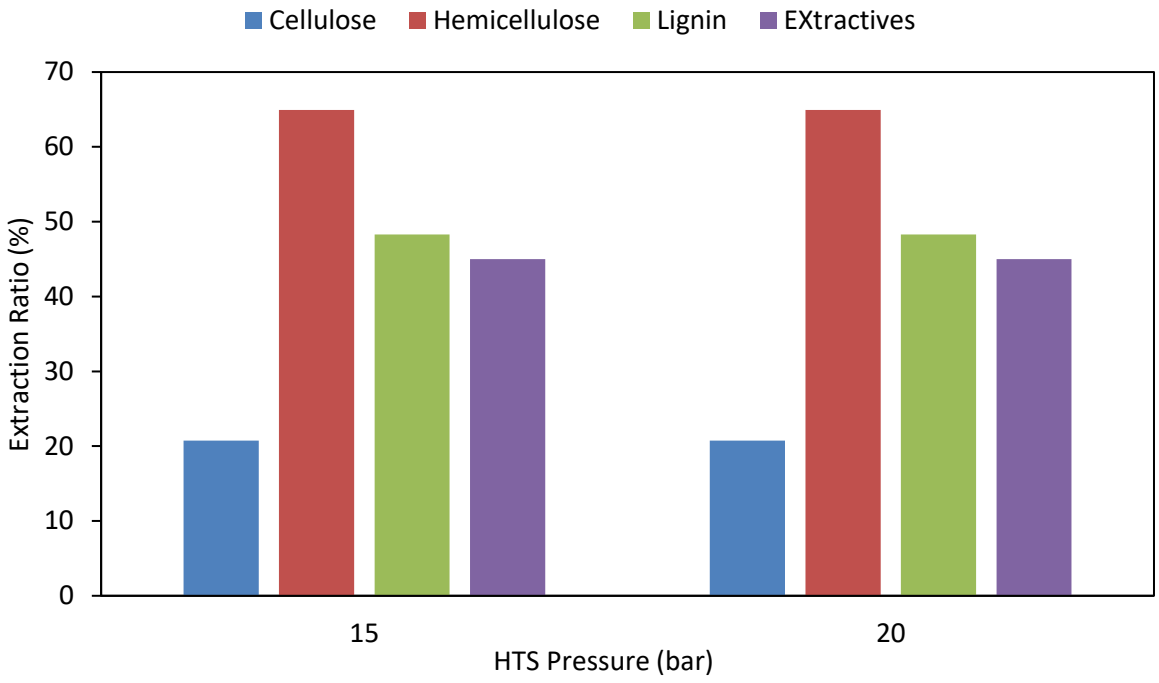

(A)

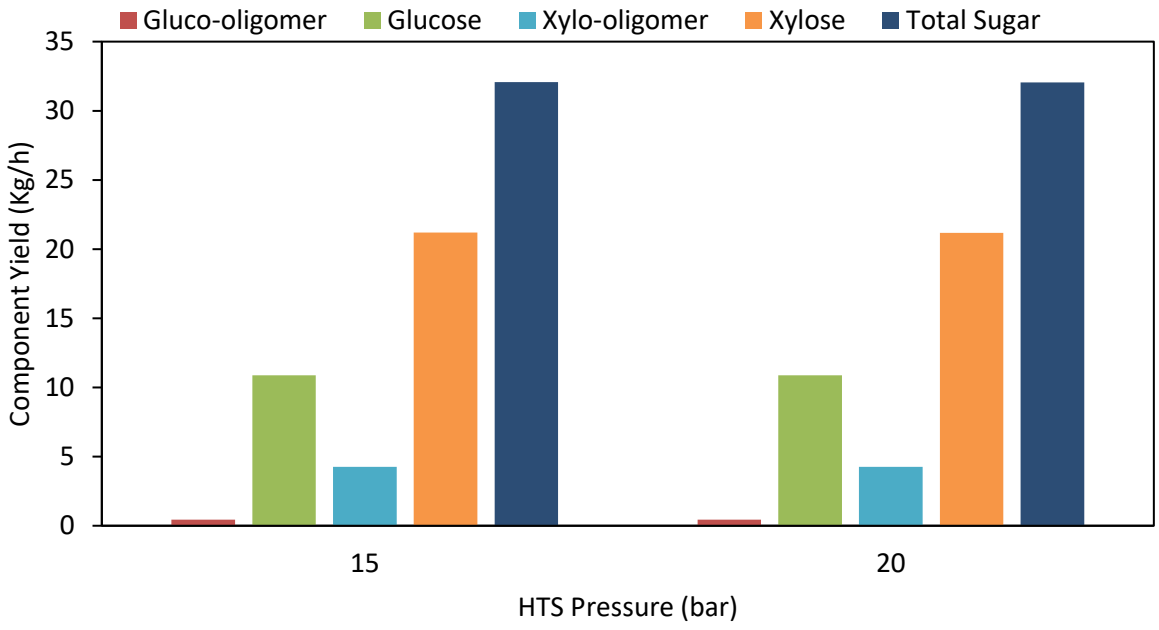

(B)

Figure 4.12: (A) Component extraction ratio and (B) Monomers and oligomers formation with HTS pressure for wheat straw (Sample 1)

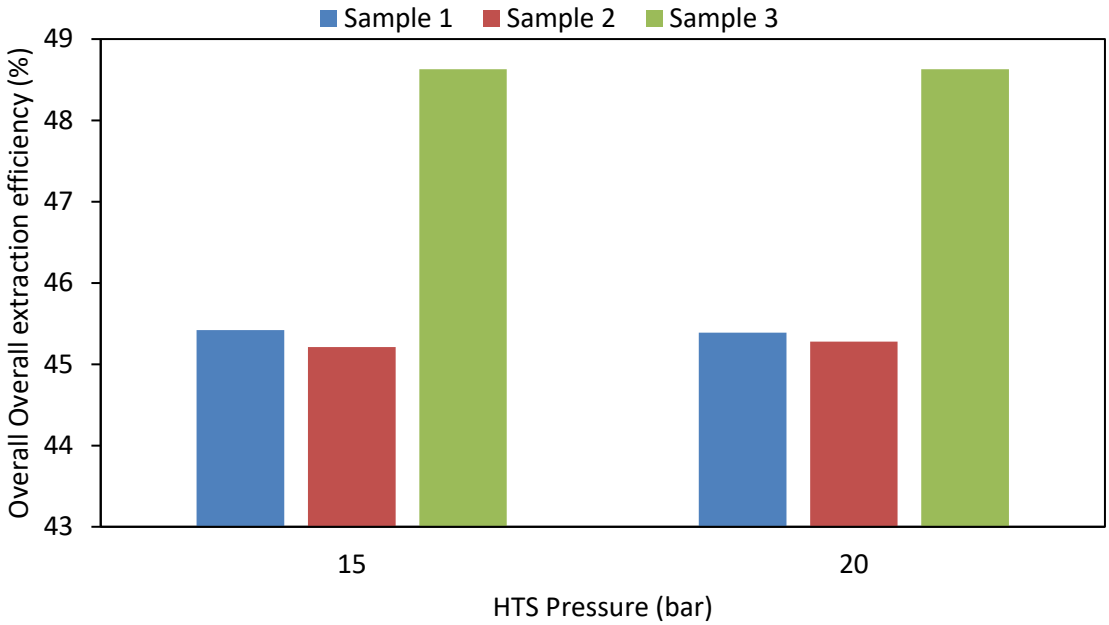

Figure 4.13: Change in overall extraction efficiency with HTS pressure for wheat straw (sample 1), corn stalk (sample 2) and woodchips (sample 3)

4.4.3. Effects of HTS Residence Time

Fig. 4.14 showed the effect of HTS residence time on components extraction ratio and formation of oligomers and sugar monomers for wheat straw (sample 1). Where, Temperature was changed in a certain interval with holding S/L of 15%, HTS temperature of 190 ℃, and HTS pressure of 20 bar.

Fig. 4.14 (A) showed that the extraction ratio of cellulose and hemicellulose increased with the HTS residence time. The hemicellulose extraction ratio was changed from 17.7% to 70.3%, and the maximum was at 25 min. In addition, cellulose gradually increased with temperature and reached its maximum at 25 minutes. This indicated that, at a certain condition, hydrolysates of cellulose and hemicellulose increased with higher residence time [71]. On the other hand, the rate of lignin and extractives extraction ratio remains unchanged over time, suggesting that these two were not affected by HTS time.

Furthermore, the formation of monomeric sugar and oligomers is shown in Fig. 4.14 (B). Results showed that the yield of monomeric sugars was increased with HTS residence time. This indicated that more residence time provide better hydrolysis and higher sugar yield [72]. On the other hand, it was observed that xylo-oligomer formation was higher at lower residence time and decreased with longer residence time. This suggests that lower residence time reduces the amount of total hydrolysate and sugar yield.

The effect of HTS residence time on components extraction ratio and monomer and oligomer formation of corn stalks (sample 2) and woodchips (sample 3) also follow the same trend as wheat straw, which is shown in Appendices B.

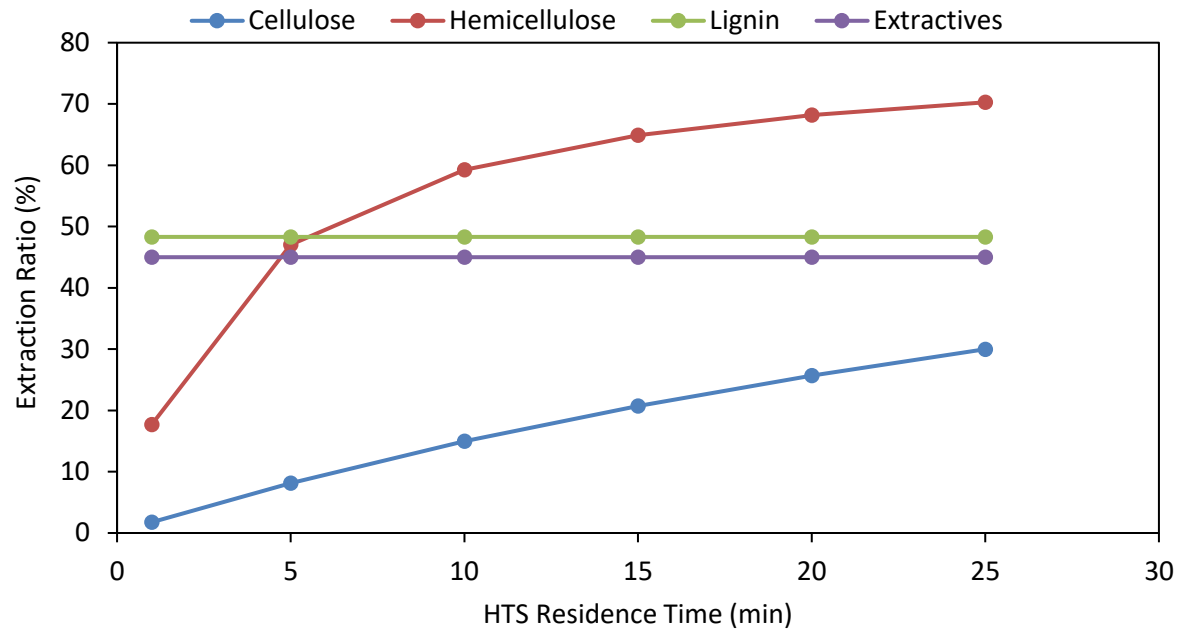

(A)

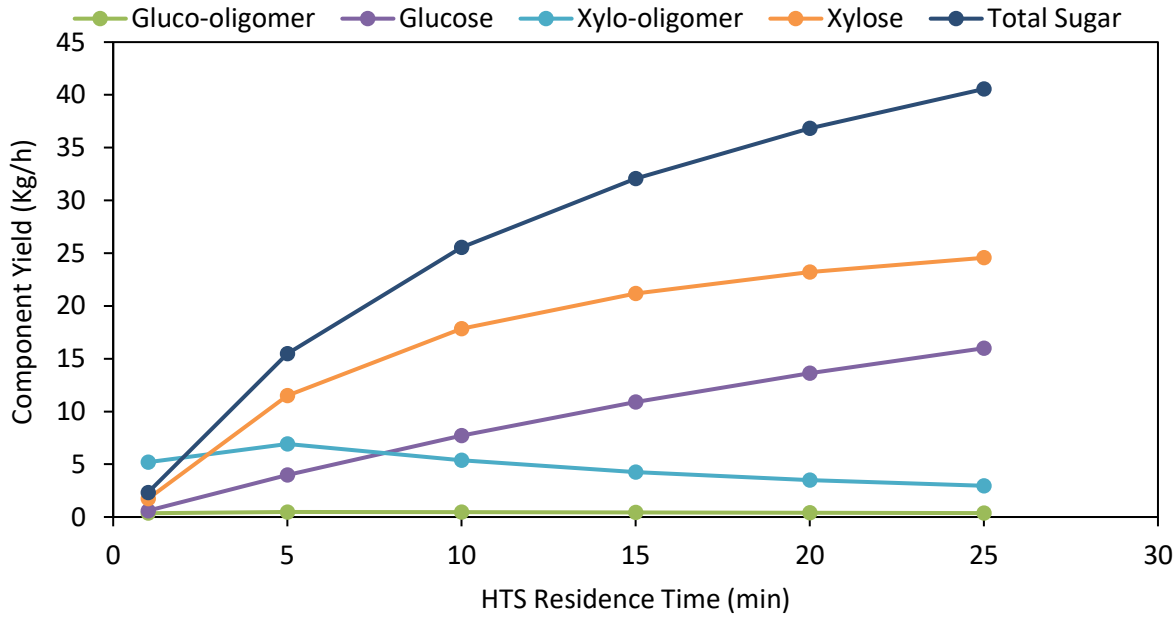

(B)

Figure 4.14: (A) Component extraction ratio and (B) Monomers and oligomers formation with HTS residence time for wheat straw (Sample 1)

Fig. 4.15 depicts the overall extraction efficiency with HTS residence time for all three samples. Results showed that overall extraction efficiency was gradually increased with HTS residence time for all the feedstocks. At the same time, corn stalk (sample 1) and woodchips (sample 2) showed approximately similar extraction between 26 to 50% over time. In addition, woodchips showed an efficiency between 28 to 53%. These suggested that overall extraction efficiency can be influenced by residence time, biomass composition and type of biomass.

.

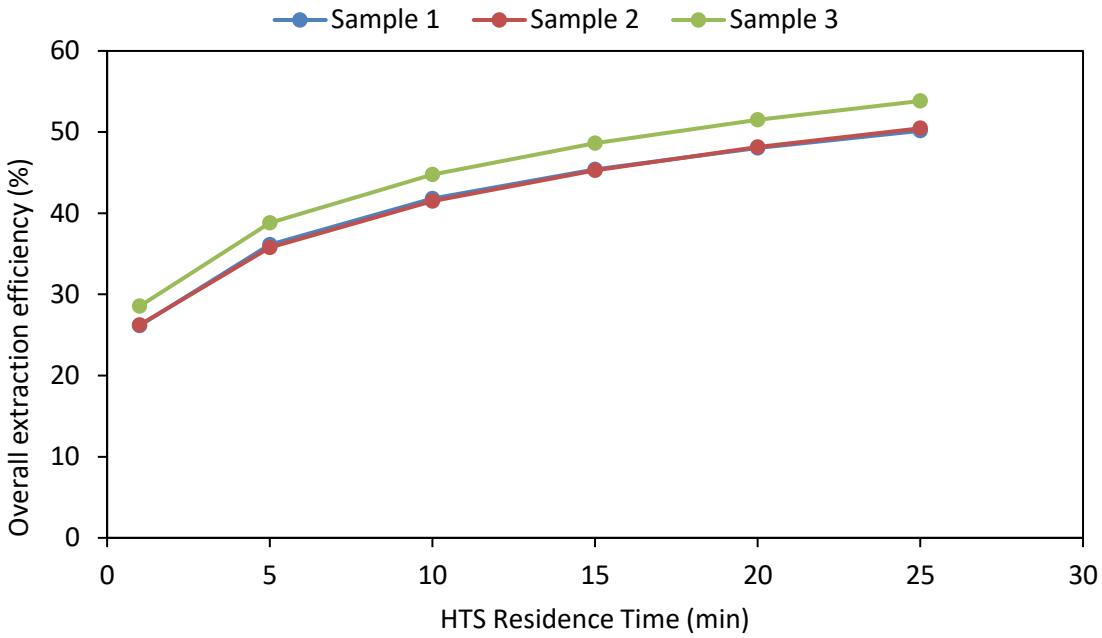

Figure 4.15: Change in overall extraction efficiency with HTS residence time for wheat straw (sample 1), corn stalk (sample 2) and woodchips (sample 3)

4.4.4. Effects of Feedstock S/L Ratio

Fig. 4.16 showed the effect of feedstock S/L ratio on components extraction ratio and formation of oligomers and sugar monomers (kg/h) for wheat straw (sample 1). Where, S/L ratio was changed two times (10% and 15%) with holding HTS temperature of 190 °C, HTS pressure of 20 bar and HTS residence time of 15 min.

Fig. 4.16 (A) represents the cellulose, hemicellulose, lignin, and extractive extraction ratios for two S/L ratios. At 10% of the S/L ratio, the extraction ratio was 20.88%, 65.03%, 48.31%, and 45% for cellulose, hemicellulose, lignin, and extractives, respectively. In the case of a 15% S/L ratio, the extraction ratio was approximately similar to that of a 10% S/L ratio. However, Fig. 4.16 (B) showed that each hydrolysate component produced a higher amount at an S/L ratio of 15% than 10%. The formation of all hydrolysates was approximately 50% higher in the S/L ratio of 15% than 10%. These results indicated that a higher solid loading results in a higher component yield. However, there should be a limit of solid loading according to the utilized process for different biomass [24].

The effect of S/L ratio on components extraction ratio and hydrolysates formation of corn stalk (sample 2) and woodchips (sample 3) also follow the same trend as wheat straw which has shown in Appendices B.

In the case of overall extraction efficiency, Fig. 4.17 showed that corn stalk had the highest overall extraction efficiency of 48.73%, followed by wheat straw and corn stalk at a 10% S/L ratio. On the other hand, at a 15% S/L ratio, all the components showed approximately the same efficiency as those at a 10% S/L ratio. Results indicated that overall extraction efficiency mostly varied with feedstock composition [72].

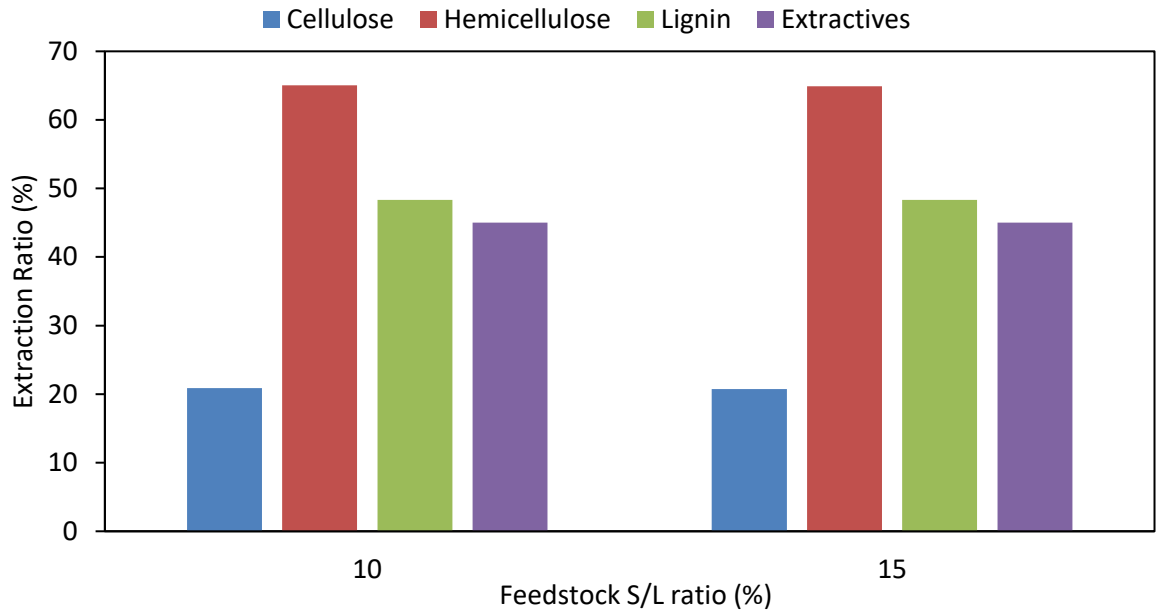

(A)

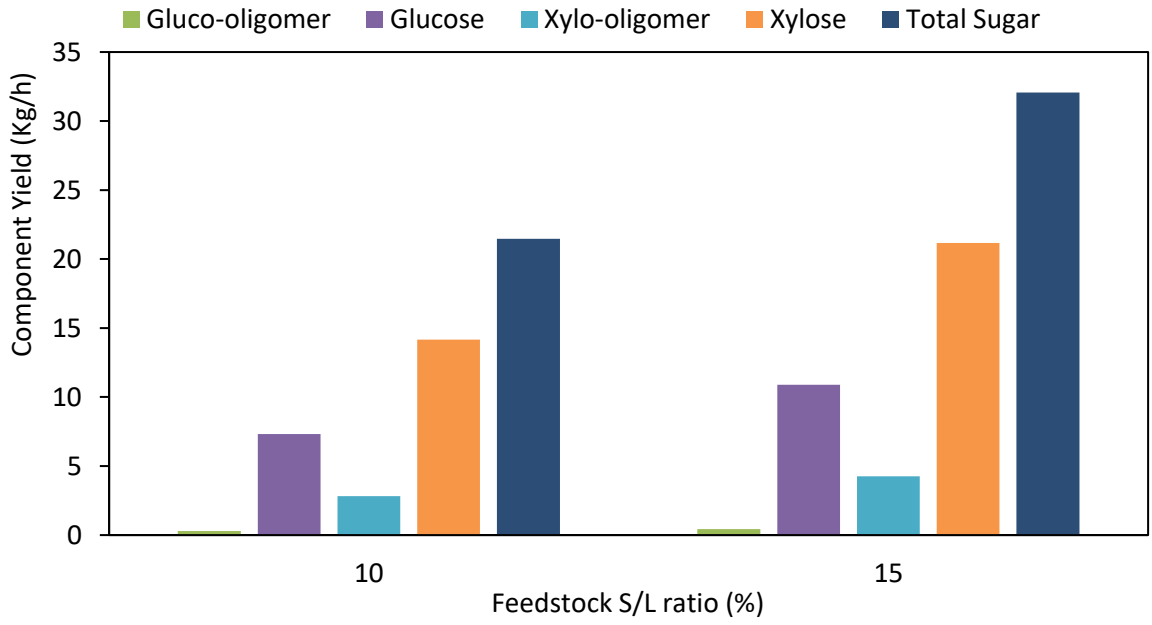

(B)

Figure 4.16: (A) Component extraction ratio and (B) Monomers and oligomers formation with feedstock S/L ratio for wheat straw (Sample 1)

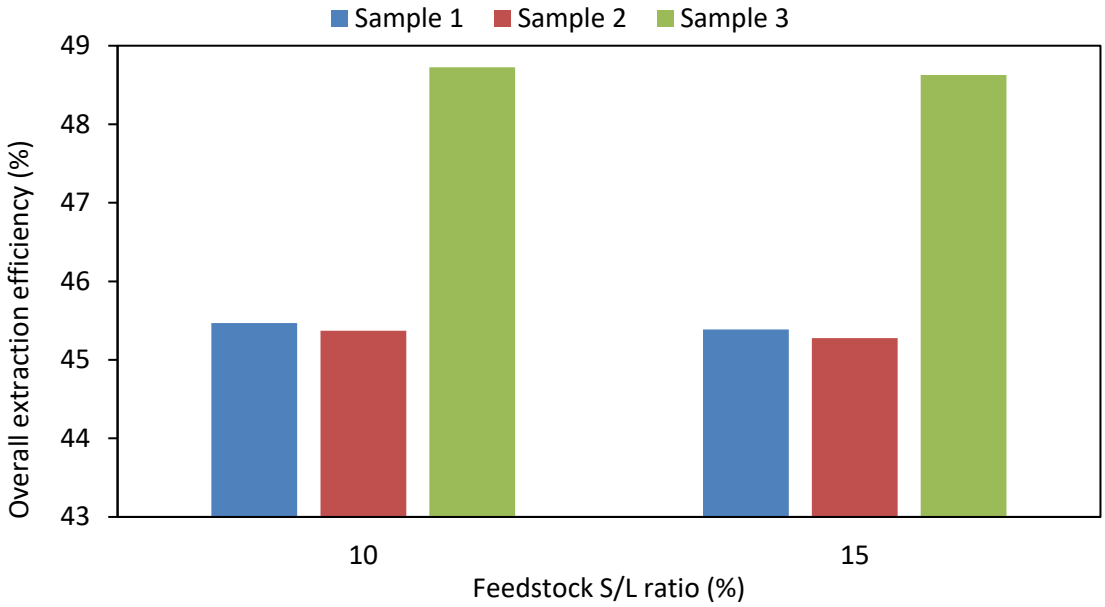

Figure 4.17: Change in overall extraction efficiency with feedstock S/L ratio for wheat straw (sample 1), corn stalk (sample 2) and woodchips (sample 3)

4.5. Optimization

Response surface methodology (RSM) was used to optimize the overall extraction efficiency aiming to maximize the efficiency. Four independent variables including, HTS temperature (X_1), HTS residence time (X_2), HTS pressure (X_3) and S/L ratio (X_4), was considered to run the simulation of coupled process (Model 3) by the Aspen Plus simulation and further statistical approach. The range of process conditions was considered as follows: HTS temperature of 180 to 210℃, HTS residence time of 5 to 25 min, HTS pressure of 15 to 20 bar and S/L ratio of 10 to 15%. A total of 31 simulation runs of four variables were designed by Central Composite Design (CCD) using the Minitab 21.4.2 statistical software.

The results of overall extraction efficiency for all three samples by Aspen Plus simulation and statistical approach (using response surface methodology) were tabulated in Table 4.1. Whereas samples 1, 2, and 3 stand for wheat straw, corn stalk, and woodchips, respectively. The data showed that the overall extraction efficiency by the Aspen Plus simulation varied between 37.93 and 64.4% for wheat straw, 37.24 and 66.8% for corn stalk, and 40.53 and 69.77% for woodchips. The maximum efficiency obtained by simulation was 64.4% for wheat straw, 66.8% for corn stalk, and 69.77% for woodchips at the 10th run (S/L ratio 12.5%, HTS temperature 210℃, HTS residence time 15 min, and HTS pressure of 17.5 bar) in Aspen Plus. As woodchips had shown the higher overall extraction efficiency among all the feedstocks, we optimized the overall extraction efficiency of the coupled process (Model 3) based on simulated results of woodchips (sample 3).

An ANOVA test was carried out to determine the response of overall extraction efficiency, and the results are shown in Table 4.2. Values were adjusted to a quadratic model (Eq. 4.1) with a correlation coefficient (R^2) of 99.33%; the adequate fit of response values to compose an equation was determined by the significance of the model (p-value < 0.05) and non-significance of lack of fit test (p-value > 0.05)

at 95% confidence level. Also, statistically predicted values for overall extraction efficiency were near to the simulated value, as shown in Table 4.1.

$$Y = 94 - 1.30\,X_1 - 0.37\,X_2 + 2.94\,X_3 - 7.16\,X_4 + 0.00466\,X_1^2 - 0.02743\,X_2^2 - 0.196\,X_3^2 + 0.283\,X_4^2 + 0.01023\,X_1X_2 + 0.0223\,X_1X_3 - 0.0003\,X_1X_4 - 0.0032\,X_2X_3 + 0.0006\,X_2X_4 - 0.006\,X_3X_4 \quad (4.1)$$

Where, Y is the overall extraction efficiency (%), X1 is the HTS temperature, X2 is HTS residence time, X3 is the HTS pressure, and X4 is the S/L ratio, respectively.

As shown in Table 4.2, the overall extraction efficiency of the coupled process was strongly influenced by HTS temperature and HTS residence time, whose coefficient in the statistical model showed a p-value less than 0.05, which also supports the simulated results of sections 4.4.1 (effect of HTS temperature) and 4.4.3 (effect of HTS residence time) . On the other hand, no significant effect was observed for HTS pressure and S/L ratio on overall extraction efficiency whose p-value was greater than 0.05, which also supports the simulated results of sections 4.4.2 (effect of HTS pressure) and 4.4.4 (effect of S/L ratio). The 3D response surface plot also showed the effects of HTS residence time and HTS temperature on overall extraction efficiency.

The overall extraction efficiency variables were optimized by statistical approach in a way that maximizes the efficiency. At optimized conditions (HTS temperature of 210 °C, HTS residence time of 25 min, HTS pressure of 19.04 bar, and S/L ratio of 10%), the overall extraction efficiency was predicted by the statistical approach of 80.20 ± 5.04% for sample 3 (woodchips). This value was also confirmed by Aspen Plus simulation results (74.34% of overall extraction efficiency) at optimal process conditions. Also, in the optimized conditions, the hemicellulose extraction ratio was 77%, the cellulose extraction ratio was 75.6%, and the total sugar (glucose and xylose) yield was 50.64 kg/h with an input of 1000 kg/h (S/L ratio 10%, biomass 100kg/h and water 900 kg/h) feed of woodchips.

Table 4.1: Overall extraction efficiency of different feed samples by Aspen Plus simulation and statistical approach

Run	HTS Temp (°C)	HTS RT (min)	HTS Press (bar)	S/L ratio (%)	Sample 1		Sample 2		Sample 3	
					Simulated (%)	Statistical (%)	Sim. (%)	Stat. (%)	Sim. (%)	Stat. (%)
1	202.5	10	18.75	11.25	54.5	52.84	65.61	59.19	58.87	58.61
2	195	15	20	12.5	50.46	51.76	50.96	52.06	54.24	53.74
3	187.5	20	16.25	13.75	45.68	46.36	45.5	49.07	48.9	49.01
4	195	15	15	12.5	50.46	50.75	50.96	51.14	51.51	52.28
5	187.5	20	18.75	11.25	45.71	45.08	45.54	43.59	48.94	49.85
6	195	5	17.5	12.5	39.82	41.88	39.64	42.82	42.76	43.99
7	195	15	17.5	12.5	50.46	50.46	50.96	50.96	54.24	54.24
8	195	15	17.5	10	41.3	45.27	46.58	48.87	57.53	56.59
9	202.5	20	16.25	11.25	59.94	58.81	62.64	60.22	65.71	65.72
10	210	15	17.5	12.5	64.4	65.97	66.8	68.84	69.77	71.09
11	195	15	17.5	15	50.42	48.04	50.91	49.9	54.21	55.42
12	202.5	20	18.75	13.75	61.42	61.46	63.38	61.58	66.43	66.24
13	187.5	10	18.75	11.25	39.93	38.14	39.48	40.72	42.74	43.16
14	202.5	10	16.25	11.25	53.66	52.09	54.75	55.52	57.9	57.41
15	195	15	17.5	12.5	50.46	50.46	50.96	50.96	54.24	54.24
16	195	15	17.5	12.5	50.46	50.46	50.96	50.96	54.24	54.24
17	195	15	17.5	12.5	50.46	50.46	50.96	50.96	54.24	54.24
18	195	15	17.5	12.5	50.46	50.46	50.96	50.96	54.24	54.24
19	202.5	10	16.25	13.75	53.65	53.31	54.74	53.83	57.89	56.83
20	195	15	17.5	12.5	50.46	50.46	50.96	50.96	54.24	54.24
21	202.5	20	18.75	11.25	61.45	60.26	55.66	59.4	66.48	66.84
22	187.5	10	18.75	13.75	39.89	40.04	39.45	39.01	42.71	42.56
23	187.5	20	16.25	11.25	45.71	45.15	45.55	45.79	48.95	49.56
24	202.5	20	16.25	13.75	58.5	59.67	62.63	62.96	65.7	65.15
25	187.5	20	18.75	13.75	45.68	46.63	45.5	46.31	48.9	49.26
26	195	15	17.5	12.5	50.46	50.46	50.96	50.96	54.24	54.24
27	202.5	10	18.75	13.75	54.46	54.4	55.61	56.95	58.74	58
28	187.5	10	16.25	11.25	39.93	38.91	39.48	38.42	42.75	42.79
29	180	15	17.5	12.5	37.93	37.95	37.24	36.48	40.53	39.49
30	195	25	17.5	12.5	55.65	55.18	56.73	54.82	59.96	59.01
31	187.5	10	16.25	13.75	39.9	40.47	39.45	37.28	42.71	42.22

Table 4.2: Analysis of variance (ANOVA) for quadratic model for overall extraction efficiency for woodchips (sample 3)

Source	DF	Adj SS	Adj MS	F-Value	P-Value	
Model	14	1870.67	133.62	168.65	<0.05	Significant
Linear	4	1841.33	460.33	581.02		
X_1	1	1497.84	1497.84	1890.55	0.0	Significant
X_2	1	338.25	338.25	426.93	0.0	Significant
X_3	1	3.2	3.2	4.04	0.062	
X_4	1	2.04	2.04	2.58	0.128	
Square	4	26.28	6.57	8.29	0.001	
X_1^2	1	1.96	1.96	2.48	0.135	
X_2^2	1	13.44	13.44	16.97	0.001	Significant
X_3^2	1	2.69	2.69	3.4	0.084	
X_4^2	1	5.58	5.58	7.05	0.017	Significant
2-Way Interaction	6	3.06	0.51	0.64	0.694	
X_1X_2	1	2.36	2.36	2.97	0.104	
X_1X_3	1	0.7	0.7	0.88	0.362	
X_1X_4	1	0	0	0	0.991	
X_2X_3	1	0.01	0.01	0.01	0.93	
X_2X_4	1	0	0	0	0.987	
X_3X_4	1	0	0	0	0.969	
Error	16	12.68	0.79			
Lack-of-Fit	10	12.68	1.27	*	*	
Pure Error	6	0	0			
Total	30	1883.35				

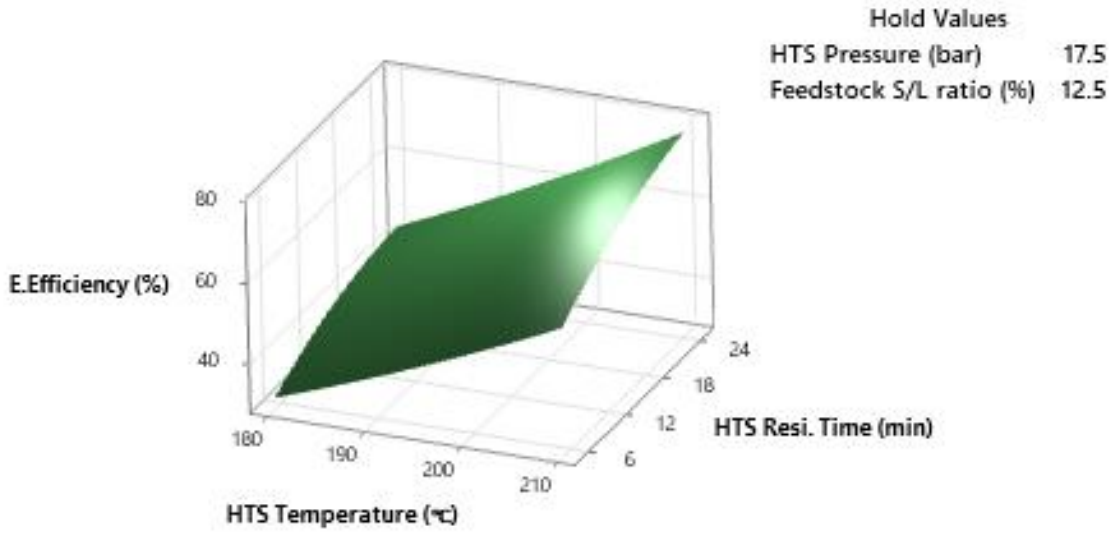

Figure 4.18: Response surface plot for optimization of overall extraction efficiency.

Chapter 5 Conclusion

The coupling process of hydrodynamic cavitation and hydrothermal separation showed an efficient technique to produce valuable products from lignocellulosic biomass rather than individual pretreatment processes. Results showed that the coupling of the HC and HTS processes had a maximum of 25.5% higher overall extraction efficiency than the single HC process and 18.2% higher efficiency than the single HTS process for woodchips. Meanwhile, the coupled process separates cellulose, hemicellulose, lignin, and extractives; conversely, single pretreatment processes focus on only certain components. Which reflects the first research question of this study.

Various parameters influenced the overall extraction efficiency and component yield in the coupled process. We studied the effects of HTS pressure, temperature, residence time, and S/L ratio among them. Results showed that overall extraction efficiency, cellulose, and hemicellulose yield were affected mainly by HTS temperature and residence time, undergoing higher with increasing temperature and pressure. The S/L ratio had shown an increased effect on all component yield, including lignin and extractives; on the other hand, HTS pressure showed a negligible effect on cellulose and hemicellulose yield and overall extraction efficiency, which was also supported by the statistical approach. However, HTS temperature, pressure, and residence had shown no effect on lignin and extractives. These results reflect the second research question of this study.

Response surface methodology was used to optimize the overall extraction efficiency, aiming to maximize efficiency. At optimal conditions (HTS temperature 210 ℃, HTS residence time 25 min, HTS pressure of 19.04 bar, S/L ratio 10%, HC pressure 3 bar, HC temperature 60℃, HC residence time 20 min), the maximum overall extraction efficiency was for woodchips, as predicted by the statistical approach of 80.20 ± 5.04% with a regression coefficient (R-sq) of 99.33%. This value was also confirmed by Aspen Plus simulation results (74.34% overall extraction efficiency for the same process conditions). Also, in the optimized conditions, hemicellulose extraction ratio was 77%, cellulose extraction ratio was 75.6%, and total sugar (glucose and xylose) yield was 50.64 kg/h with 13.43 kg/h (48.31%) of lignin and 0.855 kg/h (45%) of extractives yield for an input of 1000 kg/h (S/L ratio 10%, biomass 100 kg/h, water 900 kg/h). Finally, these results answered the third research question of this thesis work.

The coupling process employs water as its solvent, which makes it a more environmentally friendly and cost-effective option for optimizing biomass resources and minimizing waste production. This research focused on modeling and simulating the combination of hydrodynamic cavitation and hydrothermal separation process. Future investigations could involve conducting laboratory-scale experiments to gain a deeper understanding of the coupling process's behavior. Additionally, a techno-economic analysis could be performed to assess the feasibility of scaling up the entire process.

List of References

[1] A. R. Mankar, A. Pandey, A. Modak, and K. K. Pant, "Pretreatment of lignocellulosic biomass: A review on recent advances," *Bioresour. Technol.*, vol. 334, no. April, p. 125235, 2021, doi: 10.1016/j.biortech.2021.125235.

[2] E. Ahmad, T. S. Khan, M. I. Alam, K. K. Pant, and M. Ali Haider, "Understanding reaction kinetics, deprotonation and solvation of brønsted acidic protons in heteropolyacid catalyzed synthesis of biorenewable alkyl levulinates," *Chem. Eng. J.*, vol. 400, no. May, p. 125916, 2020, doi: 10.1016/j.cej.2020.125916.

[3] S. Kassaye, K. K. Pant, and S. Jain, "Hydrolysis of cellulosic bamboo biomass into reducing sugars via a combined alkaline solution and ionic liquid pretreament steps," *Renew. Energy*, vol. 104, pp. 177–184, 2017, doi: 10.1016/j.renene.2016.12.033.

[4] D. Chen, A. Gao, K. Cen, J. Zhang, X. Cao, and Z. Ma, "Investigation of biomass torrefaction based on three major components: Hemicellulose, cellulose, and lignin," *Energy Convers. Manag.*, vol. 169, pp. 228–237, 2018, doi: 10.1016/j.enconman.2018.05.063.

[5] Y. C. Lu, Y. Lu, Z. L. Lu, and X. Y. Wei, "Detailed Componential Characterization of Extractable Species with Organic Solvents from Wheat Straw," *Int. J. Anal. Chem.*, vol. 2017, 2017, doi: 10.1155/2017/7305682.

[6] S. Haghighi Mood *et al.*, "Lignocellulosic biomass to bioethanol, a comprehensive review with a focus on pretreatment," *Renew. Sustain. Energy Rev.*, vol. 27, pp. 77–93, 2013, doi: 10.1016/j.rser.2013.06.033.

[7] B. Tsegaye, C. Balomajumder, and P. Roy, "Microbial delignification and hydrolysis of lignocellulosic biomass to enhance biofuel production: an overview and future prospect," *Bull. Natl. Res. Cent.*, vol. 43, no. 1, 2019, doi: 10.1186/s42269-019-0094-x.

[8] N. Das, P. K. Jena, D. Padhi, M. Kumar Mohanty, and G. Sahoo, "A comprehensive review of characterization, pretreatment and its applications on different lignocellulosic biomass for bioethanol production," *Biomass Convers. Biorefinery*, vol. 13, no. 2, pp. 1503–1527, 2023, doi: 10.1007/s13399-021-01294-3.

[9] X. Ge *et al.*, *Conversion of Lignocellulosic Biomass Into Platform Chemicals for Biobased Polyurethane Application*, 1st ed., vol. 3. Elsevier Inc., 2018. doi: 10.1016/bs.aibe.2018.03.002.

[10] Y. Zhang *et al.*, "Recent advances in lignocellulosic and algal biomass pretreatment and its biorefinery approaches for biochemicals and bioenergy conversion," *Bioresour. Technol.*, vol. 367, no. September 2022, p. 128281, 2023, doi: 10.1016/j.biortech.2022.128281.

[11] H. Chen, *Biotechnology of Lignocellulose*. 2014. doi: 10.1007/978-94-007-6898-7.

[12] M. S. Singhvi and D. V. Gokhale, "Lignocellulosic biomass: Hurdles and challenges in its valorization," *Appl. Microbiol. Biotechnol.*, vol. 103, no. 23–24, pp. 9305–9320, 2019, doi: 10.1007/s00253-019-10212-7.

[13] A. O. Ayeni, M. O. Daramola, A. E. Adetayo, P. T. Sekoai, O. C. Nwinyi, and O. Ejekwu, *Biological and Non-Biological Methods for Lignocellulosic Biomass Deconstruction*. 2020. doi: 10.1007/978-3-030-38032-8_7.

[14] R. Terán Hilares *et al.*, "Ethanol production in a simultaneous saccharification and fermentation process with interconnected reactors employing hydrodynamic cavitation-pretreated sugarcane bagasse as raw material," *Bioresour. Technol.*, vol. 243, pp. 652–659, 2017, doi: 10.1016/j.biortech.2017.06.159.

[15] R. C. Sun, D. Salisbury, and J. Tomkinson, "Chemical composition of lipophilic extractives released during the hot water treatment of wheat straw," *Bioresour. Technol.*, vol. 88, no. 2, pp. 95–101, 2003, doi: 10.1016/S0960-8524(02)00290-0.

[16] V. B. Agbor, N. Cicek, R. Sparling, A. Berlin, and D. B. Levin, "Biomass pretreatment: Fundamentals toward application," *Biotechnol. Adv.*, vol. 29, no. 6, pp. 675–685, 2011, doi: 10.1016/j.biotechadv.2011.05.005.

[17] N. S. Mosier *et al.*, "Industrial scale-up of pH-controlled liquid hot water pretreatment of corn fiber for fuel ethanol production," *Appl. Biochem. Biotechnol. - Part A Enzym. Eng. Biotechnol.*, vol. 125, no. 2, pp. 77–97, 2005, doi: 10.1385/abab:125:2:077.

[18] L. Laureano-Perez, F. Teymouri, H. Alizadeh, and B. E. Dale, "Understanding factors that limit enzymatic hydrolysis of biomass: Characterization of pretreated corn stover," *Appl. Biochem. Biotechnol. - Part A Enzym. Eng. Biotechnol.*, vol. 124, no. 1–3, pp. 1081–1099, 2005, doi: 10.1385/ABAB:124:1-3:1081.

[19] G. Brodeur, E. Yau, K. Badal, J. Collier, K. B. Ramachandran, and S. Ramakrishnan, "Chemical and physicochemical pretreatment of lignocellulosic biomass: A review," *Enzyme Res.*, vol. 2011, no. 1, 2011, doi: 10.4061/2011/787532.

[20] T. Gagić, A. Perva-Uzunalić, Ž. Knez, and M. Škerget, "Hydrothermal Degradation of Cellulose at Temperature from 200 to 300 °c," *Ind. Eng. Chem. Res.*, vol. 57, no. 18, pp. 6576–6584, 2018, doi: 10.1021/acs.iecr.8b00332.

[21] J. A. Okolie, S. Nanda, A. K. Dalai, and J. A. Kozinski, "Chemistry and Specialty Industrial Applications of Lignocellulosic Biomass," *Waste and Biomass Valorization*, vol. 12, no. 5, pp. 2145–2169, 2021, doi: 10.1007/s12649-020-01123-0.

[22] F. J. M. Kormelink and A. G. J. Voragen, "Degradation of different [(glucurono)arabino]xylans by a combination of purified xylan-degrading enzymes," *Appl. Microbiol. Biotechnol.*, vol. 38, no. 5, pp. 688–695, 1993, doi: 10.1007/BF00182811.

[23] L. W. Doner, G. A. Sweeney, and K. B. Hicks, "Isolation of hemicellulose from corn fiber," *Cereal Chem.*, vol. 74, no. 2, pp. 176–181, 1997, [Online]. Available: https://www.google.com/patents/US6147206

[24] Z. H. Liu and A. Ragauskas, *Emerging technologies for biorefineries, biofuels, and value-added commodities*. 2021. doi: 10.1007/978-3-030-65584-6.

[25] C. H. Zhou, X. Xia, C. X. Lin, D. S. Tong, and J. Beltramini, "Catalytic conversion of lignocellulosic biomass to fine chemicals and fuels," *Chem. Soc. Rev.*, vol. 40, no. 11, pp. 5588–5617, 2011, doi: 10.1039/c1cs15124j.

[26] A. Pattiya, *Fast pyrolysis*. Elsevier Ltd., 2017. doi: 10.1016/B978-0-08-101029-7.00001-1.

[27] E. Sjostrom and U. Westermark, "Chemical Composition of Wood and Pulps :," *Anal. Methods Wood Chem. Pulping, Papermak.*, pp. 1–2, 1999.

[28] C. Yang and X. Lü, *Composition of plant biomass and its impact on pretreatment*. Elsevier, 2021. doi: 10.1016/B978-0-12-818862-0.00002-9.

[29] S. Nanda, P. Mohanty, K. K. Pant, S. Naik, J. A. Kozinski, and A. K. Dalai, "Characterization of North American Lignocellulosic Biomass and Biochars in Terms of their Candidacy for Alternate Renewable Fuels," *Bioenergy Res.*, vol. 6, no. 2, pp. 663–677, 2013, doi: 10.1007/s12155-012-9281-4.

[30] S. V. Vassilev, D. Baxter, L. K. Andersen, C. G. Vassileva, and T. J. Morgan, "An overview of the organic and inorganic phase composition of biomass," *Fuel*, vol. 94, pp. 1–33, 2012, doi:

10.1016/j.fuel.2011.09.030.

[31] A. Pettersson, M. Zevenhoven, B. M. Steenari, and L. E. Åmand, "Application of chemical fractionation methods for characterisation of biofuels, waste derived fuels and CFB co-combustion fly ashes," *Fuel*, vol. 87, no. 15–16, pp. 3183–3193, 2008, doi: 10.1016/j.fuel.2008.05.030.

[32] V. G. Deshmane, P. R. Gogate, and A. B. Pandit, "Ultrasound-assisted synthesis of biodiesel from palm fatty acid distillate," *Ind. Eng. Chem. Res.*, vol. 48, no. 17, pp. 7923–7927, 2009, doi: 10.1021/ie800981v.

[33] J. Ji, J. Wang, Y. Li, Y. Yu, and Z. Xu, "Preparation of biodiesel with the help of ultrasonic and hydrodynamic cavitation," *Ultrasonics*, vol. 44, no. SUPPL., 2006, doi: 10.1016/j.ultras.2006.05.020.

[34] T. A. Bimestre, J. A. M. Júnior, E. V. Canettieri, and C. E. Tuna, "Hydrodynamic cavitation for lignocellulosic biomass pretreatment: a review of recent developments and future perspectives," *Bioresour. Bioprocess.*, vol. 9, no. 1, 2022, doi: 10.1186/s40643-022-00499-2.

[35] R. Terán Hilares *et al.*, "Hydrodynamic cavitation as an efficient pretreatment method for lignocellulosic biomassA parametric study," *Bioresour. Technol.*, vol. 235, pp. 301–308, 2017, doi: 10.1016/j.biortech.2017.03.125.

[36] S. Raut-Jadhav, M. P. Badve, D. V. Pinjari, D. R. Saini, S. H. Sonawane, and A. B. Pandit, "Treatment of the pesticide industry effluent using hydrodynamic cavitation and its combination with process intensifying additives (H2O2 and ozone)," *Chem. Eng. J.*, vol. 295, pp. 326–335, 2016, doi: 10.1016/j.cej.2016.03.019.

[37] K. Nakashima, Y. Ebi, N. Shibasaki-Kitakawa, H. Soyama, and T. Yonemoto, "Hydrodynamic Cavitation Reactor for Efficient Pretreatment of Lignocellulosic Biomass," *Ind. Eng. Chem. Res.*, vol. 55, no. 7, pp. 1866–1871, 2016, doi: 10.1021/acs.iecr.5b04375.

[38] M. Badve, P. Gogate, A. Pandit, and L. Csoka, "Hydrodynamic cavitation as a novel approach for wastewater treatment in wood finishing industry," *Sep. Purif. Technol.*, vol. 106, pp. 15–21, 2013, doi: 10.1016/j.seppur.2012.12.029.

[39] I. Kim, I. Lee, S. H. Jeon, T. Hwang, and J. I. Han, "Hydrodynamic cavitation as a novel pretreatment approach for bioethanol production from reed," *Bioresour. Technol.*, vol. 192, pp. 335–339, 2015, doi: 10.1016/j.biortech.2015.05.038.

[40] B. Randhavane Shrikant and A. K. Khambete, "Hydrodynamic Cavitation: A Novel Treatment Approach," *Mater. Today Proc.*, vol. 4, no. 9, pp. 9680–9684, 2017, doi: 10.1016/j.matpr.2017.06.246.

[41] X. Sun, C. H. Kang, J. J. Park, H. S. Kim, A. S. Om, and J. Y. Yoon, "An experimental study on the thermal performance of a novel hydrodynamic cavitation reactor," *Exp. Therm. Fluid Sci.*, vol. 99, no. November 2017, pp. 200–210, 2018, doi: 10.1016/j.expthermflusci.2018.02.034.

[42] Z. Wu, S. Tagliapietra, A. Giraudo, K. Martina, and G. Cravotto, "Harnessing cavitational effects for green process intensification," *Ultrason. Sonochem.*, vol. 52, no. December 2018, pp. 530–546, 2019, doi: 10.1016/j.ultsonch.2018.12.032.

[43] X. Sun, S. Chen, J. Liu, S. Zhao, and J. Y. Yoon, "Hydrodynamic Cavitation: A Promising Technology for Industrial-Scale Synthesis of Nanomaterials," *Front. Chem.*, vol. 8, no. April, pp. 1–7, 2020, doi: 10.3389/fchem.2020.00259.

[44] X. Sun *et al.*, "Recent advances in hydrodynamic cavitation-based pretreatments of lignocellulosic biomass for valorization," *Bioresour. Technol.*, vol. 345, no. August 2021, p. 126251, 2022, doi: 10.1016/j.biortech.2021.126251.

[45] P. B. Baxi and A. B. Pandit, "Using cavitation for delignification of wood," *Bioresour. Technol.*, vol. 110, pp. 697–700, 2012, doi: 10.1016/j.biortech.2012.01.042.

[46] L. Lauberte *et al.*, "Lignin – Derived antioxidants as value-added products obtained under cavitation treatments of the wheat straw processing for sugar production," *J. Clean. Prod.*, vol. 303, p. 126369, 2021, doi: 10.1016/j.jclepro.2021.126369.

[47] K. Thangavelu, R. Desikan, O. P. Taran, and S. Uthandi, "Delignification of corncob via combined hydrodynamic cavitation and enzymatic pretreatment: Process optimization by response surface methodology," *Biotechnol. Biofuels*, vol. 11, no. 1, pp. 1–13, 2018, doi: 10.1186/s13068-018-1204-y.

[48] R. Terán Hilares, J. C. dos Santos, M. A. Ahmed, S. H. Jeon, S. S. da Silva, and J. I. Han, "Hydrodynamic cavitation-assisted alkaline pretreatment as a new approach for sugarcane bagasse biorefineries," *Bioresour. Technol.*, vol. 214, pp. 609–614, 2016, doi: 10.1016/j.biortech.2016.05.004.

[49] M. P. Badve, P. R. Gogate, A. B. Pandit, and L. Csoka, "Hydrodynamic cavitation as a novel approach for delignification of wheat straw for paper manufacturing," *Ultrason. Sonochem.*, vol. 21, no. 1, pp. 162–168, 2014, doi: 10.1016/j.ultsonch.2013.07.006.

[50] R. Hamidi *et al.*, "Recent developments and future outlooks of hydrodynamic cavitation as an intensification technology for renewable biofuels production," *J. Environ. Chem. Eng.*, vol. 11, no. 5, p. 110819, 2023, doi: 10.1016/j.jece.2023.110819.

[51] S. Nagarajan and V. V. Ranade, "Pretreatment of Lignocellulosic Biomass Using Vortex-Based Devices for Cavitation: Influence on Biomethane Potential," *Ind. Eng. Chem. Res.*, vol. 58, no. 35, pp. 15975–15988, 2019, doi: 10.1021/acs.iecr.9b00859.

[52] A. A. Modenbach and S. E. Nokes, "The use of high-solids loadings in biomass pretreatment-a review," *Biotechnol. Bioeng.*, vol. 109, no. 6, pp. 1430–1442, 2012, doi: 10.1002/bit.24464.

[53] S. L. Lee *et al.*, "Modernizing Pharmaceutical Manufacturing: from Batch to Continuous Production," *J. Pharm. Innov.*, vol. 10, no. 3, pp. 191–199, 2015, doi: 10.1007/s12247-015-9215-8.

[54] R. Terán Hilares, R. M. Dionízio, C. A. Prado, M. A. Ahmed, S. S. da Silva, and J. C. Santos, "Pretreatment of sugarcane bagasse using hydrodynamic cavitation technology: Semi-continuous and continuous process," *Bioresour. Technol.*, vol. 290, no. June, p. 121777, 2019, doi: 10.1016/j.biortech.2019.121777.

[55] T. A. Bimestre, J. A. M. Júnior, C. A. Botura, E. V. Canettieri, and C. E. Tuna, "Theoretical modeling and experimental validation of hydrodynamic cavitation reactor with a Venturi tube for sugarcane bagasse pretreatment," *Bioresour. Technol.*, vol. 311, no. May, p. 123540, 2020, doi: 10.1016/j.biortech.2020.123540.

[56] K. Nalawade, P. Saikia, S. Behera, K. Konde, and S. Patil, "Assessment of multiple pretreatment strategies for 2G L-lactic acid production from sugarcane bagasse," *Biomass Convers. Biorefinery*, vol. 13, no. 2, pp. 647–660, 2023, doi: 10.1007/s13399-020-01163-5.

[57] M. Li *et al.*, "The effect of liquid hot water pretreatment on the chemical-structural alteration and the reduced recalcitrance in poplar," *Biotechnol. Biofuels*, vol. 10, no. 1, pp. 1–13, 2017, doi: 10.1186/s13068-017-0926-6.

[58] J. Ralph, C. Lapierre, and W. Boerjan, "Lignin structure and its engineering," *Curr. Opin. Biotechnol.*, vol. 56, pp. 240–249, 2019, doi: 10.1016/j.copbio.2019.02.019.

[59] A. J. Ragauskas, "Pseudo-Lignin Formation during Dilute acid Pretreatment for Cellulosic Ethanol," *Recent Adv. Petrochemical Sci.*, vol. 1, no. 1, pp. 1–5, 2017, doi:

10.19080/rapsci.2017.01.555551.

[60] P. Biller and A. B. Ross, *Production of biofuels via hydrothermal conversion*. Elsevier Ltd, 2016. doi: 10.1016/B978-0-08-100455-5.00017-5.

[61] W. Zhou, M. Yang, C. Wang, J. Liu, and J. Xing, "Changes in plant cell-wall structure of corn stover due to hot compressed water pretreatment and enhanced enzymatic hydrolysis," *World J. Microbiol. Biotechnol.*, vol. 30, no. 8, pp. 2325–2333, 2014, doi: 10.1007/s11274-014-1651-y.

[62] G. Batista, R. B. A. Souza, B. Pratto, M. S. R. dos Santos-Rocha, and A. J. G. Cruz, "Effect of severity factor on the hydrothermal pretreatment of sugarcane straw," *Bioresour. Technol.*, vol. 275, no. December 2018, pp. 321–327, 2019, doi: 10.1016/j.biortech.2018.12.073.

[63] M. S. R. dos Santos Rocha, B. Pratto, R. de Sousa, R. M. R. G. Almeida, and A. J. G. da Cruz, "A kinetic model for hydrothermal pretreatment of sugarcane straw," *Bioresour. Technol.*, vol. 228, pp. 176–185, 2017, doi: 10.1016/j.biortech.2016.12.087.

[64] A. Tozluoğlu, Ö. Özyürek, Y. Çöpür, and H. Özdemir, "Integrated Production of Biofilm, Bioethanol, and Papermaking Pulp from Wheat Straw," *BioResources*, vol. 10, no. 4, pp. 7834–7853, 2015, doi: 10.15376/biores.10.4.7834-7853.

[65] P. Reyes, M. Pereira, and R. T. Mendonça, "Effect of partial pre-extraction of hemicelluloses on the properties of pinus radiata chemimechanical pulps," *BioResources*, vol. 10, no. 4, pp. 7442–7454, 2015, doi: 10.15376/biores.10.4.7442-7454.

[66] N. Ghavami, K. Özdenkçi, S. Chianese, D. Musmarra, and C. De Blasio, "Process simulation of hydrothermal carbonization of digestate from energetic perspectives in Aspen Plus," *Energy Convers. Manag.*, vol. 270, no. June, 2022, doi: 10.1016/j.enconman.2022.116215.

[67] S. Raut-Jadhav, V. K. Saharan, D. V. Pinjari, D. R. Saini, S. H. Sonawane, and A. B. Pandit, "Intensification of degradation of imidacloprid in aqueous solutions by combination of hydrodynamic cavitation with various advanced oxidation processes (AOPs)," *J. Environ. Chem. Eng.*, vol. 1, no. 4, pp. 850–857, 2013, doi: 10.1016/j.jece.2013.07.029.

[68] A. J. Barik and P. R. Gogate, "Degradation of 4-chloro 2-aminophenol using a novel combined process based on hydrodynamic cavitation, UV photolysis and ozone," *Ultrason. Sonochem.*, vol. 30, pp. 70–78, 2016, doi: 10.1016/j.ultsonch.2015.11.007.

[69] S. V. Vassilev, C. G. Vassileva, Y. C. Song, W. Y. Li, and J. Feng, "Ash contents and ash-forming elements of biomass and their significance for solid biofuel combustion," *Fuel*, vol. 208, pp. 377–409, 2017, doi: 10.1016/j.fuel.2017.07.036.

[70] Q. Yu *et al.*, "Pretreatment of sugarcane bagasse with liquid hot water and aqueous ammonia," *Bioresour. Technol.*, vol. 144, pp. 210–215, 2013, doi: 10.1016/j.biortech.2013.06.078.

[71] Q. Han, Y. Jin, H. Jameel, H. min Chang, R. Phillips, and S. Park, "Autohydrolysis Pretreatment of Waste Wheat Straw for Cellulosic Ethanol Production in a Co-located Straw Pulp Mill," *Appl. Biochem. Biotechnol.*, vol. 175, no. 2, pp. 1193–1210, 2015, doi: 10.1007/s12010-014-1349-5.

[72] C. Pronyk and G. Mazza, "Kinetic modeling of hemicellulose hydrolysis from triticale straw in a pressurized low polarity water flow-through reactor," *Ind. Eng. Chem. Res.*, vol. 49, no. 14, pp. 6367–6375, 2010, doi: 10.1021/ie1003625.

[73] https://www.kinematica.ch/productfinder/d-369/px-mfc-90-d Accessed: 18 Dec23

[74] https://www.geminibv.com/labware/termaks-ts4057-oven Accessed: 18 Dec23

Appendices A

Component specifications in Aspen Plus

The following Table A.1 shown the biomass components and their representative in Aspen Plus simulation.

Table A.1: Biomass components specification in Aspen Plus

Components of LCB	Component name in Aspen Plus
Cellulose	CELLULOS
Gluco-oligomer	DEXTROSE
Glucose	DEXTROSE
Hemicellulose	D-XYLOSE
Xylo-oligomer	D-XYLOSE
Xylose	D-XYLOSE
Lignin	TRANS-P-COUMARYL-ALCOHOL
Soluble lignin	TRANS-P-COUMARYL-ALCOHOL
Extractives	N-HEXADECANOIC ACID
Soluble Extractives	N-HEXADECANOIC ACID
Ash	CALCIUM-OXIDE

Appendices B

For Sample 2 Corn Stalk

Effect of HTS temperature

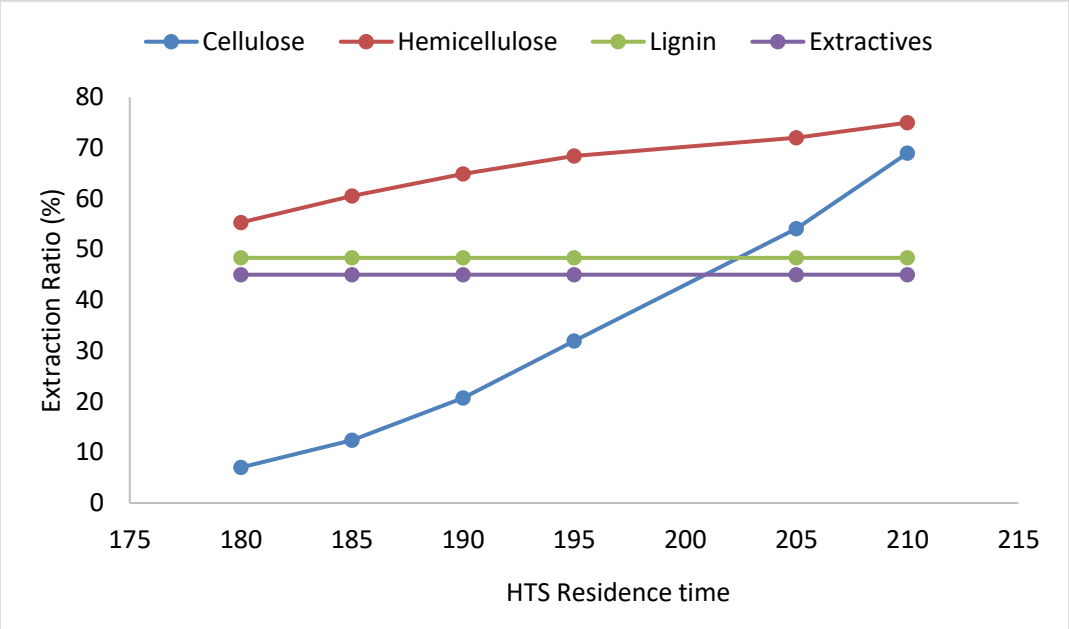

(A)

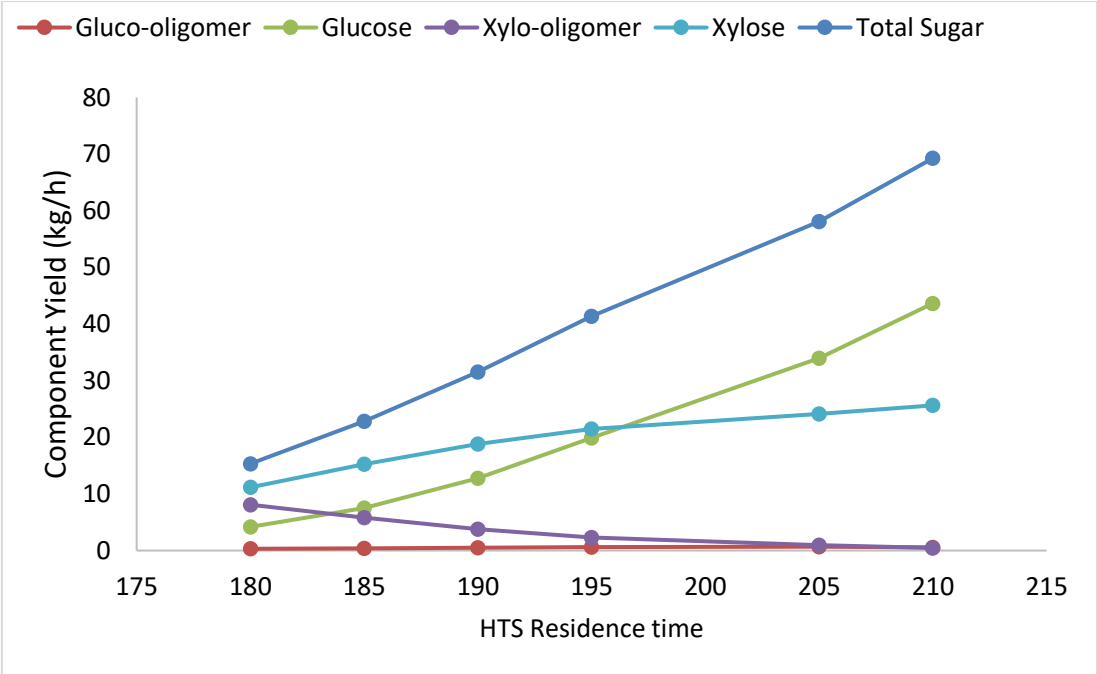

(B)

Figure A.1: (A) Component extraction ratio and (B) Monomers and oligomers formation with HTS temperature for corn stalk (Sample 2)

Effect of HTS Pressure

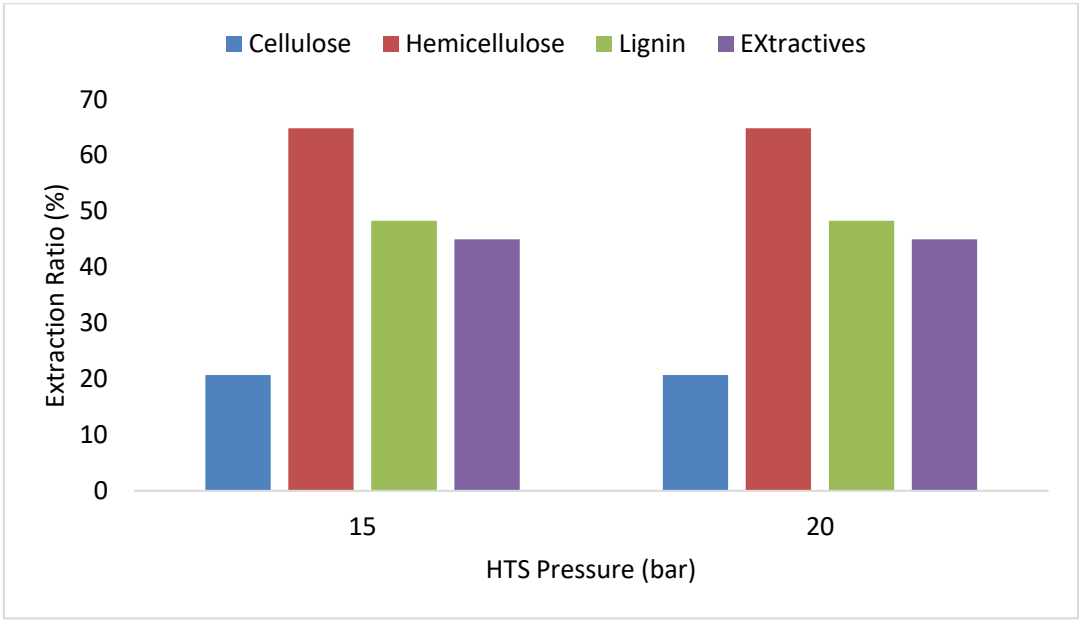

(A)

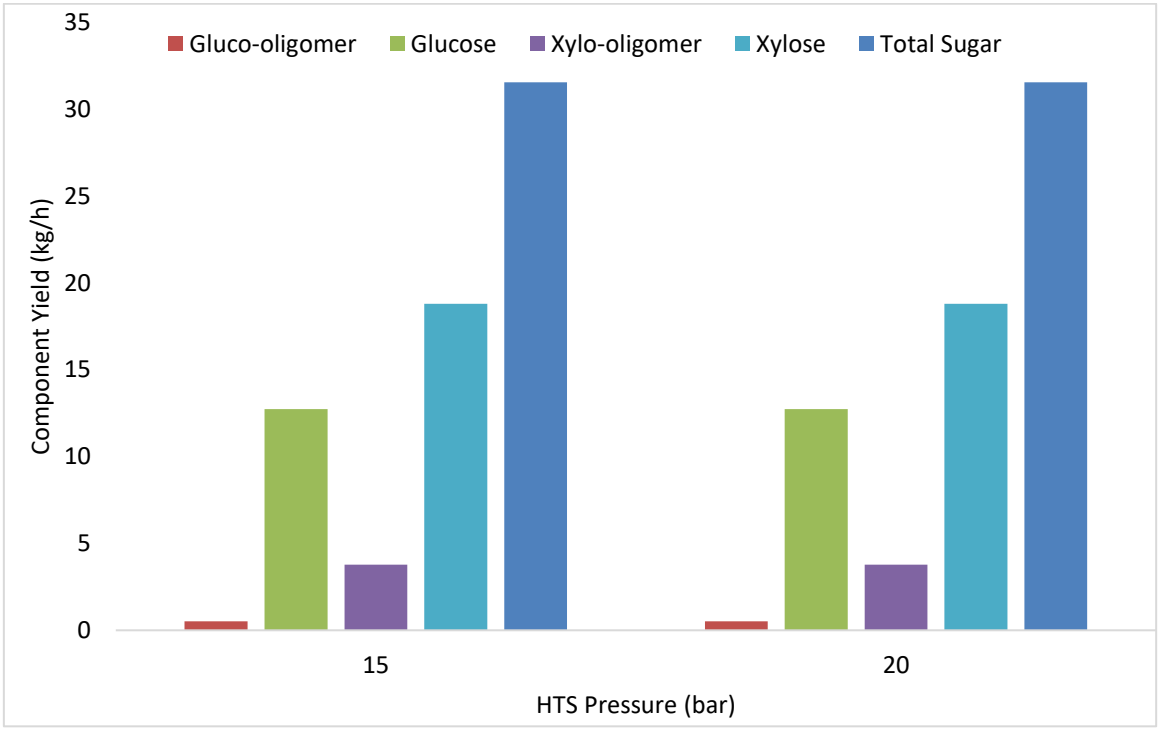

(B)

Figure A.2: (A) Component extraction ratio and (B) Monomers and oligomers formation with HTS pressure for corn stalk (Sample 2)

Effect of HTS Residence time

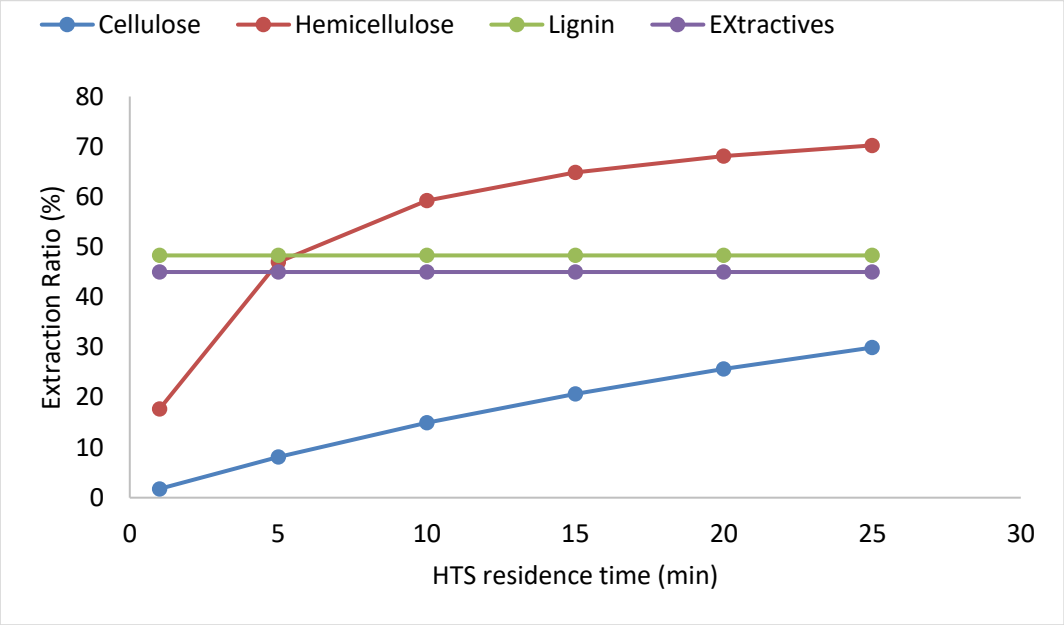

(A)

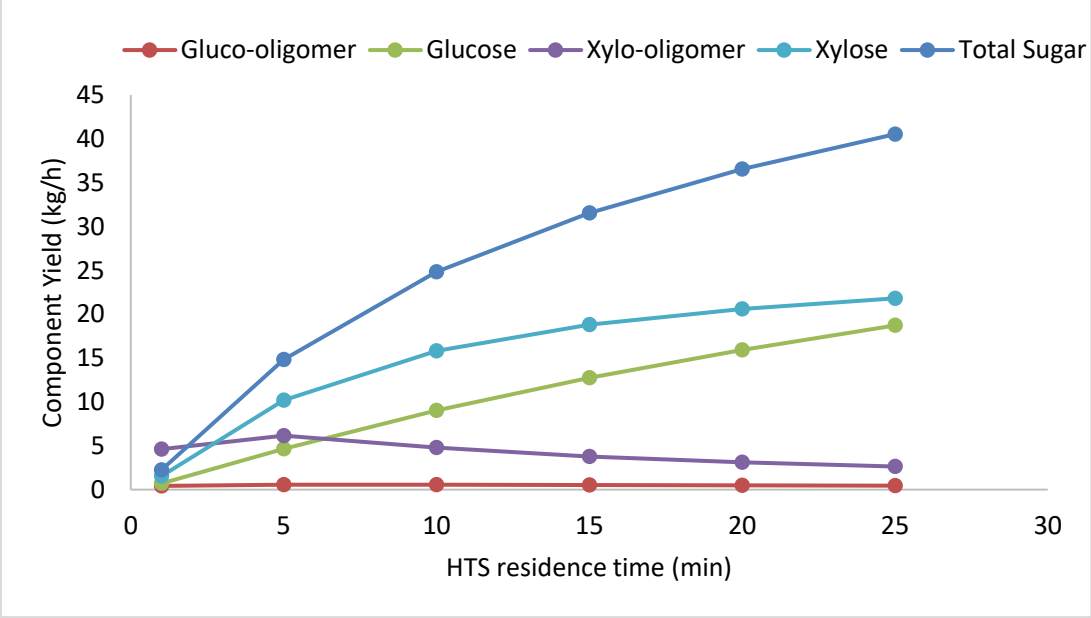

(B)

Figure A.3: (A) Component extraction ratio and (B) Monomers and oligomers formation with HTS residence time for corn stalk (Sample 2)

Effect of Feedstock S/L ratio

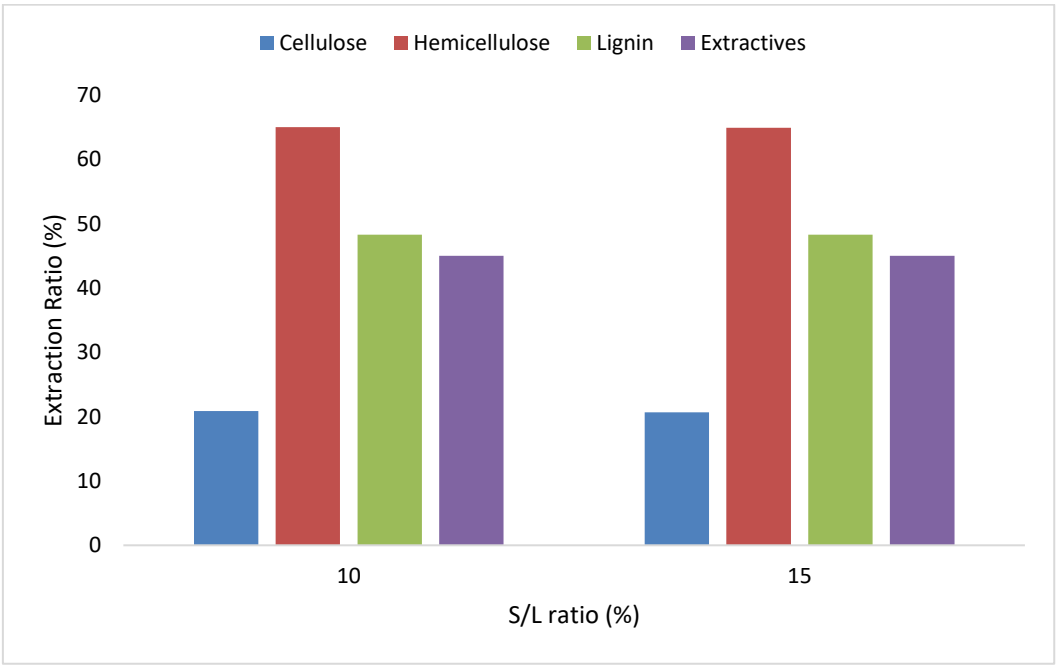

(A)

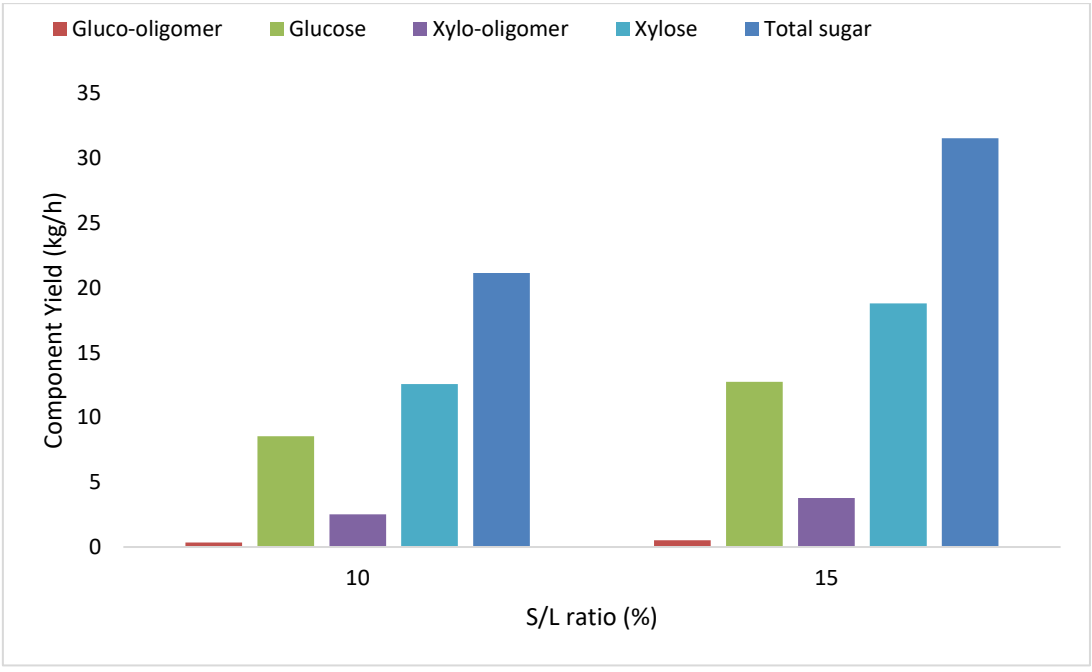

(B)

Figure A.4: (A) Component extraction ratio and (B) Monomers and oligomers formation with feedstock S/L ratio for corn stalk (Sample 2)

For Sample 3 Woodchips

Effect of HTS temperature

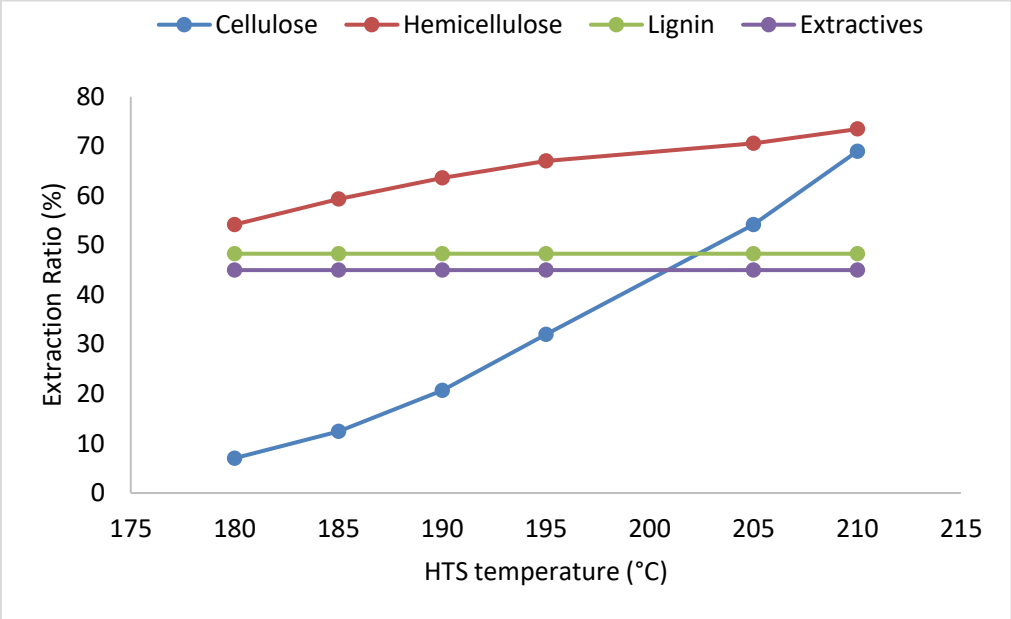

(A)

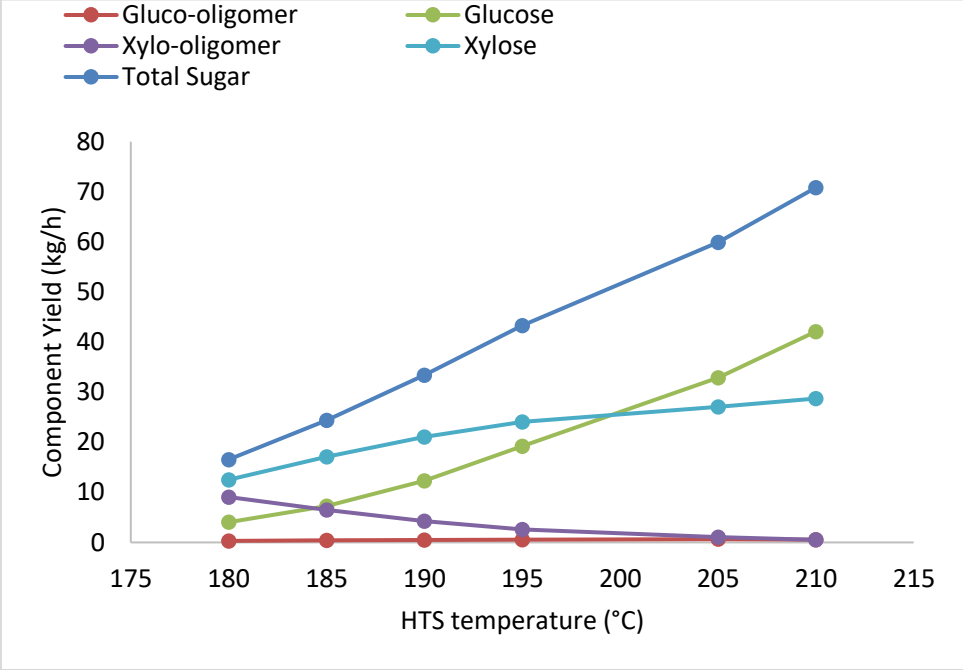

(B)

Figure A.5: (A) Component extraction ratio and (B) Monomers and oligomers formation with HTS temperature for woodchips (Sample 3)

Effect of HTS Pressure

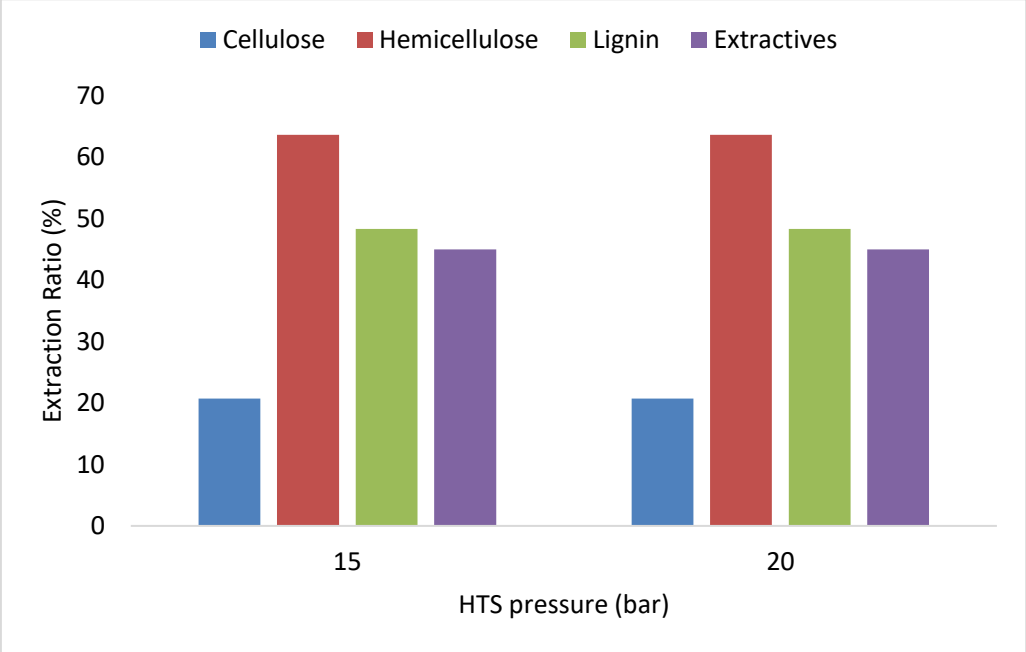

(A)

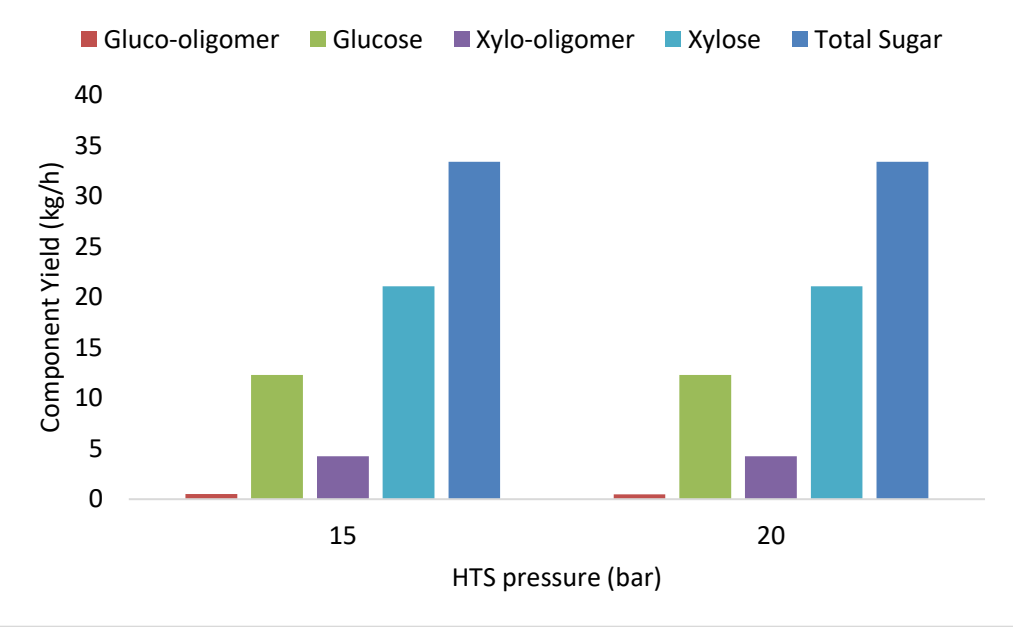

(B)

Figure A.6: (A) Component extraction ratio and (B) Monomers and oligomers formation with HTS pressure for woodchips (Sample 3)

Effect of HTS Residence Time

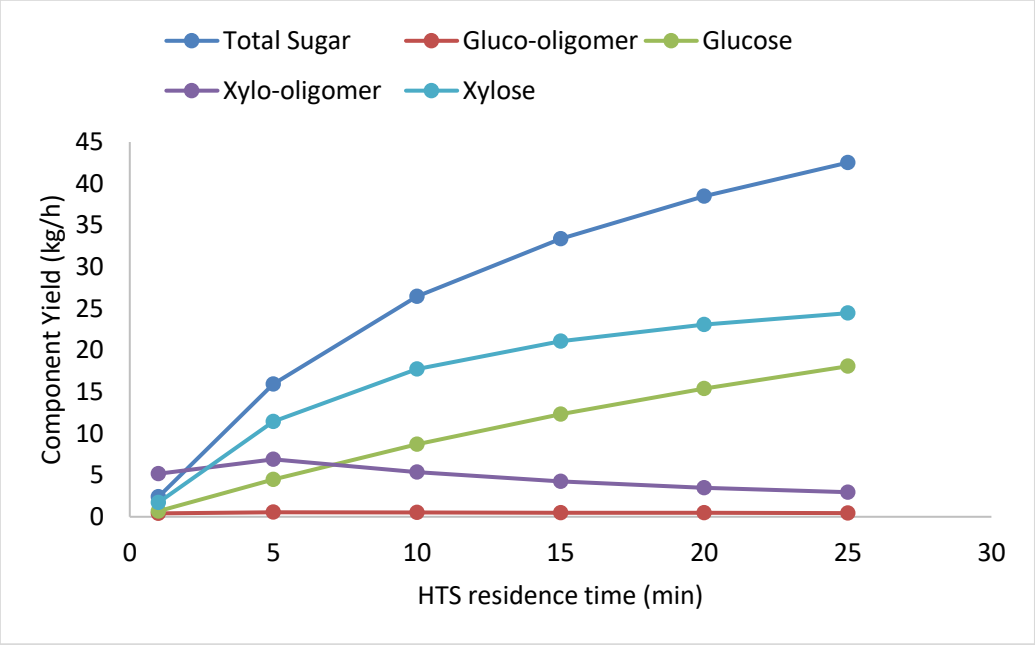

(A)

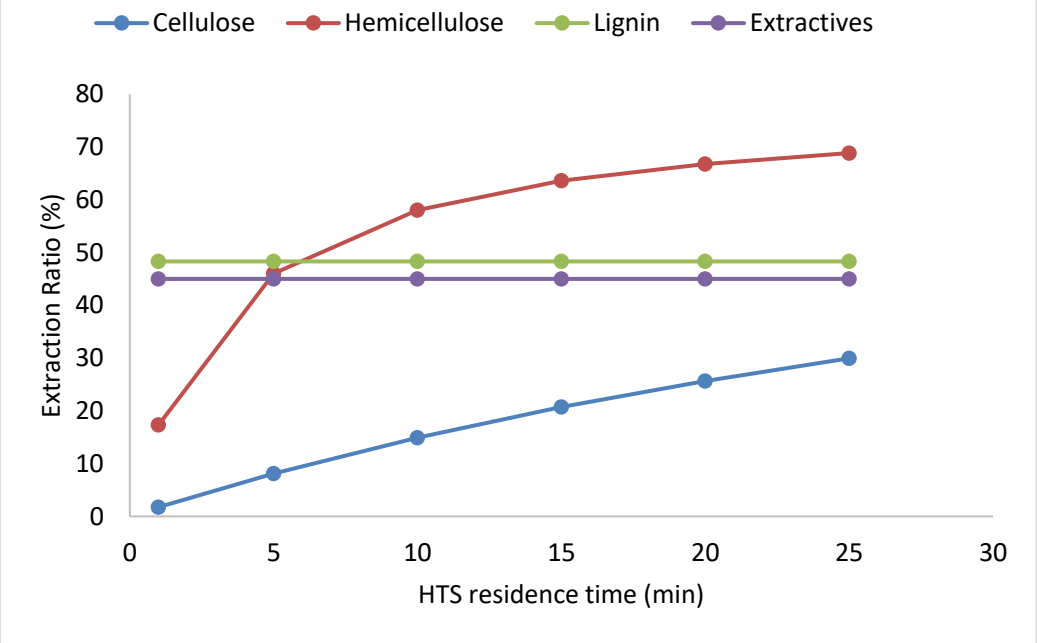

(B)

Figure A.7: (A) Component extraction ratio and (B) Monomers and oligomers formation with HTS residence time for woodchips (Sample 3)

Effect of S/L ratio

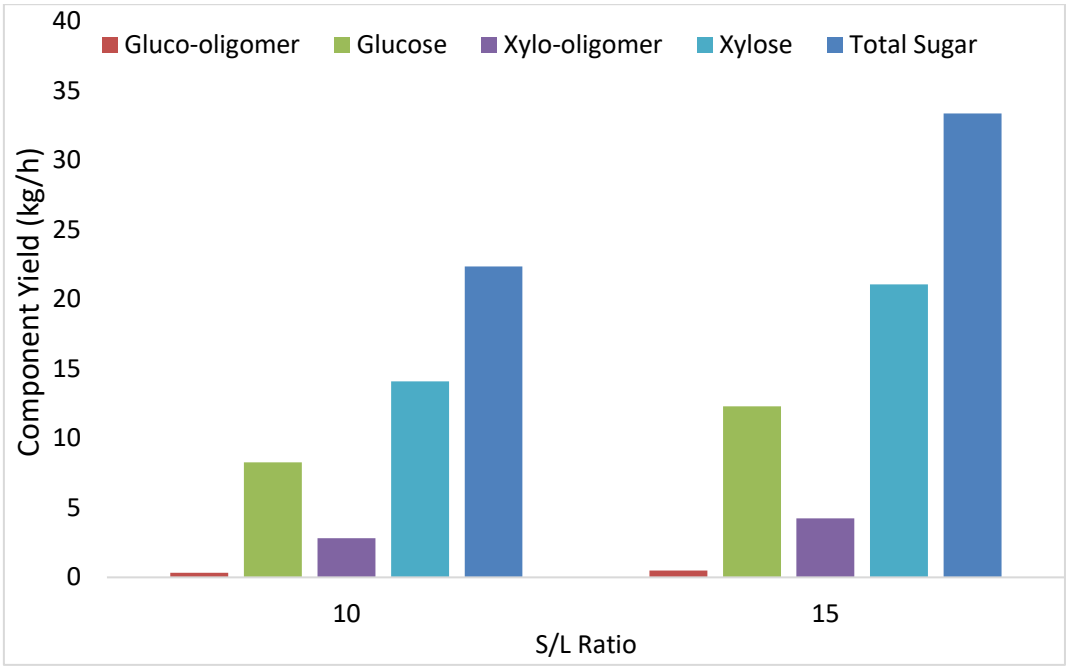

(A)

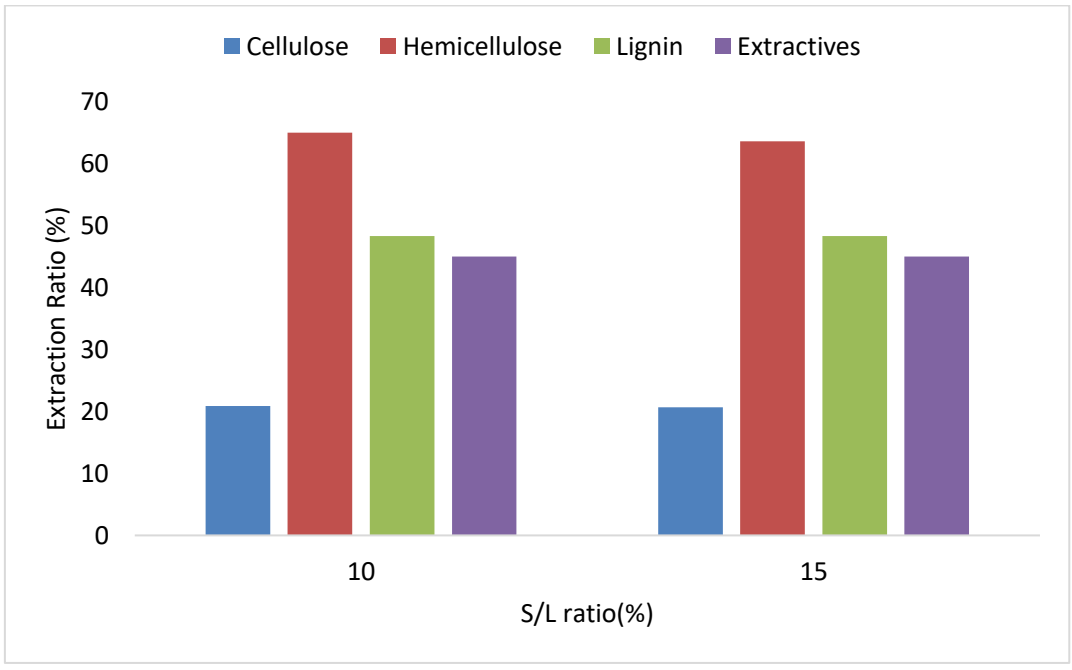

(B)

Figure A.8: (A) Component extraction ratio and (B) Monomers and oligomers formation with feedstock S/L ratio for woodchips (Sample 3)